Diameter and Coherence of Monotone Path Graphs in Low Corank

A DISSERTATION
SUBMITTED TO THE FACULTY OF THE GRADUATE SCHOOL
OF THE UNIVERSITY OF MINNESOTA
BY

Robert B. Edman

IN PARTIAL FULFILLMENT OF THE REQUIREMENTS
FOR THE DEGREE OF
Doctor of Philosophy

Victor Reiner

May, 2015

Acknowledgements

This thesis would also have not been possible without the generosity of my committee members: Kevin Leder, Pasha Pylyavskyy, Victor Reiner, and Sasha Voronov. My advisor, Victor Reiner, deserves particular credit; this would not have been possible without his patience and guidance. Vic's influence on this document was immense and the result is significantly better due to his input. Vic has always been willing to find time to work with me. I thank Vic particularly for always being willing to give me the advice and input I needed even when I didn't want to hear it.

I also gratefully acknowledge the influence of Ezra Miller on this work. Although Ezra has not seen the results contained in this document, Ezra guided me through my first years of graduate school and I look back fondly on our time together.

This dissertation was greatly improved by everyone who proofread it. My proofreaders went above and beyond in their comments and contributions. In order of perceived time spend, Victor Reiner, Victor Reiner, Victor Reiner (Vic went above and beyond in his proofreading and suggestions!), Thomas Edman, David Clark, Kyle Nelson, Jennifer Laaser, Kaisa Taipale, and both Tad and Jo of the University of Minnesota Writing Support Center.

Adventium Labs and MathCEP supported me through the final years of my PhD. In particular, Jon Rogness, Todd Carpenter, Tom Haigh, Kyle Nelson, Steve Harp, Steve Vestal, and Mark Boddy have been infinitely patient with me as I have tried to balance the commitments of multiple jobs with the demands of finishing my degree. acknowledgment should to the

Many more friends helped me stay sane through graduate school by giving me distractions. I cannot hope to list everyone who deserves an acknowledgment here but that won't stop me from trying. Friends from the University: Katy Micek, Erin Manlove, Ming Fang, Ben Rosenfield, Ole Nelson, Will Groves, David Moraski, James Swenson, Jon Rogness, and Eoin O'Hara. The HH crew, including Peter Thompson, Colin Deyong, Valentine Cadeaux, Sergio Vucci, Ben Barnhart. Skiing Friends including: Mary, Vancura, Chris Ward, Rachel Robertson, Tom Helm, Jeff Lanners, Craig Cardinal, Cheryl DuBois, Hans Harlane, David Christopherson, Mark Ahlers, Avho Taipale, Paavo Taipale, and the rest of the Vakava Racing Team. Everyone who I have sailed with including: Donovan Walker, Becky Stibbe, Sarah Wisneski, Tony Steinheigen, Leif Hegleson, Kraig Larson, Kevin Roberts, Steve Loscheider, and Charlie Gantzer.

My friends and family have earned the final acknowledgment. They believed in me even when I didn't believe in myself, and were patient with me when things dragged on. Thomas Edman, Kathleen Briggs, Sarah Edman, Jennifer Laaser, David Clark, Casey Crabb, Kaisa Taipale, Andreas Ostenso, Joe Kenney, Bob Butterbrodt, Peter Thompson, and Raphael Mudge, thank you tremendously for all your support and encouragement.

To my four day old nephew, Mordechai Edman Robashkin.

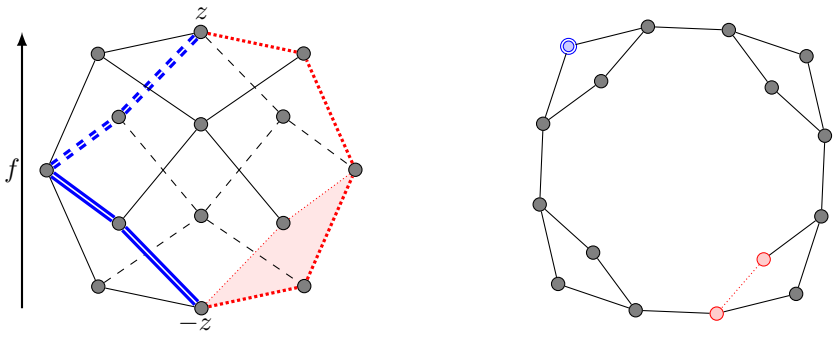

FIGURE 0.1. Three monotone paths on the zonotope and in the monotone path graph.

Abstract

A Zonotope Z is the linear projection of an n-cube into $\mathbb{R}^d$. Given a generic linear function f, an f-monotone path on Z is a path along edges from the f-minimizing vertex $-z$ to its opposite vertex z. The monotone paths of Z are the vertices of the monotone path graph in which two f-monotone paths are adjacent when they differ in a face of Z. In our illustration the two red paths are adjacent in the monotone path graph because they differ in the highlighted face. An f-monotone path is coherent if it lies on the boundary of a polygon obtained by projecting Z to 2 dimensions. The dotted, thick, red path in Figure 0.1 is coherent because it lies on the boundary after projecting Z to the page. However, there is no equivalent projection for the blue double path. The alternate red path may be coherent or incoherent based on the choice of f. The coherent f-monotone paths of Z are a set of geometrically distinguished galleries of the monotone path graph. Classifying when incoherent f-monotone paths exist is the central question of this thesis.

We provide a complete classification of all monotone path graphs in corank 1 and 2, finding all families in which every f-monotone path is coherent and showing that all other zonotopes contain at least one incoherent f-monotone path. For arrangements of corank 1, we prove that the monotone path graph has diameter equal to the lower bound suggested by Reiner and Roichman using methods of L_2-accessibility and illustrate that L_2 methods cannot work in corank 2 by finding a monotone path graph which has no L_2-accessible nodes. We provide examples to illustrate the monotone path graph and obtain a variety of computational results, of which some are new while others confirm results obtained through different methods.

Our primary methods use duality to reformulate coherence as a system of linear inequalities. We classify monotone path graphs using single element liftings and extensions, proving for when Z has incoherent f-monotone paths, then any lifting or extension of Z has incoherent f-monotone paths too. We complete our classification by finding all monotone path graphs with only coherent f-monotone paths and finding a set of minimal obstructions which always have incoherent f-monotone paths.

Contents

List of Tables

List of Figures

Conventions

c	A covector of an oriented matroid $\mathcal{M}$.
n	The number of vectors in a vector configuration
d	The dimension of each vector v of a vector configuration V
$\mathcal{A}$	A *Hyperplane Arrangement* assumed to be central, essential
$\mathcal{A}^*$	The Gale dual of $\mathcal{A}$
$\mathcal{M}(\mathcal{A})$	The oriented matroid of a hyperplane arrangement $\mathcal{A}$
γ	A *gallery* of $\mathcal{M}()$ with an acyclic orientation
$\gamma(i)$	The i^{th} hyperplane appearing in γ. (i.e., $\gamma = 1423 \implies \gamma(2) = 4$).
$\gamma^{(i)}$	The i^{th} covector appearing in γ. (i.e., $\gamma = 1423 \implies \gamma(2) = +--+$).
g_i	The g valuations, $g_i = g(a_i)$, of g on the elements of $\mathcal{A}$.
f_i	The f valuations, $f_i = f(a_i)$, of f on the elements of $\mathcal{A}$.
$\widehat{\mathcal{A}}$	A single-element lifting of $\mathcal{A}$.
$\mathcal{A}^+$	A single-element extension of $\mathcal{A}$.
a_i	Vectors of the hyperplane arrangement $\mathcal{A}$.
a_i^*	Vectors of $\mathcal{A}^*$ dual to a_i of $\mathcal{A}$.
$\mathcal{H}_i$	Hyperplane i of $\mathcal{A}$.
γ^+	An extension of γ in $\mathcal{A}^+$ a single-element extension of $\mathcal{A}$.
$\widehat{\gamma}$	An lifting of γ in $\widehat{\mathcal{A}}$ a single-element lifting of $\mathcal{A}$
$Z(\mathcal{A})$	The zonotope of hyperplane arrangement $\mathcal{A}$
$G_1(\mathcal{A})$	The 1-skeleton of $Z(\mathcal{A})$.
$G_2(\mathcal{A}, c)$	The graph of f-monotone paths$-c$ to c
$\Gamma(\mathcal{A}, c)$	The set of all galleries of $(\mathcal{A}, c)$.
$((-)^*(+)^*)^*$	A sign vector, written as a word in $\{-, 0, +\}$.
(Z, v)	A pointed zonotope
(A, c)	A pointed hyperplane arrangement
$(\mathcal{M}, (+)^n)$	An acyclically oriented matroid
(Z, f)	A generic functional f on a zonotope Z

CHAPTER 1

Introduction

In this thesis we study monotone path graphs of zonotopes and hyperplane arrangements in low corank. For a d-dimensional, centrally symmetric, zonotope in $Z \subset \mathbb{R}^d$, a linear functional $f \in \left(\mathbb{R}^d\right)^*$, which is non constant along every edge of Z determines unique f-minimal and f-maximum vertices of Z, $-z$ and z respectively. Paths along the edges of Z from $-z$ to z for which f is strictly increasing are f-monotone paths. A monotone path is coherent if it lies on the boundary of a polygon obtained by projecting Z to 2-dimensions. The set of all f-monotone paths form a geometrically distinguished subset of the vertices of the monotone path graph.

More generally a cellular string σ of Z is a sequence of faces of Z, called cells, in which consecutive faces σ_i and σ_{i+1} share a single vertex z_i, and the sequence of common vertices are (z_i) is f-monotone. An f-monotone path is a cellular string of maximal length, in which each cell is an edge of Z. A flip is a cellular string in which a distinguished cell is a 2-face of Z and all other cells are edges. Cellular strings, like f-monotone paths, are coherent when they lay on the boundary of the polygon obtained by projecting Z to 2-dimensions.

Given a hyperplane arrangement, $\mathcal{A}$ consisting of n hyperplanes in $\left(\mathbb{R}^d\right)^*$ we build the d-dimensional zonotope $Z(\mathcal{A}) \subset \mathbb{R}^d$, whose $d-k$-faces correspond to intersections of k hyperplanes. In this polytope, vertices correspond to chambers of $\mathcal{A}$, and edges are slices of hyperplanes which divide two chambers. A function $f \in \left(\mathbb{R}^d\right)^*$ which is non-constant along every edge of $Z(\mathcal{A})$ determines a unique vertex z of $Z(\mathcal{A})$ or, equivalently, a unique chamber c of $\mathcal{A}$. A path γ from $-c$ to c in $\left(\mathbb{R}^d\right)^*$ is a gallery of $\mathcal{A}$ and is a minimal gallery when γ has minimal length.

The set of all minimal galleries of $\mathcal{A}$ is the vertex set of a graph $G_2(\mathcal{A}, c)$ in which two minimal galleries are adjacent when they differ only in the path they take around an intersection of two hyperplanes of $\mathcal{A}$. Minimal galleries correspond to f-monotone paths and intersections of hyperplanes correspond to faces of $Z(\mathcal{A})$, so the graph $G_2(\mathcal{A}, c)$ is equal to the graph of f-monotone paths of $\mathcal{A}$.

We realize a hyperplane arrangement as a $d \times n$ matrix, A, whose columns are normal to the hyperplanes of $\mathcal{A}$. The corank of $\mathcal{A}$ is $n-d$ so corank 0 consists of d hyperplanes in $\mathbb{R}^d$. The zonotope of corank 0 hyperplane arrangements $\mathcal{A}$ is a d-cube and for a generic f distinguishing a chamber c, the graph $G_2(\mathcal{A}, c)$ is the d-permutohedron, as illustrated in Figure 1.1. Every gallery in $\mathcal{A}$ is coherent for f and the Permutohedron is a polytope [**BKS94**, Section 4]. In contrast, for higher corank hyperplane arrangements, the monotone path graph may contain incoherent galleries and will not be a polytope.

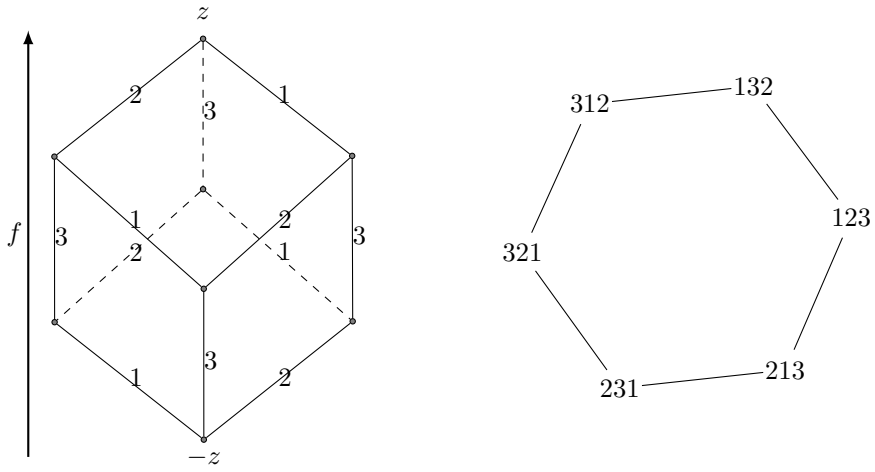

FIGURE 1.1. Zonotope (3-cube) and Monotone path graph (Permutohedron)

Our major results characterize the monotone path graphs which contain incoherent f-monotone paths in corank 1 and 2.

Behind both f-monotone paths of a zonotope and minimal galleries of a hyperplane arrangement there is a rank d acyclically oriented matroid $\mathcal{M}$. Section 2.1 reviews the relevant details of oriented matroids. Importantly $\mathcal{M} = \bigsqcup_{i=0}^{d} \mathcal{M}_i$ is the lattice of flats in which $\mathcal{M}_i$ consists of all corank i covectors of $\mathcal{M}$. Each corank k covector of $\mathcal{M}$ corresponds to a k-face of Z which in turn gives rise to a $(d-k)$ dimensional intersection of hyperplanes L_k. Since $\mathcal{M}$ is acyclically oriented, $(+)^n \in \mathcal{M}_0$ is a maximal covector of $\mathcal{M}$ and maximal covectors correspond to vertices of Z (or equivalently chambers of $\mathcal{A}$). Each edge of Z corresponds to a corank 1 covector of $\mathcal{M}$ and a gallery is a sequence of corank 1 covectors satisfying a monotone property which we will make explicit in Definition 2.9 The vertices of the graph $G_2(\mathcal{M}, (+)^n)$ are the galleries of $\mathcal{M}$; two galleries are adjacent when they differ by an element of $\mathcal{M}_2$.

The diameter of $G_2(\mathcal{A}, c)$ can be understood geometrically. Let $L = \bigsqcup_{i=0}^{d} L_i$ be the graded poset of intersection subspaces of $\mathcal{A}$, ordered by reverse inclusion. Every element of $c \in \mathcal{M}_2$ gives rise to an $X \in L_2$ however X does not uniquely determine c. We obtain a lower bound on the diameter of $G_2(\mathcal{A}, c)$ by noticing that a gallery γ and its reversal are L_2 flips apart, and that these flips are well defined as a subset of L_2 but not as a subset of $\mathcal{M}_2$. In [**RR12**] Reiner and Roichman asked "For real hyperplane arrangements $\mathcal{A}$ and a choice of base chamber c, does the graph G_2 of minimal galleries from $-c$ to c have diameter exactly $|L_2|$?" There are partial answers to this question, with [**CFGdO00**] showing equality when $\mathcal{A}$ is a hyperplane arrangement in $\mathbb{R}^3$. The diameter equals $|L_2|$ when $\mathcal{A}$ is a supersolveable hyperplane arrangement in [**RR12**]. We add to these results by proving that the diameter equals $|L_2|$ when $\mathcal{A}$ has corank 1.

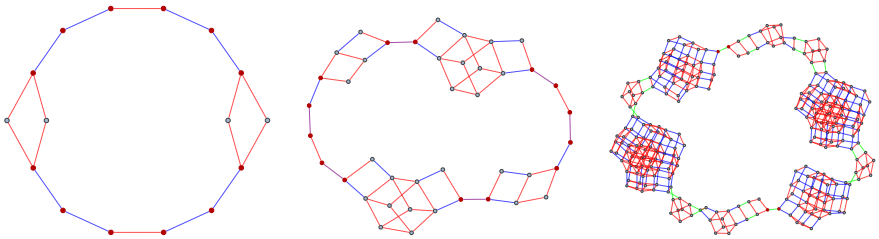

	A_3	B_3	H_3
corank=$n-3$	3	6	12
# of min. galleries	16	42	152
$\lvert L_2\rvert$	7	13	31

FIGURE 1.2. Monotone path graphs of irreducible reflection arrangements in $\mathbb{R}^3$.

It is harder to find examples in which the diameter strictly exceeds the lower bound of $|L_2|$. An example of Richter-Gerbert provides one example as a rank 4 oriented matroid [**RG93**]. We improve on this result by providing a realized hyperplane arrangement consisting of 8 hyperplanes in $\mathbb{R}^4$.

EXAMPLE 1.1. *To illustrate the structure of monotone path graphs we look at the 3 irreducible reflection arrangements in $\mathbb{R}^3$, presented in Figure 1.2. Although the graphs vary in complexity, they seem to be "bubbly" versions of a regular $2\,|L_2|$-gon in $\mathbb{R}^2$. Incoherent galleries of $\mathcal{A}$ look like nodes inside the $2\,|L_2|$-gon, forming bubbles. We notice adding hyperplanes increases corank and adds bubbles.*

We have organized this document as follows: In Chapter 2, we provide a self-contained description of the monotone path graph using the language of oriented matroids and pointed hyperplane arrangements. We begin with the relevant oriented matroid definitions in Section 2.1. Section 2.2 focuses on oriented matroids realized by vector configurations and hyperplane arrangements and develops our understanding of galleries using Gale duality. We include highlights of the classification of affine Gale diagrams, but leave details for the supporting material in Appendix B. The classification matches that of [**McM71**] and [**Grü67**] but is specifically tailored for pointed hyperplane configurations and illustrates families of monotone path graphs. Section 2.3 concludes the background material by giving the details of f-monotone paths and coherence.

Section 3 is an interlude summarizing the ideas of Chapter 2. Readers with some background in oriented matroids and monotone path graphs may choose to begin reading in this section as it contains the first new material. We say that (Z, f) is *all-coherent* for the special situation that every cellular string is coherent and (Z, v) universally all-coherent when (Z, f) is all-coherent for every (Z, f) realizing (Z, v). We conclude by reviewing the definitions of L_2-accessibility and a key proposition of [**RR12**] which uses L_2-accessibility to compute the diameter of the monotone path graph.

The theoretical tools of this dissertation are in Chapter 4, which uses the definitions of Chapter 3 to prove five key lemmas. These technical lemmas allow us prove the existence of incoherent galleries for hyperplane arrangements which are either single-element extensions or single-element liftings of

previously understood hyperplane arrangements. Of these 5 lemmas, two of them, Lemmas 4.16 and 4.24 are particularly subtle.

The rewards of Chapters 3 and 4 come in Chapters 5 and 6, which contain the main results of this dissertation. Specifically, Theorem 5.9 gives a complete classification of monotone path graphs in corank 1. Our classification identifies a unique family of corank 1, universally all-coherent pointed hyperplane arrangements. For all other monotone path graphs, we find an incoherent f-monotone path by identifying the smallest monotone path graph which contains an incoherent path for any f, then use the results of Section 4.5 to lift this incoherent path to all monotone path graphs outside of our previously identified all-coherent family. Finally, in Theorem 5.12, we prove the diameter is $|L_2|$ for all monotone path graphs of corank 1, arguing that the family of all-coherent gallery is itself a zonotope and thus its diameter is $|L_2|$ and finding a particular L_2-accessible gallery in all corank 1 hyperplane arrangements.

Chapter 6 provides a complete classification of monotone path graphs in corank 2. In Theorem 6.8 we identify two families of universally all-coherent monotone path graphs and give a set of minimal obstructions to show that all other monotone path graphs contain at least one incoherent path for every f. In contrast to Chapter 5 we are unable to use methods of L_2-accessibility to prove that the diameter equal $|L_2|$ in corank 2, which we discuss further in Section 7.

Chapter 7 presents a list of open questions, each motivated with an example. These open questions serve as a repository of hyperplane arrangements results which have motivated our thinking but found no other home in this dissertation. Chapter 7 also presents some minor theoretical and computational results we collected in the course of our research. Proposition 7.2 points out that our work also classifies cyclic hyperplane arrangements, and that the classification vaguely resembles Theorem 1.1 of [**ADLRS00**]. Some of our computational are previously unpublished, while others are confirmations of previously known results. The two new examples are:

- Example 7.1 is a hyperplane arrangement in corank 2, with a pleasantly symmetric monotone path graph, yet with no L_2-accessible galleries.
- Example 7.3 is a realized cyclic hyperplane arrangement with $d = 4$ and $n = 8$ with diameter 30 but $|L_2|$ strictly less at 28.

Finally, we hope that readers will find the appendices of this dissertation useful and amusing. Appendix B contains our classification of zonotopes of corank 1 and 2, a resource we wish was available to us at the outset of our research. Appendix A contains a rephrasing of monotone path problems as two recreational math problems for non-technical audiences.

CHAPTER 2

Oriented Matroids, Vector Configurations, and Hyperplane arrangements

This thesis is study of monotone path graphs of zonotopes and hyperplane arrangements, using oriented matroids and duality. This chapter is a review of acyclically oriented matroids, pointed hyperplane arrangements, and zonotopes with a generic functional f. A fully inclusive treatment of oriented matroids is beyond the scope of this document and we give only the details and notation needed to make our discussion self-contained. For those who wish to know more on the topic, we found [**BLVS$^+$93**] [**Zie95**], and [**Sta07**] particularly helpful. Readers with prior exposure to oriented matroids and zonotope may choose to skip this chapter in and begin reading in Chapter 3. We remark that oriented matroids realized by hyperplanes arrangements are not so far from the fully abstract notion of an oriented matroid, as the Topological Representation Theorem, presents any oriented matroid as an arrangement of pseudospheres [**FL78**].

2.1. Oriented Matroids

Oriented matroids generalize the similar combinatorial descriptions of directed graphs, orthogonal pairs of real vector subspaces, point configurations, vector configurations, and hyperplane arrangements [**BLVS$^+$93**, Ch. 3]. Each motivating description has its own system of axioms; each subtly different, but cryptomorphic. The axioms share a common notion of signed sets or sign vectors. In the setting of hyperplane arrangements sign vectors will be natural, so we restrict our attention to them.

DEFINITION 2.1. *A vector $v \in \{+,-,0\}^n$ is a* sign vector *of length n. For any vector (signed or otherwise), we will refer to component i of v as v_i. The support of a sign vector is the* set *of nonzero components, denoted:*

$$\mathit{supp}\,(v) = \{i \mid v_i \neq 0\}\,.$$

The negative $-v$ of v is the sign vector with all $+$'s and $-$'s flipped:

$$-v_i = \begin{cases} 0 & \text{if } v_i = 0, \\ - & \text{if } v_i = +, \\ + & \text{if } v_i = -. \end{cases}$$

We omit commas when writing sign vectors and use a literal notation; by viewing sign vectors as words in the symbols $\{+,-,0\}$, we write the sign vector $++++$ as $(+)^4$ or $--++$ as $(-)^2(+)^2$. The

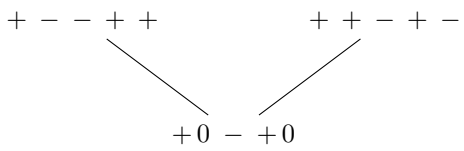

FIGURE 2.1. Poset structure of Oriented Matroids

symbols $\{+,-,0\}$ have a partial order in which $0 < +$, $0 < -$, and $+$ and $-$ are incomparable. The partial order of $\{+,-,0\}$ extends to a partial order on sign vectors in which $u < v \iff u_i < v_i$ for all i.

DEFINITION 2.2. *For sign vectors u and v, the* separation set *of u and v is the set of non-zero components where u and v are not equal:*

$$sep\,(u,v) = \{i \,:\, u_i = -v_j \neq 0\}\,.$$

EXAMPLE 2.3. *The sign vectors $++-+-$ and $+--++$ in Figure 2.1 are incomparable as they are not equal and non zero in positions 2 and 5, while both $++-+-$ and $+--++$ are greater than $+0-+0$.*

DEFINITION 2.4. *For two sign vectors u and v,* composition *of u and v decreases the separation set of u and v by building a sign vector with larger support. Formally we define composition as*

$$(u \circ v)_i = \begin{cases} u_i & \text{if } u_i \neq 0, \\ v_i & \text{else.} \end{cases}$$

We say that w eliminates j between u and v when $w_j = 0$ and $w_i = (u \circ v)_i$ for $i \notin sep\,(u,v)$.

Composition and elimination are both geometrically motivated operations and we will return to them in Section 2.2. For now we simply develop the intuition that composition and elimination are the reverse of each other.

Oriented matroids are sets of sign vectors called either vectors or covectors which satisfy oriented matroid axioms. Vectors and covectors define the same combinatorial structure using different axioms. Possible systems of axioms to choose from, and the objects which they most readily describe, include:

- Circuit axioms (coming from directed graphs),
- Orthogonality axioms (orthogonal pairs of real vector spaces),
- Chirotope axioms (point configurations and convex polytopes),
- Covector axioms (real hyperplane arrangements).

Details for all these axioms can be found in [**BLVS$^+$93**] along with equivalence proofs. Our focus is hyperplane arrangements so we use the covector axioms.

DEFINITION 2.5. *A set $\mathcal{V}^* \subset \{+, 0, -\}^n$ of sign vectors satisfies* the covector axioms *and is the set of covectors of an oriented matroid $\mathcal{M}$ when:*

- $0^n \in \mathcal{V}^*$,
- *(symmetry)* $u \in \mathcal{V} \implies -u \in \mathcal{V}^*$
- *(composition) for all* $u, v \in \mathcal{V}^*$, $u \circ v \in \mathcal{V}^*$,
- *(elimination) for all* $u, v \in \mathcal{V}^*$, $j \in S(u, v) \implies \exists w \in \mathcal{V}^*$ *so that* w *eliminates* j *between* u *and* v.

The rank of an oriented matroid is defined as the length of the longest chain of covectors

$$0 < c_1 < c_2 < \cdots < c_d$$

with c_i in $\mathcal{V}^*$. Any individual covector c also has rank and corank in $\mathcal{M}$: the rank of c is is the length of the longest chain $0 < c_1 < \ldots < c_r = c$; the corank of a vector c is the length of the longest chain

$$c = c_{d-r} < \cdots < c_d$$

in which c_d is a maximal covector of $\mathcal{M}$. The rank function gives oriented matroids a lattice structure $L(\mathcal{M}) = \bigsqcup_{i=0}^{d} \mathcal{M}_i$ in which $L_i(\mathcal{M})$ is the set of all corank i covectors of $\mathcal{M}$.

An oriented matroid also has a set of vectors $\mathcal{V}$ which carry equivalent combinatorial data. We will refer to $\mathcal{V}^*$ as the covectors of $\mathcal{M}$ and $\mathcal{V}$ as the vectors of $\mathcal{M}$. It is important to note that by way of vectors and covector, oriented matroids have duality built-in.

DEFINITION 2.6. *An oriented matroid $\mathcal{M}^*$ is the* dual *of $\mathcal{M}$ when $\mathcal{M}$ and $\mathcal{M}^*$ are related in the following way:*

- *the vectors of $\mathcal{M}^*$ are the covectors of $\mathcal{M}$, and*
- *the covectors of $\mathcal{M}^*$ are the vectors of $\mathcal{M}$.*

We do not dwell on this duality but will return when working with vector configurations.

EXAMPLE 2.7. *We check the covector axioms of Definition 2.5 for the set*

$$\mathcal{V}^* = \left\{ \begin{array}{ccccccc} +++, & 0++, & -++, & -+0, & -+-, & -0- \\ ---, & 0--, & +--, & +-0, & +-+, & +0+ \\ & & & 000 & & \end{array} \right\}.$$

Looking at the axioms one at a time we see:

- *Identity:* $0 \in \mathcal{V}^*$.
- *Symmetry:* $-c$ *is directly above or below* c.
- *Composition:* $u \circ v$ *of* u *and* v *remains in the same row as* v.
- *Elimination:* w *which eliminates* u *and* v *is either* 000 *or located between* u *and* v.
- *The rank of* $\mathcal{M}$ *is* 2.

Oriented matroids are the combinatorial structure behind zonotopes and hyperplane arrangements and we can understand galleries purely using oriented matroids [**CM93**], [**FPS01**]. Informally, galleries are paths in $L(\mathcal{M})$ from a distinguished maximal covector $-c$ to its antipodal covector c. When $\mathcal{M}$ has $(+)^n$ as a maximal covector we say that $\mathcal{M}$ has an acyclic orientation. For an oriented matroid $\mathcal{M}$ with an acyclic orientation, the choice of c determines an orientation of $\mathcal{M}$ and we assume without loss of generality that $c = (+)^n$.

DEFINITION 2.8. *A pair $(\mathcal{M}, (+)^n)$ is an* acyclically oriented matroid *if $\mathcal{M}$ is an oriented matroid and $(+)^n$ is a maximal covector of $\mathcal{M}$.*

The basic geometric objects of acyclically oriented matroids cellular strings and we are particularly interested in galleries and flips. We define cellular strings in general then specialize the definition for galleries and flips. The idea is that a gallery is a cellular string in which each cell has corank 1 in $\mathcal{M}$ and a flip is a cellular string with a distinguished cell of corank 2.

DEFINITION 2.9. *A* cellular string *of an acyclically oriented matroid $(\mathcal{M}, (+)^n)$ is a sequence of covectors $\sigma = \sigma_1 \big| \cdots \big| \sigma_m$ of $\mathcal{M}$, with $\sigma_i \circ (+)^n = \sigma_{i+1} \circ (-)^n$ for $1 \leq i \leq m$ with $\sigma_0 = (-)^n$ and $\sigma_{m+1} = (+)^n$. We call each covector σ_i a cell of σ.*

DEFINITION 2.10. *Given an acyclically oriented matroid $(\mathcal{M}, (+)^n)$ a* gallery *γ of $\mathcal{M}$ is a cellular string $\sigma_1 \big| \cdots \big| \sigma_n$ in which each cell $\sigma_i = \gamma^{(i)}$ is a corank 1 covector of $\mathcal{M}$, with $\gamma^{(i)} \circ ((-)^n) = \gamma^{(i+1)} \circ ((+)^n)$ for $1 \leq i \leq n$ with the convention $\gamma^{(0)} = (-)^n$ and $\gamma^{(n+1)} = (+)^n$. For notation ease we refer to the set of all galleries of $(\mathcal{M}, (+)^n)$ as $\Gamma(\mathcal{M}, (+)^n)$.*

DEFINITION 2.11. *Given an acyclically oriented matroid $(\mathcal{M}, (+)^n)$ a* flip *is a cellular string $\sigma_1 \big| \cdots \big| \sigma_{n-1}$ in which a distinguished cell $X = \sigma_i$ is a covector of corank 2 in $\mathcal{M}$ and all other cells are covectors of corank 1 in $\mathcal{M}$. We will refer to a flip by its distinguished corank 2 covector X. We say that galleries γ and γ' are adjacent by a flip X when both γ and γ' are refinements of X.*

DEFINITION 2.12. *The vertices of* the graph *$G_2(\mathcal{M}, (+)^n)$ are galleries of $\mathcal{M}$. Two galleries are adjacent in $G_2(\mathcal{M}, (+)^n)$ when they are adjacent by a flip.*

EXAMPLE 2.13. *Using the oriented matroid of Example 2.7 we see that there are two galleries which we write as the rows of a matrix for clarity:*

$$\gamma = \begin{pmatrix} \gamma^{(1)} = 0 - - \\ \gamma^{(2)} = + - 0 \\ \gamma^{(3)} = +0+ \end{pmatrix} \qquad \gamma' = \begin{pmatrix} \gamma'^{(1)} = -0- \\ \gamma'^{(2)} = - + 0 \\ \gamma'^{(3)} = 0 + + \end{pmatrix}$$

The two galleries are adjacent by the flip 000 which is the unique covector of corank 2. The graph $G_2(\mathcal{A}, (+)^n)$ has two nodes connected by a single flip.

Beautiful as they are, further details about abstract oriented matroids are unnecessary for our understanding of monotone path graphs, so we omit them.

2.2. Vector Configurations and Hyperplane arrangements

We now make oriented matroids concrete by introducing the closely related objects of vector configurations and hyperplane arrangements. We explain the close relationship between these two objects by describing their cocircuits and the zonotope. We then discuss galleries of pointed hyperplane arrangement and pointed zonotopes, and we make galleries and flips geometrically clear by viewing them as paths on zonotopes. Finally, we revisit oriented matroid duality, explicitly constructing the Gale dual and explaining galleries using duality. We close by recalling some highlights of a classification of pointed hyperplane arrangements, including affine Gale duals, single-element liftings, and single-element extensions, although we leave most details to the supplementary material in Appendix B.

DEFINITION 2.14. *A* hyperplane arrangement $\mathcal{A} \subset \mathbb{R}^d$ *is a set of* n *hyperplanes in* $\mathbb{R}^d$. *Each hyperplane has a specified normal vector* a_i *and we will write* $A = (a_i)$ *as* $d \times n$ *matrix in which each column vector* a_i *is normal to hyperplane* $\mathcal{H}_i$. *For our purposes, hyperplane arrangements will always be:*

- central*, so that* $0 \in \mathcal{H}_i$ *for all* i*, and*
- essential*, meaning* $\bigcap_{\mathcal{H}_i \in \mathcal{A}} \mathcal{H}_i = \{0\}$*, or equivalently, the matrix* $\mathcal{A}$ *has rank* d.

Any hyperplane divides $\mathbb{R}^d$ into positive and negative half-spaces. The set of all hyperplanes divides $\mathbb{R}^d$ into open polyhedral cones which we call *chambers*. Each of those chambers is associated to a sign vector c in which c_i is $+$ if the chamber is in the positive half space of hyperplane $\mathcal{H}_i$, and $-$ otherwise. The chambers are the maximal covectors of $\mathcal{M}(\mathcal{A})$. We refer to maximal covectors as chambers when we want to stress the geometric nature of hyperplane arrangements and maximal covectors when emphasizing the oriented matroid structure.

EXAMPLE 2.15. *We return to the oriented matroid of Example 2.7 which we realize as a hyperplane arrangement by specifying the vector* $a_i \in \mathcal{A}$ *as normal to hyperplane* $\mathcal{H}_i$.

$$\mathcal{A} = \begin{array}{c} \begin{matrix} a_1 & a_2 & a_3 \end{matrix} \\ \begin{pmatrix} 1 & 0 & 1 \\ 0 & 1 & 1 \end{pmatrix} \end{array}$$

Figure 2.2 makes clear the relationship between the maximal covectors and chambers $\mathcal{A}$. *We also now understand the geometry of the elimination axiom of Definition 2.5; the covector* $+0+$ *eliminates* 2 *between* $+++$ *and* $+-+$ *and corresponds to the part of hyperplane* 2 *which divides the chambers* $+++$ *and* $+-+$.

We have not specified the oriented matroid structure of $\mathcal{A}$, but the maximal covectors of $\mathcal{A}$ depend only on the normal vectors $\{a_i\}$. The oriented matroid structure of $\mathcal{A}$ is defined using the normal vectors. Ignoring that $\{a_i\}$ are normal to hyperplanes in $\mathcal{A}$, we call any finite set of vectors a vector configuration.

DEFINITION 2.16. *A* vector configuration V *is a finite set of vectors* $V = \{v_1 \ldots, v_n\}$ *spanning* $\mathbb{R}^d$ *and which we write as a* $d \times n$ *matrix* V. *We* d *is the rank of* V *and* $n - d$ *as the corank of* V.

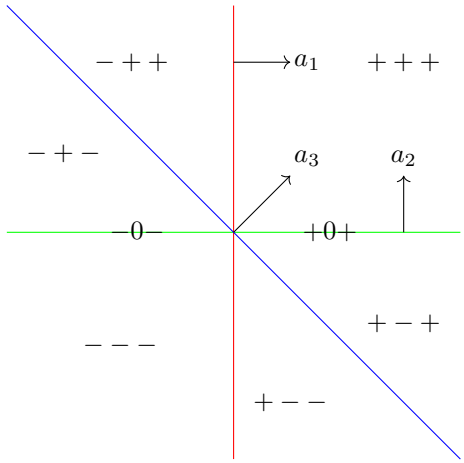

FIGURE 2.2. A simple hyperplane arrangement (Example 2.15)

Vector configurations and hyperplane arrangements are the same combinatorial objects and we use them interchangeably. Any set finite set of vectors defines a hyperplanes arrangement simply by viewing each vector as the normal vector of a hyperplane arrangement. Any set of hyperplanes are described by a configuration of normal vectors. We define $\mathcal{M}$ by specifying the covectors of $\mathcal{M}(V)$. The covectors of V are built from the valuations of linear functions $f \in \left(\mathbb{R}^d\right)^*$ on V. We favor the hyperplane terminology but often think using vector configurations. We use $\mathcal{M}(\mathcal{A})$ and $\mathcal{M}(V)$ interchangeably.

DEFINITION 2.17. *Give a vector configuration V and $f \in \left(\mathbb{R}^d\right)^*$, the vector $f^* \in \mathbb{R}^n$ whose i^{th} component $f_i = f(v_i)$ for every $v_i \in V$ is* the valuation *of f on V. The set of all valuations of V is*

$$\operatorname{val} V = \left\{ f^* \in \mathbb{R}^n \,:\, \exists f \in \left(\mathbb{R}^d\right)^* \text{ such that } f(v_i) = f_i \right\} \subset \mathbb{R}^n.$$

To any vector $f^* \in \mathbb{R}^n$ we can associate a sign vector c by mapping the sign function over the components of f.

$$c_i \operatorname{sign}(w_i) = \begin{cases} - & \text{if } w_i < 0, \\ + & \text{if } w_i > 0, \\ 0 & \text{else.} \end{cases}$$

Mapping the sign function over all valuations of V turns the set of valuations into a set of sign vectors, which we suggestively denote $\mathcal{V}^*(V) = \{\operatorname{sign} f^* : f^* \in \operatorname{val} V\}$.

LEMMA 2.18. *Given a vector configuration V, the set of sign vectors of valuations of V satisfies the covector axioms of Definition 2.5 and we say $\mathcal{V}^*(V) = \{\operatorname{sign} f^* : f^* \in \operatorname{val} V\}$ are the covectors of an oriented matroid $\mathcal{M}(V)$. When $\mathcal{M} = \mathcal{M}(V)$ we say that $\mathcal{M}$ is a* realized oriented matroid *or that $\mathcal{M}(V)$ realizes $\mathcal{M}$. When V is the set of normal to a hyperplane arrangement $\mathcal{A}$, we $\mathcal{M}(V) = \mathcal{M}(\mathcal{A})$.*

PROOF. This is a standard and well-known result [**Zie95**], [**BLVS$^+$93**] which we do not reproduce here. We point out that the matroid structure of $\mathcal{M}(V)$ depends only on the direction of v_i and not its magnitude $|v_i|$. □

EXAMPLE 2.19. *We have already realized the oriented matroid in Example 2.7 with a hyperplane arrangement in Example 2.15.The oriented matroid $\mathcal{M}$ has rank 2, and consists of sign vectors of length 3 so we expect V to be a configuration of 3 vectors in $\mathbb{R}^2$. The vectors of V are normal vectors of hyperplanes in $\mathcal{A}$ so $\mathcal{M}$ is realized by the vectors*

$$V = \begin{array}{c} \begin{matrix} v_1 & v_2 & v_3 \end{matrix} \\ \begin{pmatrix} 1 & 0 & 1 \\ 0 & 1 & 1 \end{pmatrix} \end{array}$$

To verify that $\mathcal{M} = \mathcal{M}(V)$ we must find a functional $f(x, y)$ so that $\operatorname{sign} f(v_i) = c_i$ *for every $c \in \mathcal{V}^*$. We do this explicitly and write the functionals $f(x, y)$ directly above its sign vector $f(v_i)$:*

$$\mathcal{V}^* = \left\{ \begin{array}{ccc} x+y, & y, & -x+2y, \\ +++, & 0++, & -++, \\ & & \\ -x+y, & -2x+y, & -x, \\ -+0, & -+-, & -0-, \\ & & \\ -x-y, & -y & x-2y, \\ ---, & 0-- & +--, \\ & & \\ x-y, & 2x-y, & x, \\ +-0, & +-+, & +0+, \\ & & \\ & 0 & \\ & 000, & \end{array} \right\}.$$

We describe both hyperplane arrangements and vector configurations with a $d \times n$ matrix with vectors as columns. The matrix V specifies a linear surjection $V : \mathbb{R}^n \to \mathbb{R}^d$ and the image of the n-cube $[-1, +1]^n$ is the zonotope $Z = Z(V) = Z(\mathcal{A})$ [**McM71**]. The zonotope carries all the oriented matroid information of $\mathcal{M}(\mathcal{A})$ in an easy to understand geometric package.

DEFINITION 2.20. *Given a vector configuration V, written as a $d \times n$ matrix, the* zonotope *is the image of the n-cube under the linear surjection specified by V (rep. V), written explicitly as the Minkowski sum*

$$Z(V) = \sum_{i=1}^{n} [-a_i, a_i] .$$

As always when V is the set of normal vectors to a hyperplane arrangement $\mathcal{A}$ we define $Z(\mathcal{A}) = Z(V)$. The graph $G_1(V) = G_1(\mathcal{A})$ is the 1-skeleton of the zonotope and an important special case.

In geometric terms, the zonotope is a centrally symmetric polytope in $\mathbb{R}^d$ whose vertices correspond to maximal covectors of V, and whose k faces correspond to corank k covectors of $\mathcal{M}(V)$. In geometric terms, vertices of $Z(\mathcal{A})$ are the chambers of $\mathcal{A}$ and two chambers c, c' are adjacent when they are separated by exactly 1 hyperplane.

The zonotope $Z(V)$ is a polytope and its face lattice equals the poset of covectors of the oriented matroid of $\mathcal{M}(V)$. The geometry of the zonotope $Z(V)$ depends on the choice of the vectors $v_i \in V$, however two vector configurations have the same oriented matroid if and only if their zonotopes have equal face lattices [**Zie95**].

To define galleries for vector configurations we want a geometric understanding of acyclic orientations of $\mathcal{M}(V)$. An acyclic orientation of $\mathcal{M}$ is the choice of a maximal covector, and maximal covectors of $\mathcal{M}(V)$ are vertices of $Z(V)$. A realized acyclically oriented matroid is a zonotope with a distinguished vertex v.

DEFINITION 2.21. *A* pointed zonotope *is a pair (Z, v) with Z a zonotope in $\mathbb{R}^d$ and v a vertex of Z. When V is the set of normal vectors to a hyperplane arrangement $\mathcal{A}$, and c is the chamber corresponding to v we say $(\mathcal{A}, c)$ is a pointed hyperplane arrangement; we use $(\mathcal{A}, c)$ and (Z, v) interchangeably.*

We say that (Z, v) or $(\mathcal{A}, c)$ realizes the acyclically oriented matroid $(\mathcal{M}, (+)^n)$ when $Z = Z(V) = Z(\mathcal{A})$, $\mathcal{M} = \mathcal{M}(V)$ and $v = \sum v_i$ is the vertex corresponding to $(+)^n$.

Galleries of an acyclically oriented matroid are sequences of corank 1 covectors of $\mathcal{M}$. The corank 1 vectors of $\mathcal{M}(V)$ are the edges of $Z(V)$ so the galleries of (Z, v) of a pointed zonotope are paths on the edges of $Z(V)$ between $-v$ and v.

DEFINITION 2.22. *Given a pointed zonotope (Z, v), a* gallery *γ is a path of minimal length on the edges of Z from $-v$ to v.*

A gallery of a pointed hyperplane arrangement $(\mathcal{A}, c)$ is a gallery of the pointed zonotope $(Z(\mathcal{A}), v)$ in which the chamber c corresponds to the vertex v of $Z(\mathcal{A})$ is a path in $\left(\mathbb{R}^d\right)^*$ from $-c$ to c.

It is clear that this is equivalent to Definition 2.10 when (Z, v) realizes the acyclically oriented matroid $(\mathcal{M}, (+)^n)$.

DEFINITION 2.23. *A polygonal face X of $Z(\mathcal{A})$ is a S*flip *between two galleries γ and γ' of a pointed hyperplane arrangement $(Z(\mathcal{A}), v)$ when γ and γ' differ on X and agree elsewhere on $Z(\mathcal{A})$ as illustrated in Figure 2.3* [**AS01**].

This zonotope definition of a flip is consistent with Definition 2.11 but not nearly as precise. The polygonal face X corresponds to a codimension 2 intersection of hyperplanes in $\mathcal{A}$ which gives rise to a corank 2 covector of $\mathcal{M}(\mathcal{A})$. From this information we can build a cellular string σ in which X gives rise to the distinguished cell σ_k and γ and γ' define corank 1 covectors. Although we defined both galleries and flips of acyclically oriented matroids using cellular strings, we omit cellular strings in current level of generality. Such definitions are possible but are not be necessary for our understanding. We return to cellular strings in Section 2.3 and we refer interested readers to [**BKS94**].

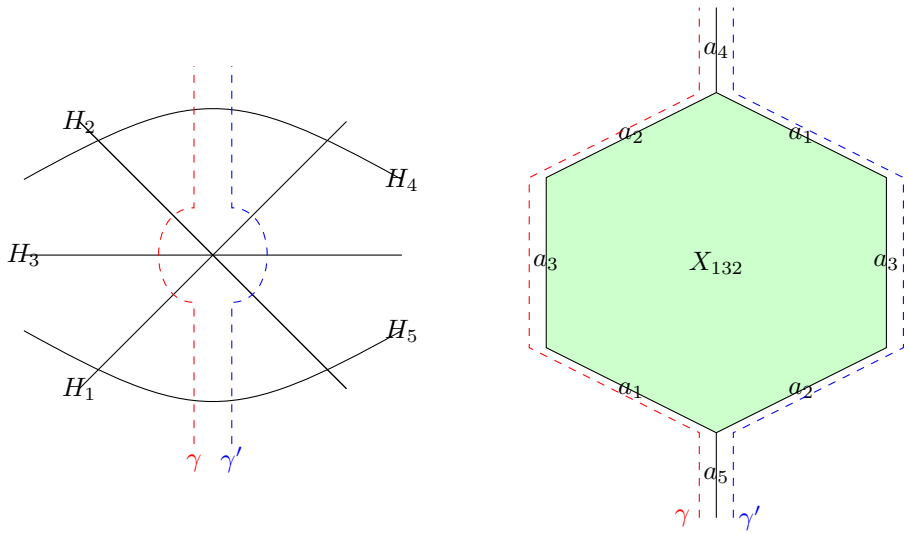

FIGURE 2.3. Flips as hyperplane intersections and faces of the zonotope

DEFINITION 2.24. *Given a pointed zonotope (Z, v) the* graph $G_2(Z, v)$ *is the graph whose vertices are galleries and in which two galleries are adjacent when they differ by a flip. The graph $G_2(\mathcal{A}, c) = G_2(Z, v)$ when $Z = Z(V)$ is a set of normal vectors of a hyperplane arrangement $\mathcal{A}$ and v corresponds to the chamber c of $\mathcal{A}$.*

EXAMPLE 2.25. *Revisiting Example 2.19 we recall the vector configuration*

$$V = \begin{array}{c} \begin{matrix} v_1 & v_2 & v_3 \end{matrix} \\ \begin{pmatrix} 1 & 0 & 1 \\ 0 & 1 & 1 \end{pmatrix} \end{array}.$$

Figure 2.4 shows that the zonotope is a hexagon and we pick the vertex $+++$ to make (Z, v) a pointed zonotope. We see the galleries from Example 2.13 as the two paths between $---$ and $+++$ and the flip between them is the lone $Z(V)$ since V has rank 2.

We can easily see galleries in flips in dimension 2 and 3 however, as we increase dimension we will need more powerful tools to understand galleries and flips. To make galleries easier to work with, we define and illustrate oriented matroid duality. The idea of duality is to reverse the roles of vectors and covectors of $\mathcal{M}$ allowing us to understand the covectors of V by understanding the vectors of V^*. We must first describe the vectors of $\mathcal{M}(V)$ and will then build V^* whose vectors are covectors of V. The vectors of $\mathcal{M}(V)$ are the sign vectors of linear dependencies of V.

DEFINITION 2.26. *A* linear dependence *of V is a vector $w \in \mathbb{R}^n$ such that $V \cdot w = 0$, which we denote by:*

$$\operatorname{dep} V = \{w \in \mathbb{R}^n \,:\, V \cdot w = 0\} \subset \mathbb{R}^n.$$

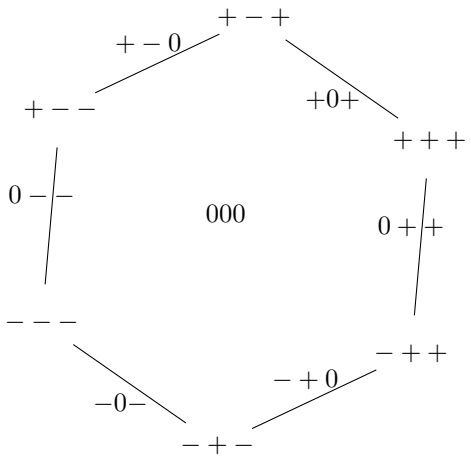

FIGURE 2.4. $(Z(V), + + +)$ and $G_2(Z(V), + + +)$ for example 2.25

The vectors of $\mathcal{M}(V)$ are the sign vectors of linear dependencies of V, that is

$$\mathcal{V}(V) = \{\operatorname{sign} v : v \in \operatorname{dep} V\}.$$

The dual vector configuration V^* is a configuration of n vectors whose linear dependencies correspond to valuations of V. To find V^* of V we must find a basis for the kernel of V. We will illustrate this with an example.

EXAMPLE 2.27. *Building from Example 2.19 we understand the covectors of V in terms of oriented matroid duality. Recall that*

$$V = \begin{array}{c} \begin{matrix} v_1 & v_2 & v_3 \end{matrix} \\ \begin{pmatrix} 1 & 0 & 1 \\ 0 & 1 & 1 \end{pmatrix} \end{array}.$$

We find a basis for $\ker V$ *which we treat as a row vector.*

$$V^* = \begin{array}{c} \begin{matrix} v_1^* & v_2^* & v_3^* \end{matrix} \\ \begin{pmatrix} 1 & 1 & -1 \end{pmatrix} \end{array}$$

We saw the covector $+ + +$ of V as a valuation of V but we can now also understand it as a linear dependence. The sum $v_1^* + v_2^* + 2v_3^* = 0$ is a linear dependence of V^* so $+ + +$ is a vector of V^* and a covector of V. Similarly we can understand all covectors of V. As in Example 2.19, we write each sign

vector under the corresponding linear dependence:

$$\mathcal{V}^* = \left\{ \begin{array}{ccc} \begin{array}{c} v_1^*+v_2^*+2v_3^*=0, \\ +++, \end{array} & \begin{array}{c} v_2^*+v_3^*=0, \\ 0++, \end{array} & \begin{array}{c} -v_1^*+2v_2^*+v_3^*=0 \\ -++, \end{array} \\ \begin{array}{c} -v_1^*+v_2^*=0, \\ -+0, \end{array} & \begin{array}{c} -2v_1^*+v_2^*-v_3^*=0, \\ -+-, \end{array} & \begin{array}{c} -v_1^*+v_3^*=0, \\ -0-, \end{array} \\ \begin{array}{c} -v_1^*-v_2^*-2v_3^*=0, \\ ---, \end{array} & \begin{array}{c} -v_2^*-v_3^*=0, \\ 0--, \end{array} & \begin{array}{c} v_1^*-2v_2^*-v_3^*=0 \\ +-- \end{array} \\ \begin{array}{c} v_1^*-v_2^*=0, \\ +-0, \end{array} & \begin{array}{c} 2v_1^*-v_2^*+v_3^*=0, \\ +-+, \end{array} & \begin{array}{c} -v_1^*+v_3^*=0 \\ +0+ \end{array} \\ & \begin{array}{c} 0v_1^*+0v_2^*+0v_3^*=0, \\ 000 \end{array} & \end{array} \right\}.$$

The crucial idea is that valuations of V correspond to linear dependencies on V^*. Duality will be essential in many of our definitions and proofs, particularly: Definition 2.39 and Lemmas and Chapter 4.

Given V, a configuration of n vectors in $\mathbb{R}^d$, the dual V^* is a configuration of n vectors in $\mathbb{R}^{n-d}$. When $n-d$ is small we can replace vectors in $\mathbb{R}^n$ with the dual vectors in $\mathbb{R}^{n-d}$, which we can visualize. Duality is the primary tool we use to classify and understand low corank vector configurations and we include a classification of pointed vector configuration in coranks 1 and 2 as Appendix B. Our classification includes the details of affine gale diagrams, however we will recall the definition of single-element liftings extensions and recall a few key highlights here.

DEFINITION 2.28. *A vector configuration V^+ is a* single-element extension *of V when*

$$V^+ = V \cup \{v_{n+1}\}.$$

Single-element extensions are inverse to oriented matroid deletion and we recall $\mathcal{A} = \mathcal{A}^+ \setminus \{a_{n+1}\}$.

We illustrate single-element extensions with a simple example.

EXAMPLE 2.29. *The vector configuration V^+ is a single-element extension of the vector configuration V from Example 2.19*

$$V = \begin{array}{c} \begin{array}{ccc} v_1 & v_2 & v_3 \end{array} \\ \begin{pmatrix} 1 & 0 & 1 \\ 0 & 1 & 1 \end{pmatrix} \end{array} \qquad V^+ = \begin{array}{c} \begin{array}{cccc} v_1 & v_2 & v_3 & v_4 \end{array} \\ \begin{pmatrix} 1 & 0 & 1 & 1 \\ 0 & 1 & 1 & 2 \end{pmatrix} \end{array}$$

DEFINITION 2.30. *We say that a vector configuration $\widehat{V} = \left\{\widehat{v}_i \in \mathbb{R}^{d+1} \,\middle|\, 1 \le i \le n+1\right\}$ is a* single-element lifting *of $V = \left\{v_i \in \mathbb{R}^d \,\middle|\, 1 \le i \le n\right\}$ if there is a linear surjection $\mathbb{R}^{d+1} \overset{\pi}{\longmapsto} \mathbb{R}^d$ so*

that

$$\pi(\hat{v}_{n+1}) = 0$$
$$\pi(\hat{v}_i) = c_i \cdot v_i \, 1 \leq i \leq n$$

Without loss of generality, we typically assume that $c_i = 1$. *Single-element liftings are inverse to oriented matroid contractions* [**Zie95**, Prop. 6.11] *and we recall that* $\mathcal{A} = \widehat{\mathcal{A}}/\{a_{n+1}\}$.

When $\gamma^+ \in \Gamma(\mathcal{A}^+, c)$ we write $\gamma^+\backslash(a_{n+1})$ for the gallery of $(\mathcal{A}, c\backslash(a_{n+1})$ obtained by deleting the hyperplane corresponding to a_{n+1}. Likewise when $\widehat{\gamma} \in \Gamma(\widehat{\mathcal{A}}, c)$ we write $\gamma^+/(a_{n+1})$ for the gallery of $(\mathcal{A}, c/(a_{n+1})$ obtained the contraction of a_{n+1}. We will later show liftings $\widehat{\gamma}$ and extensions γ^+ of a gallery γ exist using deletion and contraction ideas and write $\gamma = \widehat{\gamma}/a_{n+1}$ and $\gamma = \gamma^+\backslash a_{n+1}$. Confusingly $\widehat{\gamma}/a_{n+1}$ and $\gamma^+\backslash a_{n+1}$ are equal as words in $\{a_i\}$ but we retain the deletion and contraction notation as a reminder of how we obtain $\widehat{\mathcal{A}}$ or $\mathcal{A}^+$ from $\mathcal{A}$.

In comparison to single-element extensions, single-element liftings have two desirable properties.

- Single element-liftings preserve corank making them useful for our classification and Lemma 4.24 in particular.
- Acyclic orientations of $\mathcal{A}$ can always be lifted to acyclic orientations of $\widehat{\mathcal{A}}$, using Lemma 4.11.

We illustrate with an example of single-element liftings.

EXAMPLE 2.31. *The configurations*

$$\widehat{V} = \begin{pmatrix} 1 & 0 & 0 & 1 \\ 0 & 1 & 0 & 1 \\ 0 & 0 & 1 & 1 \end{pmatrix} \quad \textit{and} \quad V = \begin{pmatrix} 1 & 0 & 1 \\ 0 & 1 & 1 \end{pmatrix}$$

are related by the linear surjection

$$\pi(x) = \begin{pmatrix} 1 & 0 \\ 0 & 1 \\ 1 & 1 \\ 0 & 0 \end{pmatrix} x.$$

We know $\widehat{V}$ *is a single-element lifting of* V *because* $\pi(\widehat{V}) = V$.

The relationship between single-element liftings and single-element extensions is duality.

- If $\widehat{V}$ is a single-element lifting of V then $\widehat{V}^*$ is a single-element extension of V^*
$$\left(\widehat{V}\right)^* = (V^*)^+ .$$
- If V^+ is a single-element extension of V then $(V^+)^*$ is a single-element lifting of V^*
$$\left(V^+\right)^* = \widehat{(V^*)}.$$

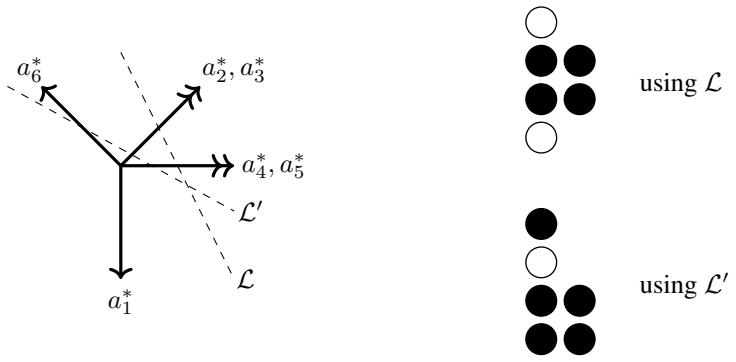

FIGURE 2.5. V^* as a vector configuration and two of its affine Gale diagram

PROPOSITION 2.32. *The following facts allow us to produce a classification of pointed vector configurations in coranks* 1 *and* 2*. Explanation of these facts along with a detailed classification can be found in Appendix B*

- *In corank* 1*, pointed vector configurations are uniquely determined by the number* n *of vectors in* V *and the number* k *of negative vectors in* V^**.*
- *Affine Gale diagrams describe dual vector configuration in coranks* 1 *and* 2*. Our convention when drawing affine Gale diagrams will be to draw positive vectors as black dots and negative vectors as white dots. We will draw affine Gale diagrams so that classes of parallel vectors will "line up" on the* x *axis, while non parallel vectors have distinct* y *values form a "stack".*
- *We organize our classification by single-element liftings of* V *but draw pictures of* V^* *and liftings of* V *are extensions of* V^**.*

EXAMPLE 2.33. *As an illustration of affine Gale diagram we introduce a vector configuration that will be the focus of Section 6.3. It consists of* 6 *vectors in* $\mathbb{R}^4$*,*

$$V = \begin{array}{c} \begin{matrix} v_1 & v_2 & v_3 & v_4 & v_5 & v_6 \end{matrix} \\ \begin{pmatrix} 1 & 0 & 0 & 0 & 1 & 2 \\ 0 & 1 & 0 & 0 & -1 & -1 \\ 0 & 0 & 1 & 0 & -1 & -1 \\ 0 & 0 & 0 & 1 & -1 & 0 \end{pmatrix} \end{array} \quad \textit{with dual, } V^* = \begin{array}{c} \begin{matrix} v_1^* & v_2^* & v_3^* & v_4^* & v_5^* & v_6^* \end{matrix} \\ \begin{pmatrix} 0 & 1 & 1 & 1 & 1 & 1 \\ -1 & 1 & 1 & 0 & 0 & -1 \end{pmatrix} \end{array}.$$

There are 4 parallelism classes of V^* *and the first 5 vectors are in standard position;* v_6^* *has a cross-ratio of* $\mu = 1$*. Depending on the choice of affine hyperplane we can have multiple equivalent affine Gale diagrams, as in Figure 2.5.*

EXAMPLE 2.34. *To illustrate the classification of Appendix B we highlight the details of* 5 *vectors in* $\mathbb{R}^3$ *when* V^* *has no parallelism. The dual vector configuration will be* 5 *vectors in* $\mathbb{R}^2$ *and the affine*

diagram	size of eq. class
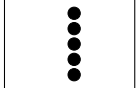	10
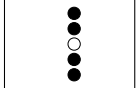	10
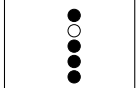	10
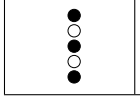	2

TABLE 2.1. Vector configurations of 5 vectors in $\mathbb{R}^3$ with no parallelism

Gale diagram will consist of 5 *distinct signed vectors, each colored black or white. Initially there are* $2^5 = 32$ *ways to color these* 5 *vectors which we break up into equivalence classes. Affine Gale diagrams are equivalent when one can be obtained from the other by*

- *Pulling a row of dots from the bottom of the diagram, changing the color of every dot, inserting it on top of the pile*
- *Turning the pile upside down, reversing the order of the rows.*

Repeatedly applying these two rules we break the 32 *affine Gale duals into the* 4 *equivalence classes listed in Table 2.1.*

Example 2.34 illustrates classifications in low corank are possible and useful, but tedious and best left to a computer, which is just how we produced the Tables in B.

2.3. Realized Acyclic orientations and f-monotone paths

We now focus on coherent f-monotone paths. This is a level of detail which we have not previously used and requires working directly with functions f rather than the sign vectors of valuations of f. In Definition 2.22 we noted that pointed zonotopes (Z, v) and hyperplane arrangements $(\mathcal{A}, c)$ realize acyclically oriented matroids $(\mathcal{M}, (+)^n)$. Specification of a chamber of c, or vertex of v, was equivalent to specifying maximal covector of $\mathcal{M}(V)$, which we could assume was $(+)^n$ without loss of generality. Chambers of $\mathcal{A}$, vertices of $Z(\mathcal{A})$, and maximal covector of $\mathcal{M}(\mathcal{A})$ are all sign vectors of valuations of f on V. When the vertex v of $Z(V)$ is the sign vector of a valuation of the functional f on V, an f-monotone path is a gallery (Z, v).

DEFINITION 2.35. *Given Z, a d-dimensional, centrally symmetric zonotope and $f \in \left(\mathbb{R}^d\right)^*$, function on Z, we say the pair (Z, f) is a* generic function on Z *if f is non-constant on every edge of Z.*

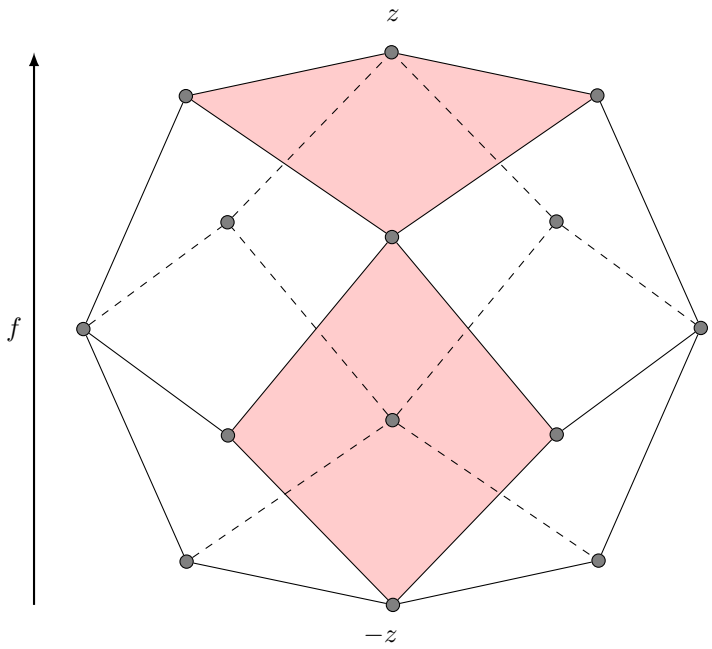

FIGURE 2.6. A cellular string of (Z, f)e.

Equivalently, when $Z = Z(V)$, f is generic when $f(v_i) > 0$ for all $v_i \in V$, so f realizes the acyclic orientation on $\mathcal{M}(V)$.

A generic functional on a zonotope is directly analogous to an acyclically oriented matroid, a pointed zonotope, or a pointed hyperplane arrangement and allows us to define a cellular string of (Z, f).

DEFINITION 2.36. *For $(Z(V), f)$ a generic function on Z with $-v$ and v being the f-minimal and f-maximal vertices of Z a* cellular string $\sigma = \sigma_1|\sigma_2|\dots|\sigma_m$ *is disjoint union of V with each block σ_i being a zonotopal face $Z(\sigma_i)$ of $Z(V)$ in which adjacent faces intersect in a single vertex $Z(\sigma_i) \cap Z(\sigma_{i+1}) = v_i$ for $1 \leq i < m$ and with*

- $-v \in Z(\sigma_1)$,
- $v \in Z(\sigma_m)$,
- $f(-v) < f(v_1) < \cdots < f(v_m) < f(v)$.

It is clear that any cellular string of Definition 2.9 is a cellular string of Definition 2.36 and we say (Z, f) realizes (Z, v) or $(\mathcal{A}, c)$. In this realization, k-faces of $Z(V)$ correspond to corank k covectors of $\mathcal{M}(V)$. The realization f of $(+)^n$ allows us to reinterpret the condition $\sigma_i \circ (-)^n = \sigma_{i+1} \circ (+)^n$ as a series inequalities. We now define f-monotone paths as and f-monotone flips in an analogous way.

DEFINITION 2.37. *Given (Z, f) a generic function on Z a* f-monotone path γ *is a cellular string in which each cell is a single vector of V. This nice case of a cellular string can be expressed as an*

ordering of vertices $(v_0, \cdots, v_n)$ of Z so that v_i and v_{i+1} share an edge of Z and which are f-monotone in the sense that

$$f(v_0) < f(v_1) < \cdots < f(v_n).$$

Note that v_0 must be f-minimal vertex of Z and v_n is the f-maximal vertex of Z.

DEFINITION 2.38. *Given (Z, f) a generic function on Z a* flip *X_F is a cellular string $\sigma_1 | \cdots | \sigma_{n-1}$ in which a distinguished cell $F = \sigma_i$ is a face of $Z(V)$ of dimension 2 and all other cells are contain a single vector of V. We say that galleries γ and γ' are adjacent by a flip X when both γ and γ' are both refinements of X_F and sometimes refer to X_F simply as F.*

DEFINITION 2.39. *For (Z, f) a generic function on Z, an f-monotone path γ is* coherent *if there exists a $g \in \left(\mathbb{R}^d\right)^*$ which selects γ in the sense*

$$\frac{g(a_{\gamma(1)})}{f(a_{\gamma(1)})} < \cdots < \frac{g(a_{\gamma(n)})}{f(a_{\gamma(n)})}.$$

It is cumbersome to write $g(v_i)$ repeatedly, so often use shorthand for valuations of functions on V. We will write $g_i = g(a_i)$ and use $g^* = (g_1, \ldots, g_n) \in \mathbb{R}^n$ to refer to the valuation of g on V. When a g exists making an f-monotone path γ coherent, we say that $\{g_i\}$ are γ ordered. When there are no $\{g_i\}$ we say that γ is incoherent in $\mathcal{A}$ for f.

We visualize a coherent f-monotone path γ on Z by projecting $\mathbb{R} \to \mathbb{R}^2$ via the map $x \to (f(x), g(x))$; the f-monotone paths which are coherent are those which appear on boundary of Z for some projection. The incoherent f-monotone paths are the paths which wrap around Z to such an extent that no projection places them on the boundary.

EXAMPLE 2.40. *Continuing with the vector configuration last seen in Example 2.25 we recall that*

$$V = \begin{array}{c} \begin{matrix} v_1 & v_2 & v_3 \end{matrix} \\ \begin{pmatrix} 1 & 0 & 1 \\ 0 & 1 & 1 \end{pmatrix} \end{array}.$$

We realize the acyclic orientation $(+)^n$ of $\mathcal{M}(V)$ using $f(x, y) = x + y$ and draw in Figure 2.7. There are two f-monotone paths of (Z, f), $\gamma = 132$ and $\gamma' = 231$, which are the upper and lower faces of Z. We make γ and γ' explicitly coherent by finding $g(x, y) = -x + y$ and $h(x, y) = x - y$ and checking

$$\frac{g_1}{f_1} = \frac{-1}{1} < \frac{g_3}{f_3} = \frac{0}{1/2} < \frac{g_3}{f_3} = \frac{1}{1}, \text{ and}$$
$$\frac{h_2}{f_2} = \frac{-1}{1} < \frac{h_3}{f_3} = \frac{0}{1/2} < \frac{h_1}{f_1} = \frac{1}{1}.$$

In addition to γ and γ' being coherent the unique flip X_{132} is also coherent and picked out by $g(x, y) = 0$. Every cellular string of (Z, f) is coherent, so this is our first example of what we will later define as all-coherent *(see Definition 3.1.*

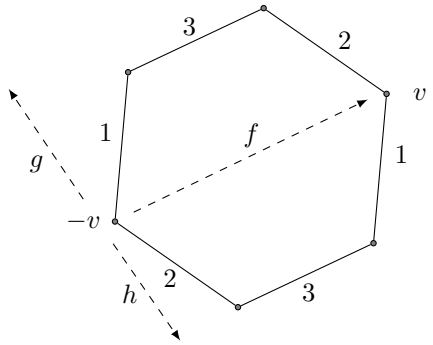

FIGURE 2.7. Pointed zonotope from Example 2.40 with g and h shown.

We can extend the definition of coherent to cellular strings of (Z, f). Cellular strings are coherent when there is a linear functional g selecting all the zonotopal faces of σ.

DEFINITION 2.41. *For $(Z(V), f)$ a generic function on Z, a cellular string $\sigma_1|\sigma_2|\dots|\sigma_m$ of $(Z(V), f)$, with V ordered so that*

$$\sigma = \underbrace{\{v_1, \dots, v_{|\sigma_1|}\}}_{\sigma_1} \Bigg| \cdots \Bigg| \underbrace{\left\{v_{\left(1+\sum_{i=1}^{k-1}|\sigma_i|\right)}, \dots, v_{\left(\sum_{i=1}^{k}|\sigma_i|\right)}\right\}}_{\sigma_k} \Bigg| \cdots \Bigg| \underbrace{\{v_{1+n-|\sigma_{n-m}|}, \dots, v_n\}}_{\sigma_{n-m}}$$

σ is coherent *if there exists a $g \in \left(\mathbb{R}^d\right)^*$ which selects σ in the sense that*

$$\underbrace{\frac{g_1}{f_1} = \cdots = \frac{g_{|\sigma_1|}}{f_{|\sigma_1|}}}_{\sigma_1} < \cdots < \underbrace{\frac{g_{\left(1+\sum_{i=1}^{k-1}|\sigma_i|\right)}}{f_{\left(1+\sum_{i=1}^{k-1}|\sigma_i|\right)}} = \ldots = \frac{g_{\left(\sum_{i=1}^{k}|\sigma_i|\right)}}{f_{\left(\sum_{i=1}^{k}|\sigma_i|\right)}}}_{\sigma_k} < \cdots < \underbrace{\frac{g_{n-|\sigma_{n-m}|+1}}{f_{n-|\sigma_{n-m}|+1}} = \cdots = \frac{g_n}{f_n}}_{\sigma_{n-m}}$$

To show that an f-monotone path γ or cellular string σ is coherent we must find a function g which selects γ; Using Section 2.2 we understand galleries of $(Z(V), v)$ with the dual V^*. We extend this understanding to coherence of f-monotone paths. Functionals on V are linear dependencies on V^*, so we coherence of an f-monotone path is a linear dependence which must satisfy inequalities.

LEMMA 2.42. *An f-monotone path γ is coherent for f if and only if there exist a linear dependence $\sum_{i=1}^{n} g_i a_i^* = 0$ with $(g_1, \dots, g_n) \in \mathbb{R}^n$ such that*

$$\frac{g_{\gamma(1)}}{f_{\gamma(1)}} < \cdots < \frac{g_{\gamma(n)}}{f_{\gamma(n)}}$$

This lemma has an extension to coherent cellular strings which we omit because of the complex notation involved in coherent cellular string. The statement of the Lemma for cellular strings and the proof are unsurprising. We also note that after Lemma 4.16 we will be able to prove coherence of a cellular string by proving coherence of a cellular string σ by proving coherence of any gallery γ which refines σ.

PROOF. This proof is an exercise in duality. To begin we will show that if γ is coherent and let g be a functional which selects γ; define $g_i = g(a_i)$ satisfy Definition 2.39. We then know that

$$\frac{g_{\gamma(1)}}{f_{\gamma(1)}} < \cdots < \frac{g_{\gamma(n)}}{f_{\gamma(n)}}$$

while duality tells us that

$$\sum_{i=1}^{n} g_i a_i^* = 0.$$

We conclude that if γ is coherent, there exist the desired $\{g_i\}$. For the reverse, suppose there are $\{g_i\}$ which satisfy Equation 2.39. By assumption we have

$$\frac{g_{\gamma(1)}}{f_{\gamma(1)}} < \cdots < \frac{g_{\gamma(n)}}{f_{\gamma(n)}}.$$

Since $\sum_{i=1}^{n} g_i a_i^* = 0$ we know there exists $g \in \left(\mathbb{R}^d\right)^*$. □

We close with the reminder that *galleries* depend only the pointed zonotope (Z, v), while *coherent galleries* depend on which f realizes v. Coherent f-monotone paths of (Z, f) with coherent flips form a subgraph of the monotone path graph, which is equal to the graph $G_2(Z, v)$ when $Z = Z(V)$ and f realizes the covector corresponding to v. What is not yet clear is how the choice of f dictates which galleries of (Z, v) correspond to coherent f-monotone paths.

DEFINITION 2.43. *Given (Z, f) a generic function on $Z = Z(V)$ a with $-v$ and v being the f-minimal and f-maximal vertices of Z, the* monotone path graph *is the graph whose vertices are all f-monotone paths of (Z, f) in which two f-monotone paths are adjacent when they differ by a flip X_F.*

The monotone path graph of (Z, f) is equal to the graph $G_2(Z, v)$ when (Z, f) realizes (Z, v). We draw the distinction between f-monotone paths and galleries thus: f-monotone paths may be coherent (for a particular f) however galleries cannot be coherent, lacking any reference to f.

CHAPTER 3

Interlude

This chapter serves as a brief interlude with three functions before diving into our theoretical tools . First, it is a chance to summarize the background material we have just completed. Second, it serves as an entry point for readers with a background in oriented matroids. Third, and most importantly, it is an opportunity focus on the several specific problems and give a few new definitions which did not fit into the background material.

Our presentation so far has moved from oriented matroids, to vector configurations and hyperplane arrangements, and finally to zonotopes with a generic linear functional f. At each step along we have defined a gallery-like object, a flip between gallery-like objects, and a graph whose vertices are gallery-like objects and edges are flips.

We now discuss the monotone path graph and $G_2(Z, v)$ in greater detail. We first review the key definitions of galleries and f-monotone paths. We then focus on the monotone path graph and its distinguished subgraph of *coherent* f-monotone paths and *coherent* flips drawing attention to the special cases of monotone path graphs in which every f-monotone path is coherent. We reverse our presentation and work inductively from the specific setting of generic functionals on zonotopes to the general setting of acyclically oriented matroids. We make several key definitions including *all-coherent*, *universally all-coherent*, and *L_2-accessible* which will guide the rest of our work. All of our examples thus far have been rank 2 to illustrate key ideas and we now allow ourselves to discuss more examples in rank 3 and above to illustrate more interesting behavior.

The three levels of generality we have worked with so far are

(1) (Most Specific) The pair (Z, f) is a *zonotope with a generic linear functional* f. Equivalently, f is generic on $Z(V)$ when $f(v_i) > 0$ for all $v_i \in V$ (or generic on $\mathcal{A}$ when $f_{a_i} > 0$ for all $a_i \in \mathcal{A}$.

An *f-monotone path* of (Z, f) is a path from the f-minimal vertex $-v$ to the f-maximal vertex v on the edges of Z, which is f-monotone in the sense of Definition 2.37. f-monotone paths are coherent when selected by a functional $g \in \left(\mathbb{R}^d\right)^*$ (see Definition 2.39). The set of all f-monotone paths are the vertices of the monotone path graph, whose edges are flips across faces of Z.

(2) (Intermediate) When $v = \sum v_i$ is the f-maximal vertex of $Z = Z(V)$ the pair (Z, v) is a *pointed zonotope* (or, equivalently, for the chamber c corresponding to v, a pointed hyperplane arrangement $(\mathcal{A}, c)$) and a *gallery* of (Z, v) is a path from $-v$ to v of minimal length (see

Definition 2.22). Galleries of (Z, v) correspond to f-monotone paths of (Z, f); when (Z, f) realizes (Z, v) a gallery of (Z, v) is an f-monotone path of (Z, f). The galleries of (Z, v) are the vertices of the graph $G_2(Z, v)$ and $G_2(\mathcal{A}, c)$.

At this level of generality we talk about the intersection lattice $L(\mathcal{A}) = \bigsqcup L_k(\mathcal{A})$ of $\mathcal{A}$. The elements X of $\in L_k(\mathcal{A})$ are k-dimensional subspaces which are intersections of hyperplanes in $\mathcal{A}$. Every corank k covector of $\mathcal{M}(\mathcal{A})$ gives rise to an element X of $L_k(\mathcal{A})$, but an element X of $L_k(\mathcal{A})$ does not uniquely determine a covector of $\mathcal{M}(\mathcal{A})$. Flips between galleries are cellular strings σ with a distinguished non-trivial cell σ_k of corank 2, and all other cells of corank 1. For ease of notation we will often refer to X, the element of $L_2(\mathcal{A})$ rather than σ.

(3) (Most General) The face lattice of $Z(V)$ defines the oriented matroid structure of $\mathcal{M} = \mathcal{M}(V)$ and the choice of v gives $\mathcal{M}(V)$ an acyclic orientation. We say that the pair $(\mathcal{M}, (+)^n)$ is an *acyclically oriented matroid* and its *galleries* and *cellular strings* are defined in Definitions 2.9 and 2.10. The galleries of $(\mathcal{M}(V), (+)^n)$ are galleries of (Z, v) when (Z, v) realizes $(\mathcal{M}(V), (+)^n)$. The galleries of $G_2(\mathcal{M}, (+)^n)$ are the vertices of the graph $G_2(\mathcal{M}, (+)^n)$ and two galleries are adjacent when they differ by cellular string with a single distinguished cell of corank 2.

All of Chapter 2 was devoted to defining the basic objects of generic functions on zonotopes, pointed zonotopes and pointed hyperplane arrangements, and acyclically oriented matroids. From these objects we defined galleries, monotone path graphs, coherent f-monotone paths, flips, cellular strings, etc... We add to these definitions with two new definitions which apply to the pairs themselves.

DEFINITION 3.1. *A zonotope with a generic linear functional is* all-coherent *if every cellular string of* (Z, f) *is* coherent.

We saw an all-coherent pair (Z, f) in Example 2.40. We will later prove Lemma 4.16 which says that every cellular string will be coherent when every f-monotone path is coherent. If we prove that every $(Z(V), f)$ which realizes the pair (Z, v) is all-coherent we will call (Z, v) universally all coherent.

DEFINITION 3.2. *The pair* (Z, v)*, a pointed zonotope is* universally all-coherent *if every gallery of* (Z, v) *is a coherent* f*-monotone path for every* (Z, f) *realizing* (Z, v).

We have not discussed it in detail, however Example 2.40 is universally all-coherent because it is of corank 2. Lest we give the impression that all pointed vector configurations are universally all-coherent we now give our first example with *incoherent* f-monotone paths, which also serves to illustrate the interplay of our 3 levels of abstraction.

EXAMPLE 3.3. *We consider $\mathcal{A}$ to the corank 1 hyperplane arrangement consisting of 4 hyperplanes in $\mathbb{R}^3$, in which $\mathcal{A}^*$ has exactly 2 negative vectors. We specify $\mathcal{A}$ and $\mathcal{A}^*$ as*

$$\mathcal{A} = \begin{array}{c} \begin{matrix} a_1 & a_2 & a_3 & a_4 \end{matrix} \\ \begin{pmatrix} 1 & 0 & 0 & 1 \\ 0 & 1 & 0 & 1 \\ 0 & 0 & 1 & -1 \end{pmatrix} \end{array}, \qquad \mathcal{A}^* = \begin{array}{c} \begin{matrix} a_1^* & a_2^* & a_3^* & a_4^* \end{matrix} \\ \begin{pmatrix} -1 & -1 & 1 & 1 \end{pmatrix} \end{array}.$$

The functional $f(x,y,z) = x+y+z$ is maximized at the point $(2,2,0)$ corresponding to the covector $+++-$. We can check that $\gamma = 1423$ is a gallery of $\mathcal{A}$ using each definition independently.

To check that $\gamma = 1423$ is a gallery of the acyclically oriented matroid $(\mathcal{M}(\mathcal{A}),(+)^n)$ we use Definition 2.10 and find covectors $(0--,+-0,+0-,++0)$ of $\mathcal{M}(\mathcal{A})$. While the set $\mathcal{C}^* \subset \mathcal{V}^*$ of covectors is longer than we are willing to list here, we can easily check that each element in the sequence for $\gamma^{(i)}$ is a covector using $\mathcal{A}^*$

To check that $\gamma = 1423$ is a gallery of $(\mathcal{A},c)$, we use Definition 2.22 and simply notice that each chamber listed for γ is a vertex of $Z(\mathcal{A})$, and we can check that they are adjacent in $Z(\mathcal{A})$ by using duality, checking that $0--,+-0,+0-,++0$ are still covectors of $\mathcal{A}$.

Finally, to check that $\gamma = 1423$ is a f-monotone path of (Z,f) we use Definition 2.37. We give coordinates to the vertices of $Z(\mathcal{A})$:

$$\begin{aligned} v_0 &= ---- = (-2,-2,0), \\ v_1 &= +--- = (0,-2,0), \\ v_2 &= +--+ = (2,0,-2), \\ v_3 &= ++-+ = (2,2,-2), \\ v_4 &= +++- = (2,2,0). \end{aligned}$$

We evaluate f on each of these vertices and find $(f(v_i)) = (-4,-2,0,2,4)$ so this is an f-monotone path.

For $f(x,y,z) = x+y+z$ the f-monotone path 1423 is incoherent. Suppose that $g(x,y,z) = Ax+By+Cz$ selects γ, then we would have

$$A < A+B-C < B < C$$

but $B-C<0$ so $A+B-C<A$ which contradicts $A<A+B-C$. We will explore this example further in Section 5.3.

The function $f(x,y,z) = 3x+2y+z$ also makes (Z,f) realize (Z,v) since $f(a_i)>0$. The f-monotone path 1423 is coherent because the functional $g(x,y,z) = -33x+34y+31z$ selects it in the sense that

$$\frac{g_1}{f_1} = \frac{-33}{3} < \frac{g_4}{f_4} = \frac{-32}{4} < \frac{g_2}{f_2} = \frac{34}{2} < \frac{g_3}{f_3} = \frac{31}{1}$$

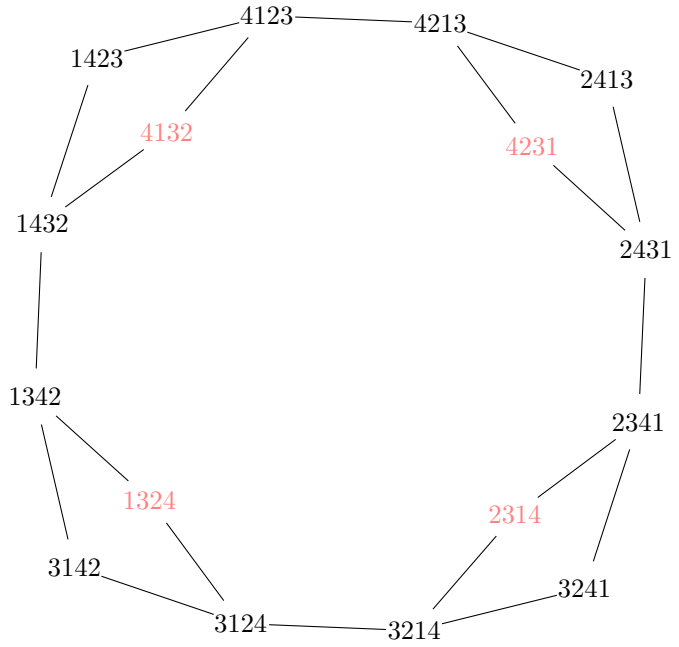

FIGURE 3.1. The monotone path graph for $f(x, y, z) = 3x + 2y + z$ with incoherent f-monotone paths in red.

We can check computationally that $\{1324, 2314, 4132, 4231\}$ *is a complete list of incoherent galleries for* $f(x, y, z) = 3x + 2y + z$*. The monotone path graph of* (Z, f) *is shown in Figure 3.1 with incoherent galleries drawn in red.*

Curiously, $h(x, y, z) = -30x + 36y + 32z$ *also make* γ *coherent since*

$$\frac{g_1}{f_1} = \frac{-30}{3} < \frac{g_4}{f_4} = \frac{-38}{4} < \frac{g_2}{f_2} = \frac{36}{2} < \frac{g_3}{f_3} = \frac{32}{1}.$$

The choice of g in Example 3.3 is important. The g which selects γ is not unique and how we pick g_i will be fundamental to most of our arguments, so we pause briefly to understand the flexibility we have in the choice of $\{g_i\}$.

LEMMA 3.4. *Given* $(Z(\mathcal{A}), f)$*, a zonotope with a generic functional* f *and an* f*-monotone path* γ*, if* $h_1, \ldots, h_n$ *satisfy*

$$\frac{h_{\gamma(1)}}{f_{\gamma(1)}} < \cdots < \frac{h_{\gamma(n)}}{f_{\gamma(n)}} \text{ and}$$
$$\sum h_i a_i^* = 0$$

then for any B and any $0 < A$, $g_i = Ah_i + Bf_i$ satisfies

$$\frac{g_{\gamma(1)}}{f_{\gamma(1)}} < \cdots < \frac{g_{\gamma(n)}}{f_{\gamma(n)}} \text{ and}$$
$$\sum g_i a_i^* = 0.$$

PROOF. Suppose h_i satisfies

$$\frac{h_{\gamma(1)}}{f_{\gamma(1)}} < \cdots < \frac{h_{\gamma(n)}}{f_{\gamma(n)}} \text{ and}$$
$$\sum h_i a_i^* = 0$$

then we must check that $\sum_{i=1}^{n} (Ah_i + Bf_i)\, a_i^* = 0$. We compute this directly

$$\begin{aligned}\sum_{i=1}^{n}(Ah_i + Bf_i)a_i^* &= \sum_{i=1}^{n} Ah_i a_i^* + \sum Bf_i a_i^* \\ &= A\sum_{i=1}^{n} h_i a_i^* + B\sum_{i=1}^{n} f_i a_i^* \\ &= A \cdot 0 + B \cdot 0 = 0.\end{aligned}$$

We must also check that $(Ah_i + Bf_i)$ is γ monotone. We see that for any $\frac{h_i}{f_i} < \frac{h_k}{f_k}$ we have

$$\begin{aligned}\frac{g_i}{f_i} = \frac{Ah_i + Bf_i}{f_i} &= \frac{Ah_i}{f_i} + B \\ &< \frac{Ah_k}{f_k} + B = \frac{Ah_k + Bf_k}{f_k} = \frac{g_k}{f_k}.\end{aligned}$$

□

COROLLARY 3.5. *For any coherent f-monotone path γ of (Z, f), we may pick $\{g_i\}$ which realize the coherent of γ so that:*

- *for any bound C, $g_i < C$ for all i (or, symmetrically $C < g_i$), and*
- *we may scale $\{g_i\}$ so that $|g_i - g_j| = \delta$ for specific i, j and any $\delta > 0$.*

PROOF. Since γ is a coherent f-monotone path we know there must exist $\{h_i\}$ which satisfy

$$\frac{h_{\gamma(1)}}{f_{\gamma(1)}} < \cdots < \frac{h_{\gamma(n)}}{f_{\gamma(n)}} \text{ and}$$
$$\sum h_i a_i^* = 0$$

Given any C, we will use Lemma 3.4 to pick A and B making $g_i < C$ for all i. Pick $A = 1$ and $B < \frac{C-h_i}{f_i}$ for all i, define $g_i = h_i + Bf_i$ so that

$$g_i = h_i + Bf_i < h_i + \left(\frac{C - h_i}{f_i}\right) f_i = h_i + C - h_i = C$$

To scale we use Lemma 3.4 with $A = \delta / |g_i - g_j|$ to make $|g_i - g_j| = \delta$ for any $\delta > 0$. □

We now describe the subgraph of coherent f-monotone paths in the monotone path graph. These subgraphs are induced by all the coherent galleries and equal to the 1 skeleton of the *fiber zonotope* of the projection $f : Z(\mathcal{A}) \to \mathbb{R}$. The fiber zonotope is a particular fiber polytope [**BS92**] which generalizes the secondary polytopes of [**GKZ94**]. Although we will not give the full details of fiber zonotopes here, we will refer the reader to Chapter 9 of [**Zie95**] and [**BS92**]. We give an explicit construction of the fiber zonotope restated in a manner which will be useful to us [**BS92**], [**RR12**].

DEFINITION 3.6. *The* fiber zonotope *of the projection $f : Z(\mathcal{A}) \to \mathbb{R}$ is the $n - d$ dimensional zonotope $Z(\mathcal{A}')$ generated by the vectors*

$$\mathcal{A}' = \{v_{ij} \mid \textit{where } v_{ij} = f(v_i)v_j - f(v_j)v_i\} \textit{ and } 1 \leq i < j \leq n.$$

The vertices of fiber zonotope correspond to coherent f-monotone paths and any cellular string on $Z(\mathcal{A}')$ is a coherent cellular string of (Z, f). The 1-skeleton of $Z(\mathcal{A}')$ will be the subgraph of the monotone path graph consisting of all coherent f-monotone paths.

EXAMPLE 3.7. *We will continue Example 3.3 in the context of the fiber zonotope. Recall that* $\mathcal{A}^* = \begin{pmatrix} -1 & -1 & 1 & 1 \end{pmatrix}$. *For* $f(x, y, z) = 3x + 2y + z$ *we find* $\{v_{ij}\}$.

$$v_{12} = \begin{pmatrix} -2 \\ 3 \\ 0 \end{pmatrix} \quad v_{13} = \begin{pmatrix} -1 \\ 0 \\ 3 \end{pmatrix} \quad v_{14} = \begin{pmatrix} -1 \\ 3 \\ -3 \end{pmatrix}$$
$$v_{23} = \begin{pmatrix} 0 \\ -1 \\ 2 \end{pmatrix} \quad v_{24} = \begin{pmatrix} 2 \\ -1 \\ -2 \end{pmatrix} \quad v_{34} = \begin{pmatrix} 1 \\ 1 \\ -5 \end{pmatrix}.$$

When we construct the Zonotope of $\{v_{ij}\}$ we obtain a polytope whose 1-skeleton we can embed in the monotone path graph of $\mathcal{A}$. We have already seen this monotone path graph in Example 3.3 and illustrated it Figure 3.1 where the vertices corresponding to $Z\mathcal{A}'$ are the black, coherent f-monotone paths.

The major results of this dissertation are that, in coranks 1 and 2,

- (Z, v) being universally all-coherent depends only on $(\mathcal{M}, (+)^n$, and
- when (Z, v) is not universally all-coherent every (Z, f) realizing (Z, v) contains at least one incoherent gallery.

The final definitions of this Chapter are taken from [**RR12**] which we will use for our diameter computation in corank 1.

DEFINITION 3.8. *For a pointed hyperplane arrangement $(\mathcal{A}, c)$, the L_2 separation set of galleries γ and γ' is the set of elements $X \in L_2(\mathcal{A})$ in which γ and γ' differ. That is, given a path $(\gamma = \gamma_0, \gamma_1, \ldots, \gamma_k = \gamma')$ the separation set*

$$L_2(\gamma, \gamma') = \{X_i | \quad \gamma_{i-1} \text{ and } \gamma_i \text{ are adjacent by the flip } X_i\}$$

Remarkably $L_2(\gamma, \gamma')$ is well-defined and does not depend on the path in $G_2(\mathcal{A}, c)$ [**RR12**, Example 3.3]. *It is important to note that $X \in L_2(\mathcal{A})$ is the codimension 2 subspace of $\mathbb{R}^d$ corresponding to the flip between γ_{i-1} and γ_i and* not *a cellular string. The separation $L_2(\gamma, \gamma')$ is only well-defined on $L(\mathcal{A})$, not on $L(\mathcal{M})$.*

Its not hard to see that the graph distance $d_{G_2(\mathcal{A},c)}(\gamma, \gamma') \geq L_2(\gamma, \gamma')$ for all $\gamma, \gamma' \in \Gamma(\mathcal{A}, c)$. For a fixed gallery γ, when the standard graph distance $d(\gamma, \gamma')$ equals the L_2-separation for every γ', we say that γ is L_2-accessible.

DEFINITION 3.9. *A gallery γ of $G_2(\mathcal{A}, c)$ is* L_2-accessible *when $d_G(\gamma, \gamma') = |L_2(\gamma, \gamma')|$ for every $\gamma' \in G_2(\mathcal{A}, c)$.*

The graph $G_2(\mathcal{A}, c)$ is nicely symmetric with an involution from γ to its reversal, so L_2-accessibility is the key for the following proposition from [**RR12**, Proposition 3.12].

PROPOSITION 3.10. *If $G_2(\mathcal{A}, c)$ contains an L_2-accessible vertex γ, then the diameter of $G_2(\mathcal{A}, c)$ is exactly $|L_2(\mathcal{A})|$.*

In the case of corank 1, Theorem 5.10 shows that a particular gallery of $G_2(\mathcal{A}, c)$ is L_2-accessible and proves that the diameter of $G_2(\mathcal{A}, c)$ equals $|L_2|$.

CHAPTER 4

Five Useful Lemmas

We are now ready to provide the new theoretical tools of this thesis. In this Chapter, we use the definitions presented in Sections 2 and 3 to prove 5 new lemmas. Our lemma are essential to understanding coherent, incoherent, and L_2-accessible galleries of single-element liftings, single-element extensions, and disjoint unions. The central question of these lemmas is: when does $G_2(\mathcal{A}, c)$ contain incoherent f-monotone paths. All lemmas will be illustrated with examples as well as interesting special cases and counter-examples. We in particular draw the reader's attention to Example 4.10 which serves as cautionary tale. Lemma 4.16 also deserves some attention and might surprise readers with some knowledge of regular triangulations.

4.1. The Product Lemma

Our first lemma is about the f-monotone paths of $\mathcal{A}$, when $\mathcal{A} = \mathcal{A}_1 \sqcup \mathcal{A}_2$ is a disjoint union of hyperplanes. Disjoint unions aren't enough to classify hyperplane arrangements but the intuition provided by disjoint unions serves us well. We describe the structure of $G_2(\mathcal{A}_1 \sqcup \mathcal{A}_2, (c, c'))$ explicitly in terms of $G_2(\mathcal{A}_1, c)$ and $G_2(\mathcal{A}_2, c')$ in Lemma 4.8. As an immediate corollary, we will be able to find L_2-accessible galleries when both $\mathcal{A}_1$ and $\mathcal{A}_2$ have L_2 accessible galleries. We will later return to disjoint unions in Corollary 5.8 and describe when $\mathcal{A}$ has incoherent f-monotone paths in terms of $\mathcal{A}_1$ and $\mathcal{A}_2$.

DEFINITION 4.1. *Given hyperplane arrangements $\mathcal{A}$ consisting of n hyperplanes in $\mathbb{R}^d$ and $\mathcal{A}'$ consisting of n' hyperplanes in $\mathbb{R}^{d'}$, the* disjoint union $\mathcal{A} \bigsqcup \mathcal{A}'$ *is the arrangement of $n + n'$ hyperplanes in $\mathbb{R}^{d+d'}$ formed by embedding $\mathbb{R}^d$ in $\mathbb{R}^{d+d'}$ as the first d coordinates and $\mathbb{R}^{d'}$ in $\mathbb{R}^{d+d'}$ as the last d' coordinates. We say that a hyperplane arrangement is* reducible *when it can be written as $\mathcal{A} \bigsqcup \mathcal{A}'$ for some $\mathcal{A}, \mathcal{A}'$ in $\mathbb{R}^d, \mathbb{R}^{d'}$ and* irreducible *when there are no such $\mathcal{A}$ and $\mathcal{A}'$. When $\mathcal{A}$ or $\mathcal{A}'$ is a single vector a_{n+1} in $\mathbb{R}^1$ we say a_{n+1} is an* isthmus.

We remark that $\mathcal{A}$ is reducible when it can be written as a block matrix and functionals $\widehat{f} : \mathbb{R}^{d+d'} \to \mathbb{R}$ can be decomposed into two functions $f_1 : \mathbb{R}^d \to \mathbb{R}$ and $f_2 : \mathbb{R}^{d'} \to \mathbb{R}$ with $\widehat{f}(x, x') = f_1(x) + f_2(x')$. We ask: what is the structure of $Z(\mathcal{A} \sqcup \mathcal{A}')$ in terms of $Z(\mathcal{A})$ and $Z(\mathcal{A}')$. Isthmuses are an important

example of this because the dual of an isthmus is the zero vector. When $\mathcal{A}'$ is an isthmus, we have:

$$\left(\mathcal{A} \bigsqcup \mathcal{A}'\right)^* = \mathcal{A}^* \cup \left\{ \begin{pmatrix} 0 \\ \vdots \\ 0 \end{pmatrix} \right\}.$$

EXAMPLE 4.2. *Our first example of disjoint unions is an isthmus, in which $\mathcal{A}'$ is a single hyperplane in $\mathbb{R}^1$, and $\mathcal{A}$ is the arrangement of 3 hyperplanes in $\mathbb{R}^2$ from Example 2.15. We embed both $\mathcal{A}$ and $\mathcal{A}'$ into $\mathbb{R}^3$ as*

$$\mathcal{A} = \begin{array}{c} \begin{matrix} a_1 & a_2 & a_3 \end{matrix} \\ \begin{pmatrix} 1 & 0 & 1 \\ 0 & 1 & 1 \\ 0 & 0 & 0 \end{pmatrix} \end{array}, \quad \textit{and} \quad \mathcal{A}' = \begin{array}{c} \begin{matrix} a_4 \end{matrix} \\ \begin{pmatrix} 0 \\ 0 \\ 1 \end{pmatrix} \end{array}.$$

We draw attention to $a^*_{n+1} = 0$, the dual of a_{n+1}. The zonotope $Z(\mathcal{A}')$ is simple; it is the line segment. The zonotope $Z(\mathcal{A})$ is already familiar to us from Example 2.25 and consists of 6 vertices and 6 edges arranged as a hexagon in $\mathbb{R}^2$. The zonotope $Z(\mathcal{A} \sqcup \mathcal{A}')$ has 12 vertices and 18 edges; it is a prism with a hexagonal base, as illustrated in Figure 4.1.

This motivates Lemma 4.3, which identifies $Z(\mathcal{A} \sqcup \mathcal{A}')$ as the Cartesian product of $Z(\mathcal{A})$ and $Z(\mathcal{A}')$. While $Z(\mathcal{A})$ is a polytope, we state our lemma in purely graph theoretic terms. A zonotope version will also be true but we limit our attention to the 1-skeleton to use Definition 2.37.

Before we state Lemma 4.3, we remind the reader of the graph theoretic notion of a Cartesian product [**HIK11**]. Given graphs G and H, the graph Cartesian product $G \square H$ is the graph with

$$V(G \square H) = V(G \square H) = V(G) \times V(H)$$

$$E(G \square H) = \left\{ ((v,w),(v',w')) \text{ with } \begin{array}{c} v = v' \text{ and } (w,w') \in E(H) \\ \text{or} \\ w = w' \text{ and } (v,v') \in E(G) \end{array} \right\}.$$

LEMMA 4.3. *If $\mathcal{A} = \{a_i, \ldots a_n\}$ and $\mathcal{A}' = \{a_{n+1}, \ldots a_{n+n'}\}$ in $\mathbb{R}^{d'}$ and $\mathbb{R}^d$, with zonotopes $Z(\mathcal{A})$ and $Z(\mathcal{A}')$ then*

$$G_1(\mathcal{A} \sqcup \mathcal{A}') = G_1(\mathcal{A}) \square G_1(\mathcal{A}').$$

PROOF. Covectors of $\mathcal{M}(\mathcal{A} \sqcup \mathcal{A}')$ are the vertices of $G_1(\mathcal{A} \sqcup \mathcal{A}')$ and have the form (c, c') in which c is a covector of $\mathcal{M}(\mathcal{A})$ and c' is a covector of $\mathcal{M}(\mathcal{A}')$. The vertex set of $V(G_1(\mathcal{A} \sqcup \mathcal{A}'))$ is then the Cartesian product $V(G_1(\mathcal{A})) \times V(G_1(\mathcal{A}'))$.

We know that two vertices (c, c') and (d, d') are adjacent in $G_1(\mathcal{A} \sqcup \mathcal{A}')$ when $|\text{sep}\,((c, c'), (d, d'))| = 1$ so $c = d$ and c' and d' are adjacent in $G_1(\mathcal{A}')$ or $c' = d'$ and c and d are adjacent in $G_1(\mathcal{A})$. Thus $G_1(\mathcal{A} \sqcup \mathcal{A}') = G_1(\mathcal{A}) \square G_1(\mathcal{A}')$. □

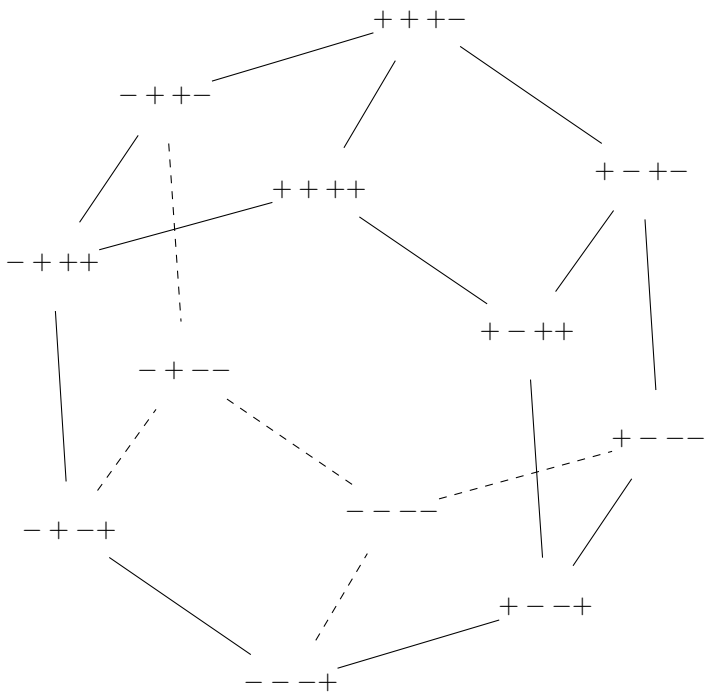

FIGURE 4.1. Zonotopes of $Z(\mathcal{A} \sqcup \mathcal{A}')$ in Example 4.2

Understanding $G_1(\mathcal{A} \sqcup \mathcal{A}')$ as a graph product gives us a way to understand the graph $G_2(\mathcal{A} \sqcup \mathcal{A}', (c, c'))$. Vertices of $G_2(\mathcal{A}, c)$ are paths on $G_1(\mathcal{A})$; we investigate how paths on $G_1(\mathcal{A} \sqcup \mathcal{A}')$ relate to paths on $G_1(\mathcal{A})$ and $G_1(\mathcal{A}')$ before proceeding to state and proving our next lemma.

EXAMPLE 4.4. *Continuing from Example 4.2 we again have*

$$\mathcal{A} = \begin{array}{c} \begin{matrix} a_1 & a_2 & a_3 \end{matrix} \\ \begin{pmatrix} 1 & 0 & 1 \\ 0 & 1 & 1 \\ 0 & 0 & 0 \end{pmatrix} \end{array} \quad \textit{and} \quad \mathcal{A}' = \begin{array}{c} \begin{matrix} a_4 \end{matrix} \\ \begin{pmatrix} 0 \\ 0 \\ 1 \end{pmatrix} \end{array}$$

Using the vertices $v = +++$ and $v' = +$ we compute $G_2(\mathcal{A} \sqcup \mathcal{A}', (v, v'))$ from $G_2(\mathcal{A}, v)$ and $G_2(\mathcal{A}', v')$. The graph $G_2(\mathcal{A}', +)$ consists of a single gallery $\gamma = 4$ and no edges. The monotone path graph of $\mathcal{A}$ consists of the two galleries $\gamma = 132$ and $\gamma' = 231$ with a single flip between them as we saw in Example 2.13.

The monotone path graph $G_2(\mathcal{A} \sqcup \mathcal{A}')$ consists of 8 galleries and 8 edges (Figure 4.2). We see that the galleries of $G_2(\mathcal{A} \sqcup \mathcal{A}', (c, c'))$ are the galleries of $G_2(\mathcal{A}, c)$ with a 4 shuffled in.

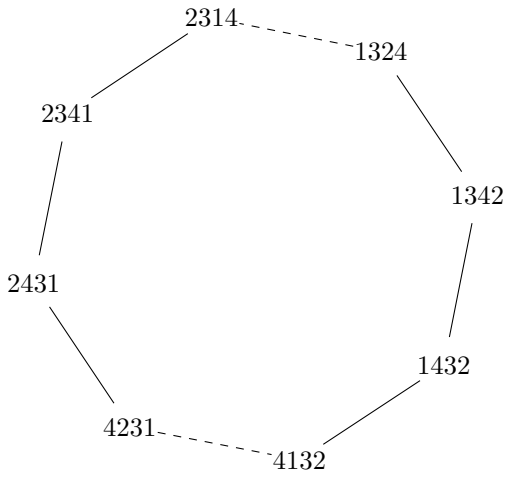

FIGURE 4.2. Monotone path graph of the disjoint union

We suspect that galleries of $(\mathcal{A} \sqcup \mathcal{A}', (c, c'))$ will be shuffles of the galleries of $(\mathcal{A}, c)$ and the galleries of $(\mathcal{A}', c')$. Shuffles are intuitive but need a precise definition that we adapt from [**Sta97**, p.70] and [**Sta99**, p.482].

DEFINITION 4.5. *A gallery $\widehat{\gamma}$ of $(\mathcal{A} \sqcup \mathcal{A}', (c, c'))$ is a shuffle of a gallery γ of $(\mathcal{A}, c)$ and γ' of $(\mathcal{A}', c')$ when both γ and γ' are subsequences of $\widehat{\gamma}$.*

Examples 4.2 and 4.4 made galleries clear using shuffle products, but did not explain the flips of $G_2(\mathcal{A}, c)$. We now give a more in-depth example to illustrate the flips.

EXAMPLE 4.6. *We extend Example 4.2 to better illustrate flips. We start with the hyperplane arrangement*

$$\mathcal{A} = \begin{array}{c} \begin{matrix} a_1 & a_2 & a_3 & a_4 \end{matrix} \\ \begin{pmatrix} 1 & 0 & 1 & 0 \\ 0 & 1 & 1 & 0 \\ 0 & 0 & 0 & 1 \\ 0 & 0 & 0 & 0 \end{pmatrix} \end{array} \quad \textit{and} \quad \mathcal{A}' = \begin{array}{c} \begin{matrix} a_5 \end{matrix} \\ \begin{pmatrix} 0 \\ 0 \\ 0 \\ 1 \end{pmatrix} \end{array}.$$

We recognize $\mathcal{A}$ from Example 4.4, so we understand $G_2(\mathcal{A}, c)$ and $\mathcal{A}'$ is an isthmus. Likewise, we know the galleries of $\mathcal{A} \sqcup \mathcal{A}'$ are galleries $G_2(\mathcal{A}, c)$ with 5 inserted. Figure 4.3 shows $G_2(\mathcal{A} \sqcup \mathcal{A}')$, with vertices colored according to how 5 was shuffled into γ. Notice that the top and bottom, where galleries take the form 5γ and $\gamma 5$, are copies of $G_2(\mathcal{A}, c)$ In this picture we see that there is an edge $X_{1,2,3}$ between 51324 and 52314 but not between 15324 and 25314 since 5 separates the 132 substring.

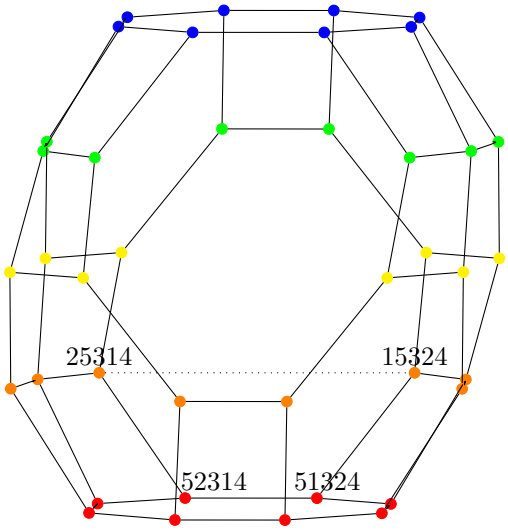

FIGURE 4.3. $G_2(\mathcal{A}, c)$ illustrating flips for shuffle products.

The flips of $\mathcal{A} \sqcup \mathcal{A}'$ are a subset of the flips of $\mathcal{A}$, the flips of $\mathcal{A}'$, and changes in the shuffle. We cannot apply flip $X_{i,\dots k}$ to γ if i and k are not adjacent in γ. This allows us to define a flip between two shuffles.

PROPOSITION 4.7. *Given two pointed hyperplane arrangements $(\mathcal{A}, c)$ and $(\mathcal{A}', c')$, a flip $X_{\widehat{\gamma}(i)\dots,\widehat{\gamma}(k)}$ of a gallery $\widehat{\gamma} = \gamma \sqcup\!\sqcup \gamma'$ for γ a gallery of $(\mathcal{A}, c)$ and γ' a gallery of $(\mathcal{A}', c')$ has one of the three following forms:*

- *A flip X from $(\mathcal{M}(\mathcal{A}), c)$ (with γ and γ' both refinements of X).*
- *A flip X from $(\mathcal{M}(\mathcal{A}'), c')$ (with γ and γ' both refinements of X).*
- *A flip $X_{i,j}$ with c_i a corank 1 covector of $\mathcal{A}$ and c_j a corank 1 covector of $\mathcal{A}'$.*

PROOF. This is clear from our understanding of the galleries of $(\mathcal{A} \sqcup \mathcal{A}', (c, c'))$. The corank two covectors of $\mathcal{A} \sqcup \mathcal{A}'$ are the corank 2 covectors of $\mathcal{A}$, the corank 2 covectors of $\mathcal{A}'$, and the new corank 2 covectors corresponding to the separation sep (c, c') of corank 1 covectors of $c \in \mathcal{M}(\mathcal{A})$ and $c' \in \mathcal{M}(\mathcal{A}')$ respectively. Cellular strings are likewise built from the cellular strings of $\mathcal{A}$ and $\mathcal{A}'$, giving flips the form described above. □

Now that we understand galleries and the flips of $(\mathcal{A} \sqcup \mathcal{A}', (c, c'))$ we have a complete description of $G_2(\mathcal{A} \sqcup \mathcal{A}', (c, c'))$.

LEMMA 4.8. *For two pointed hyperplane arrangements $(\mathcal{A}, c)$ and $(\mathcal{A}', c')$, the vertices of the graph $G_2(\mathcal{A} \sqcup \mathcal{A}', (c, c'))$ are shuffles $\widehat{\gamma} = \gamma \sqcup\!\sqcup \gamma'$ for galleries γ of $(\mathcal{A}, c)$ and γ' of $(\mathcal{A}', c')$. The edges of $G_2(\mathcal{A} \sqcup \mathcal{A}', (c, c'))$ are the flips $X_{\widehat{\gamma}(i)\dots,\widehat{\gamma}(k)}$ described in proposition 4.7*

PROOF. The proof follows the construction. Galleries of $\mathcal{A} \sqcup \mathcal{A}'$ are paths on $G_1(\mathcal{A} \sqcup \mathcal{A}')$, which are in turn shuffles of galleries of $(\mathcal{A}, c)$ and $(\mathcal{A}', c')$. Adjacency between monotone paths in $\mathcal{A} \sqcup \mathcal{A}'$ is either adjacency in $(\mathcal{A}, c)$, adjacency in $(\mathcal{A}', c')$, or a change in shuffle from between $\mathcal{A}$ and $\mathcal{A}'$. □

While the proof of Lemma 4.8 is simple, it has a important consequence. Since we understand the monotone path graph of $\mathcal{A} \sqcup \mathcal{A}'$, we can write the graph distance and the L_2 distance and understand L_2-accessibility for some galleries.

COROLLARY 4.9. *If γ is an L_2-accessible gallery in $\mathcal{A}$ and γ' is an L_2-accessible gallery in $\mathcal{A}'$ then the trivial shuffle gallery $\gamma\gamma'$ is L_2-accessible in $\mathcal{A} \sqcup \mathcal{A}'$*

PROOF. To show that $\gamma = \gamma_{\mathcal{A}}\gamma_{\mathcal{A}'}$ is L_2-accessible we must describe the separation set and the graph distance between $\gamma\gamma'$ and another gallery $\gamma' = {\gamma'}_{\mathcal{A}} \sqcup\!\sqcup \gamma_{\mathcal{A}'}$. Since both $\gamma_{\mathcal{A}}$ and $\gamma_{\mathcal{A}'}$ are L_2-accessible we know the graph distance equals the L_2 distance between $\gamma_{\mathcal{A}}$ and ${\gamma'}_{\mathcal{A}}$ as well as $\gamma_{\mathcal{A}'}$ and ${\gamma'}_{\mathcal{A}'}$.

To find a path between γ and γ' we first take the path from $\gamma_{\mathcal{A}}$ to ${\gamma'}_{\mathcal{A}}$ in $G_2(\mathcal{A}, c)$ which has graph distance equal to L_2 distance. We then take the path from $\gamma_{\mathcal{A}'}$ to ${\gamma'}_{\mathcal{A}'}$ in $G_2(\mathcal{A}')$ which also has L_2 distance equal to graph distance. Finally, we shuffle ${\gamma'}_{\mathcal{A}}\ {\gamma'}_{\mathcal{A}'}$ using a minimal number transpositions [**Sta97**]: each transposition is a flip in $G_2(\mathcal{A} \sqcup \mathcal{A}')$ and that each flip is distinct from both previous transpositions the paths in $G_2(\mathcal{A}, c)$ and $G_2(\mathcal{A}', c')$:

$$\begin{aligned}\gamma &= \gamma_{\mathcal{A}}\gamma_{\mathcal{A}'} \\ &\to {\gamma'}_{\mathcal{A}}\gamma_{\mathcal{A}'} \\ &\to {\gamma'}_{\mathcal{A}}{\gamma'}_{\mathcal{A}'} \\ &\to {\gamma'}_{\mathcal{A}} \sqcup\!\sqcup {\gamma'}_{\mathcal{A}'}.\end{aligned}$$

With an expression for distances of subpaths we can compute both the L_2 distance and the graph distance as a sum [**Dij59**]. Both the graph and L_2 distances were equal at every step so we conclude that $d(\gamma, \gamma') = d_{L_2}(\gamma, \gamma')$, so γ is L_2 accessible. □

Lemma 4.8 provides a tool to compute diameter by way of L_2-accessibility, but it is not powerful enough for coherence. The following example shows that coherence need not be preserved by disjoint unions.

EXAMPLE 4.10. *We illustrate that a shuffle of two coherent monotone paths may be incoherent. We use $f_{\mathcal{A}_1} = (1, 1, 1) = f_{\mathcal{A}_2}$ and*

$$\mathcal{A}_1 = \mathcal{A}_2 = \begin{pmatrix} 1 & 0 & 1/2 \\ 0 & 1 & 1/2 \end{pmatrix}$$

So that $f = (1, 1, 1, 1, 1, 1)$ *and*

$$\mathcal{A} = \mathcal{A}_1 \bigsqcup \mathcal{A}_2 = \begin{array}{c} \begin{matrix} a_1 & a_2 & a_3 & a_4 & a_5 & a_6 \end{matrix} \\ \begin{pmatrix} 1 & 0 & 1/2 & 0 & 0 & 0 \\ 0 & 1 & 1/2 & 0 & 0 & 0 \\ 0 & 0 & 0 & 1 & 0 & 1/2 \\ 0 & 0 & 0 & 0 & 1 & 1/2 \end{pmatrix} \end{array}.$$

Since both $\mathcal{A}_1$ *and* $\mathcal{A}_2$ *are arrangements in dimension* 2 *each arrangement only has two galleries. The* f*-monotone paths* 132 *and* 465 *of* $\mathcal{A}_1$ *and* $\mathcal{A}_2$ *respectively are both coherent and, have* 20 *shuffles, which we illustrate in Figure 5.3. We then know that the shuffle* $\gamma = 146325$ *is an* f*-monotone paths of* $\mathcal{A}_1 \sqcup \mathcal{A}_2$*, but is not coherent itself. Were* γ *coherent, there would be a function* $g(x_1, x_2, x_3, x_4) = g_1x_1 + g_2x_2 + g_3x_3 + g_4x_4$ *whose valuations would satisfying the following chain of inequalities.*

$$g_1 < g_4 < \frac{g_3 + g_4}{2} < \frac{g_1 + g_2}{2} < g_2 < g_4.$$

The left and right terms inequalities, $g_1 < g_3$ *and* $g_2 < g_4$ *imply* $g_1 + g_2 < g_3 + g_4$ *but above we have* $g_3 + g_4 < g_1 + g_2$*, a contradiction, so* γ *is incoherent.*

This example is interesting and complete enough that it can be generalized to any disjoint union, however we do not yet have all the tools necessary to deal with the proper generalization. Corollary 5.8 will extend this example to the disjoint union of arbitrary hyperplane arrangements. Disjoint unions are a good first example for inductive reasoning about monotone path graphs, however they are not enough. To work towards a classification, we will need to use the more powerful tools of single-element liftings and single-element extensions.

It is worth commenting here that working with coherence seems more subtle than L_2-accessibility. Example 1.1 indicates that coherent galleries will be more common than L_2-accessible galleries however L_2-accessibility is the primary tool we have for bounding diameter. Further, we are able to use L_2-accessibility without any reference to functional f realizing the acyclic orientation of $\mathcal{A}$. When we talk about coherence properties, we must make reference to f.

4.2. The Acyclic Orientation Liftings Lemma

Our second lemma discusses acyclic orientations and galleries of single-element liftings. We defined single-element liftings in Section 2.2 and we recall the key idea: A single-element lifting $\widehat{\mathcal{A}}$ of $\mathcal{A}$ preserves corank and when $\mathcal{A}$ consists of n vectors in $\mathbb{R}^d$, $\widehat{\mathcal{A}}$ will consist of $n + 1$ vectors in $\mathbb{R}^{d+1}$. Our goal is to understand the galleries of $(\widehat{\mathcal{A}}, \widehat{c})$ from the galleries of $(\mathcal{A}, c)$. The answer is elegant and complete; every gallery γ of $\mathcal{A}$ has exactly $n + 1$ liftings in $\widehat{\mathcal{A}}$, however not every gallery of $\widehat{\mathcal{A}}$ will be a lifting.

We begin by understanding the acyclic orientations of $\widehat{\mathcal{A}}$. This understanding of acyclic orientations of $\widehat{\mathcal{A}}$ serves double duty providing an understanding of when $\widehat{\mathcal{A}}$ has an acyclic orientation (always)

and which galleries $\widehat{\gamma}$ of $(\widehat{\mathcal{A}},\widehat{c})$ are liftings of galleries of $(\mathcal{A},c)$. Galleries are sequences of acyclic orientations of $\{\pm a_i^*\}$ and by lifting each acyclic orientation into an appropriately chosen $\widehat{\mathcal{A}}^*$ we can build galleries $\widehat{\gamma}$ in $\widehat{\mathcal{A}}^*$. We rely heavily on the notation introduced in Lemma 2.8 of $f_i = f(a_i)$.

LEMMA 4.11. *If $\widehat{\mathcal{A}}$ is a single-element lifting of $\mathcal{A}$ and f is a generic functional on $Z(\mathcal{A})$ realizing $(\mathcal{A},c)$ there is a lifting $\widehat{c}$ of c and $\widehat{f}$ of f which is generic on $Z(\widehat{\mathcal{A}})$ and realizes $(\widehat{\mathcal{A}},\widehat{c})$.*

PROOF. Since $\widehat{\mathcal{A}}$ is a single-element lifting of $\mathcal{A}$, we know that $\widehat{\mathcal{A}}^* = \{a_1^*,\ldots,a_n^*\} \cup \left\{a_{n+1}^*\right\}$ is a single-element extension of $\mathcal{A}^* = \{a_1^*,\ldots,a_n^*\}$. The function f induces an acyclic orientation on $\mathcal{A}$ so $f_i > 0$ for $1 \le i \le n$. Our goal is to find $\left\{\widehat{f}_i > 0\right\}$ for $1 \le i \le n+1$.

Since f induces an acyclic orientation on $\mathcal{A}$, we know there are strictly positive $f_i,\ldots,f_n > 0$ which satisfy $\sum f_i a_i^* = 0$. Since $\mathcal{A}$ is essential, we also know a_{n+1}^* is a linear combination of $\{a_1^*,\ldots,a_n^*\}$ so there exist $\alpha_1,\ldots,\alpha_n \in \mathbb{R}$, such that $\sum_{i=1}^n \alpha_i a_i^* - a_{n+1}^* = 0$. For some $N > \max(\{\alpha_i/f_i\} \cup \{0\})$ define

$$\widehat{f}_i = \begin{cases} f_i - \frac{\alpha_i}{N} & \text{if } 1 \le i \le n, \\ \frac{1}{N} & \text{when } i = n+1. \end{cases}$$

We claim that $\widehat{f}_i > 0$ come from some functional $\widehat{f} \in \left(\mathbb{R}^{d+1}\right)^*$, as

$$\begin{aligned} \sum_{i=1}^{n+1} \widehat{f}_i a_i^* &= \sum_{i=1}^{n} \left(f_i - \frac{\alpha_i}{N}\right) a_i^* * + \frac{1}{N} a_{n+1}^* \\ &= \sum_{i=1}^{n} f_i a_i^* + \frac{1}{N}\left(a_{n+1}^* - \sum_{i=1}^{n} \alpha_i a_i^*\right) \\ &= 0 + 0 = 0. \end{aligned}$$

Further, as $\alpha_i/f_i < N$ for any i we know that $\widehat{f}_i = \widehat{f}_i - \alpha_i/N > 0$ for $1 \le i \le n$ and since $N > 0$, $\widehat{f}_{n+1} = 1/N > 0$. This proves that:

- $\widehat{f}_i = \widehat{f}(\widehat{a}_i)$ is an acyclic orientation of $\widehat{\mathcal{A}}$,
- $\widehat{c} = (+)^{n+1}$ is a chamber of $\widehat{\mathcal{A}}$, and
- $\widehat{f}$ is generic on $\widehat{\mathcal{A}}$.

□

According to Definition 2.37 a gallery γ of $(\mathcal{A},c)$ is path on $G_1(\mathcal{A})$, each vertex of which is a maximal covector of $\mathcal{M}(\mathcal{A})$. Each maximal covector is an acyclic orientation of $\mathcal{A}$ so we can use Lemma 4.11 on every covector maximal covector γ to build a covector in $\widehat{\mathcal{A}}$ and a gallery $\widehat{\gamma}$ of $\widehat{\mathcal{A}}$.

DEFINITION 4.12. *Given a pointed hyperplane arrangement $(\mathcal{A},c)$, a generic functional f on $Z(\mathcal{A})$ realizing $(\mathcal{A},c)$ and the lifting $(\widehat{\mathcal{A}},\widehat{c})$ of Lemma 4.11, we say a gallery $\widehat{\gamma}$ of $(\widehat{\mathcal{A}},\widehat{c})$ is a lifting of gallery γ if $\widehat{\gamma}/(n+1) = \gamma$*

COROLLARY 4.13. *If $\widehat{\mathcal{A}}$ is a single-element lifting of $\mathcal{A}$ and γ is a gallery for $\mathcal{A}$ then any $\widehat{\gamma}$ such that $\widehat{\gamma}/(n+1) = \gamma$ is a gallery for $\widehat{\mathcal{A}}$.*

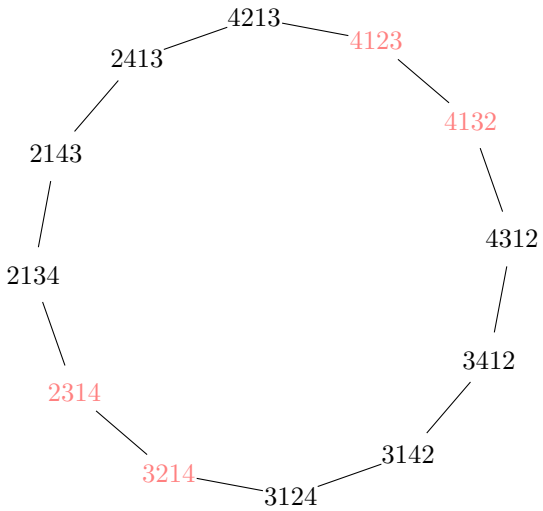

FIGURE 4.4. Graph $G_2(\mathcal{A}, c)$ from Example 4.14 with non-lifted nodes highlighted in red.

PROOF. Viewed geometrically, a gallery γ is a path from $(-)^n$ to $(+)^n$ on $G_1(\mathcal{A})$. Every vertex $\gamma^{(i)}$ of γ is a chamber of $\mathcal{A}$, which gives an acyclic orientation of $\{\pm a_i\}$. By repeated application of 4.11 each acyclic orientation of $\{\pm a_i\}$ with $1 \leq i \leq n$ can be lifted to an acyclic orientation of $\{\pm a_i\}$. Picking where to insert $n+1$ is picking we switch from lifting into $\mathcal{A}^* \cup \{-a_{n+1}\}$ or $\mathcal{A}^* \cup \{a_{n+1}\}$. □

Corollary 4.13 tells us that liftings of galleries always exist which we illustrate with an example.

EXAMPLE 4.14. *We return to the configurations from Examples 2.31 and 4.2, which we specify in the dual.*

$$\mathcal{A}^* = \begin{pmatrix} -1 & 1 & 1 \end{pmatrix}$$
$$\widehat{\mathcal{A}}^* = \begin{pmatrix} -1 & 1 & 1 & 1 \end{pmatrix}$$

We can check that $\Gamma(\mathcal{A}) = \{213, 312\}$ *(e.g. Example 2.15). Corollary 4.13 produces* 8 *galleries of* $\widehat{\mathcal{A}}$*,*

$$\{4213, 4312, 2413, 3412, 2143, 3142, 2134, 3124\} \subseteq \Gamma(\widehat{\mathcal{A}}).$$

We can list the galleries of $\widehat{\mathcal{A}}$ *by hand using* $\widehat{\mathcal{A}}^*$

$$\Gamma(\widehat{\mathcal{A}}) = \left\{ \begin{array}{lll} \textit{4213,} & \textit{4312,} & \textit{4123,} \\ \textit{2413,} & \textit{3412,} & \textit{4132,} \\ \textit{2143,} & \textit{3142,} & \textit{2314,} \\ \textit{2134,} & \textit{3124,} & \textit{3214} \end{array} \right\}.$$

$$\begin{pmatrix} - & - & \dots & - & - \\ - & - & \dots & - & + \\ + & - & \dots & - & + \\ \vdots & \vdots & \ddots & \vdots & \vdots \\ + & + & \dots & + & + \end{pmatrix} \qquad \begin{pmatrix} - & - & \dots & - & - \\ + & - & \dots & - & - \\ + & + & \dots & - & - \\ \vdots & \vdots & \ddots & \vdots & \vdots \\ + & + & \dots & + & + \end{pmatrix}$$

FIGURE 4.5. $\widehat{\gamma}_g$ and $\widehat{\gamma}_h$ as a column of covectors

We see that all the galleries predicted by Corollary 4.13 are present in $\widehat{\mathcal{A}}$ along with 4 additional galleries. The galleries $2314, 3214, 4123$, and 4132 are not liftings of any galleries of $\mathcal{A}$ as they do not contain either 213 or 312 as subwords.

Corollary 4.13 guarantees the lifting of galleries, however Example 4.14 illustrates that there is no converse in general. There is a partial converse which relies only on the acyclically oriented matroid $(\mathcal{M}(\mathcal{A}), (+)^n)$ realized by $(\mathcal{A}, c)$.

LEMMA 4.15. *For $\widehat{\mathcal{A}}$ a single-element lifting of $\mathcal{A}$ and an acyclically oriented matroid $(\mathcal{M}(\widehat{\mathcal{A}}), (+)^{n+1})$, if both $(n+1, \gamma)$ and $(\gamma, n+1)$ are galleries of $(\mathcal{M}(\widehat{\mathcal{A}}), (+)^n)$, then*

- *$(+)^n$ is a maximal covector of $\mathcal{M}(\mathcal{A})$ so $(\mathcal{M}(\mathcal{A}), (+)^n)$ is an acyclically oriented matroid,*
- *and γ is a gallery of $(\mathcal{M}(\mathcal{A}), (+)^n)$.*

PROOF. We assume we have ordered $\widehat{\mathcal{A}}$ so that $\widehat{\mathcal{A}}^* = \widehat{\mathcal{A}} \cup \{\widehat{a}_{n+1}\}$. We show that $\mathcal{A}$ has an acyclic orientation and $\gamma = (1, 2, \dots, n)$ is a gallery of $\mathcal{A}$ by repeatedly applying the elimination property of oriented matroids to $\widehat{\gamma}_g$ and $\widehat{\gamma}_h$.

Both $\widehat{\gamma}_g$ and $\widehat{\gamma}_h$ are galleries of $\widehat{\mathcal{A}}$ and we know each covector of $\widehat{\gamma}^{(i)}$ and $\widehat{\gamma}_h^{(i)}$. Figure 4.5 illustrates the covectors of $\widehat{\gamma}_g^{(i)}$ and $\widehat{\gamma}_h^{(i)}$. In particular, $\widehat{\gamma}_g^{(0)}(0) = \widehat{\gamma}_h^{(0)} = -^{n+1}$ and $\widehat{\gamma}_g^{(1)} = -^n+$ so the elimination axiom forces $-^n 0 \in \mathcal{M}(\widehat{\mathcal{A}})$ and thus $-^n \in \mathcal{M}(\mathcal{A})$. We then also know, using the symmetry axiom, that $(+)^n \in \mathcal{M}(\mathcal{A})$ so $(\mathcal{A}, (+)^n)$ is an acyclically oriented matroid.

Likewise for $1 \leq k \leq n$ we know

$$(+)^k(-)^{n-k}- = \widehat{\gamma}_h^{(k)} \text{ and } (+)^k(-)^{n-k}+ = \widehat{\gamma}_g^{(k+1)}$$

are covectors of $\mathcal{M}(\widehat{\mathcal{A}})$, so $(+)^k(-)^{n-k}0$ is a covector of $\mathcal{M}(\widehat{\mathcal{A}})$ also and $(+)^k(-)^{n-k}$ is a covector of $\mathcal{M}(\mathcal{A})$. We have constructed $\gamma^{(k)}$ for any k so $(1, 2, \dots, n)$ is a gallery of $\mathcal{A}$.

□

This converse will be useful for Lemma 4.24. For now we have an adequate understanding of lifting of galleries and move on to ask "Which galleries are coherent?"

4.3. The Coherent Cellular String Lemma

Our third lemma is a labor-saving device for classifying all-coherent monotone path graphs of generic functionals on zonotopes. Our goal is showing that, if every f-monotone path of (Z, f) is

coherent, then (Z, f) is all-coherent. This result is a surprise because of examples in which two coherent triangulations are adjacent by an incoherent bistellar flip. Our result will have implications for Section 5.2 when we find functionals for any cellular string, even though describing galleries alone would be enough. We will rely on this result in Sections 6.1 and 6.2 where it is arduous to describe the functionals of an arbitrary cellular strings. The labor-saving aspect of this lemma allows us to describe functionals which select any f-monotone path, then extend the functionals to any cellular string using the results of this section.

We recall that a cellular string $\sigma = \sigma_1 \big| \sigma_2 \big| \dots \big| \sigma_{n-m}$ of $(Z(\mathcal{A}), f)$, a generic functionals on a zonotope, is a disjoint union of the vectors of $\mathcal{A}$ satisfying conditions spelled out in Definition 2.36. A cellular string is coherent when selected by a functional; proving coherence of cellular strings means finding a linear dependence $\{g_i\}$ on $\mathcal{A}^*$ and satisfying

$$\underbrace{\frac{g_1}{f_1} = \dots = \frac{g_{|\sigma_1|}}{f_{|\sigma_1|}}}_{\sigma_1} < \dots < \underbrace{\frac{g_{\left(1+\sum_{i=1}^{k-1}|\sigma_i|\right)}}{f_{\left(1+\sum_{i=1}^{k-1}|\sigma_i|\right)}} = \dots = \frac{g_{\left(\sum_{i=1}^{k}|\sigma_i|\right)}}{f_{\left(\sum_{i=1}^{k}|\sigma_i|\right)}}}_{\sigma_k} < \dots < \underbrace{\frac{g_{n-|\sigma_{n-m}|+1}}{f_{n-|\sigma_{n-m}|+1}} = \dots = \frac{g_n}{f_n}}_{\sigma_{n-m}}.$$

LEMMA 4.16. *Let f be a generic functional on a zonotope $Z(\mathcal{A})$ and σ a cellular string of $(Z(\mathcal{A}), f)$. If every f-monotone path refining σ is coherent then σ is coherent.*

PROOF. Without loss of generality, we assume that a_i have been scaled so $f_i = 1$ for all i. Let $\sigma' = \sigma'_1 \big| \sigma'_2 \big| \dots \big| \sigma'_{n-m'}$ be a cellular string of $(Z(\mathcal{A}), f)$ which refines σ.

We will work by induction on m. When $m' = 0$, σ' is a gallery of $\mathcal{A}$ and coherent for f by hypothesis. We now assume that all cellular strings $\sigma' = \sigma'_1 \big| \sigma'_2 \big| \dots \big| \sigma'_{n-m'}$ refining σ are coherent, so $m' < m$. Assume that $\mathcal{A}$ is ordered so

$$\sigma = \underbrace{\{a_1, \dots, a_{|\sigma_1|}\}}_{\sigma_1} \Bigg| \dots \Bigg| \underbrace{\left\{a_{\left(1+\sum_{i=1}^{k-1}|\sigma_i|\right)}, \dots, a_{\left(\sum_{i=1}^{k}|\sigma_i|\right)}\right\}}_{\sigma_k} \Bigg| \dots \Bigg| \underbrace{\{a_{1+n-|\sigma_{n-m}|}, \dots, a_n\}}_{\sigma_{n-m}}.$$

To make σ' coherent we must find a linear dependence $\{x_i\}$ of $\mathcal{A}^*$ ordered so that

$$\underbrace{x_1 = \dots = x_{|\sigma_1|}}_{\sigma_1} < \dots < \underbrace{x_{\left(1+\sum_{i=1}^{k-1}|\sigma_i|\right)} = \dots = x_{\left(\sum_{i=1}^{k}|\sigma_i|\right)}}_{\sigma_k} < \dots < \underbrace{x_{n-|\sigma_{n-m}|+1} = \dots = x_n}_{\sigma_{n-m}}.$$

For $m > 1$ there is a cell σ'_k which is zonotopal face $Z(\sigma'_k)$ of $Z(\mathcal{A})$ having $|\sigma_k| > 1$. We take ${\sigma_k}' = \sigma_{(k,1)} \big| \sigma_{(k,2)} \big| \dots \big| \sigma_{(k,\ell)}$, a maximal, proper cellular string of $(Z(\sigma_k), f)$. The refinement ${\sigma_k}'$ exists because $|\sigma_k| > 1$. We build two longer cellular strings using σ with the cell σ_k replaced by ${\sigma_k}'$ and its reversal:

$$\sigma^g = \sigma_1 \big| \dots \big| \sigma_{k-1} \big| \underbrace{\sigma_{(k,1)} \big| \dots \big| \sigma_{(k,\ell)}}_{\sigma_k, \text{ refined to } {\sigma_k}'} \big| \sigma_{k+1} \big| \dots \Big| \sigma_{n-m},$$

$$\sigma^h = \sigma_1 \big| \dots \big| \sigma_{k-1} \big| \underbrace{\sigma_{(k,\ell)} \big| \dots \big| \sigma_{(k,1)}}_{{\sigma_k}' \text{ reversed}} \big| \sigma_{k+1} \big| \dots \Big| \sigma_{n-m}.$$

The cellular strings σ^g and σ^h are of length $n-m+\ell-1 > n-m$ and coherent for $(Z(\mathcal{A}), f)$. Let $a_{\alpha_1} \in \sigma_{(k,1)}$ and $a_{\alpha_2} \in \sigma_{(k,2)}$ and use Lemma 3.4 to pick $\{g_i\}$ and $\{h_i\}$ making σ^g and σ^h coherent to satisfy $g_{\alpha_2} - g_{\alpha_1} = h_{\alpha_1} - h_{\alpha_2}$ guaranteeing that $g_{\alpha_1} + h_{\alpha_1} = g_{\alpha_2} + h_{\alpha_2}$. We define

$$x_i = g_i + h_i \qquad \text{for } 1 \leq i \leq n.$$

We check that $\{x_i\}$ are a linear dependence of $\mathcal{A}^*$ and thus $x_i = x(a_i)$ with the computation:

$$\begin{aligned}\sum_{i=1}^{n} x_i a_i^* &= \sum_{i=1}^{n} (g_i + h_i)\, a_i^* \\ &= \sum_{i=1}^{n} g_i a_i^* + \sum_{i=1}^{n} h_i a_i^* \\ &= 0 + 0 = 0.\end{aligned}$$

Since σ^g and σ^h agree outside of σ_k we know that x selects a cellular string that agrees with σ outside of σ_k. We must show that the constants $x_{(\sigma_{k,i})}$ are equal for all $1 \leq i \leq \ell$. From our choice of $\{g_i\}$ and $\{h_i\}$ we know

$$\begin{aligned}x_{(\sigma_{k,1})} &= x_{\alpha_i} \\ &= g_{\alpha_1} + h_{\alpha_1} = g_{\alpha_2} + h_{\alpha_2} \\ &= x_{\alpha_2} = x_{(\sigma_{k,2})}.\end{aligned}$$

The function x then selects a cellular string through $Z(\sigma_k)$ which is coarser than the maximally course, proper $\sigma_k{}'$ cellular string $Z(\sigma_k)$, so x must be constant on all σ_k. We now know that

$$\underbrace{x_1 = \cdots = x_{|\sigma_1|}}_{\sigma_1} < \cdots < \underbrace{x_{\left(1+\sum_{i=1}^{k-1}|\sigma_i|\right)} = \cdots = x_{\left(\sum_{i=1}^{k}|\sigma_i|\right)}}_{\sigma_k} < \cdots < \underbrace{x_{n-|\sigma_{n-m}|+1} = \cdots = x_n}_{\sigma_{n-m}},$$

so σ is coherent for f. We conclude that any cellular string σ' refining σ, including σ itself, is coherent for $(Z(\mathcal{A}), f)$ by induction. □

The key idea here was to use Lemma 3.4 and divide by a positive number. We remark that this lemma is surprising in light of [**DLRS10**, Example 5.3.4] which exhibits a pair of coherent triangulations of a point configuration having an incoherent bistellar flip between them. The central symmetry of $Z(\mathcal{A})$ distinguishes f-monotone path graphs from coherent triangulations. When $Z(\mathcal{A})$ is centrally symmetric there is symmetry which gives an involution $\sigma \to -\sigma$ on cellular strings of $(Z(\mathcal{A}), f)$. This involution is missing for triangulations and fiber polytopes in general.

The final theorem of this section was pointed out to us by V. Reiner.

THEOREM 4.17. *The pair $(\mathcal{A}, c)$ is universally all-coherent if and only if there exists some generic f on $\mathcal{A}$ inducing c for which $(\mathcal{A}, f)$ is all-coherent.*

PROOF. It is clear that if $(\mathcal{A}, c)$ is universally all-coherent then there exists a generic f inducing c for which $(\mathcal{A}, f)$ is all-coherent by definition.

Now suppose that $(\mathcal{A}, f)$ is all-coherent and let f' be another generic functional on $\mathcal{A}$ inducing c. Let Z and Z' be be the fiber zonotopes of f and f' respectively, both of dimension $d-1$. Denote by P and P' the face posets of Z and Z', after omitting the empty face $\emptyset$ from each. Hence, the order complexes ΔP and $\Delta P'$ both triangulate $d-2$ spheres, namely the barycentric subdivisions of the boundaries of Z and Z'

Since (A, f) is all-coherent every cellular string σ of $(\mathcal{A}, c)$ appears in L and hence one has an inclusion $P' \hookrightarrow P$ as an induced subposet. Then $P' = P$ using [**ADLRS00**, Lemma 3.3], so we conclude $(\mathcal{A}, f')$ is also all-coherent. □

This insightful Theorem was understood only after we gave several proofs of universal all-coherent explicitly for every f. We leave our proofs intact to illustrate the remarkable nature of universal all-coherence and gladly include this theorem as a labor-saving device for future researchers.

4.4. The Incoherent Extension Lemma

This section presents our first tool to prove existence of incoherent galleries; when $\mathcal{A}^+$ is a single-element extension of $\mathcal{A}$ we prove that when $\mathcal{A}$ has incoherent f-monotone paths $\mathcal{A}^+$ does too. The intuition here is clear:

$$\frac{g_{\gamma(1)}}{f_{\gamma(1)}} < \cdots < \frac{g_{\gamma(n)}}{f_{\gamma(n)}} < \frac{g_{\gamma(n+1)}}{f_{\gamma(n+1)}}$$

cannot be satisfied without also satisfying

$$\frac{g_{\gamma(1)}}{f_{\gamma(1)}} < \cdots < \frac{g_{\gamma(n)}}{f_{\gamma(n)}}.$$

Using a contrapositive statement and interpreting these inequalities as coherence we will show that if γ is incoherent then γ has a extension γ^+ which is also incoherent.

DEFINITION 4.18. *For $\mathcal{A}^+ = \{a_i, \ldots, a_{n+1}\}$, a single-element extension of $\mathcal{A}$, an f-monotone path γ^+ of $(Z(\mathcal{A}^+), f)$ is an extension of an f-monotone path γ of $(Z(\mathcal{A}), f)$ when $\gamma^+ \backslash (n+1) = \gamma$.*

Lemma 4.19 will be geometrically intuitive yet only useful in corank 2 and above. Using Lemma 4.19 will require finding a projection $(\mathcal{A}^+)^* \to \mathcal{A}^*$. Unlike 4.8 this will not provide structural insight into the monotone path graph, it will only allow us to efficiently prove incoherence.

LEMMA 4.19. *Suppose $\mathcal{A}^+ = \{a_i, \ldots, a_{n+1}\}$ is a single-element extension of $\mathcal{A}$ and f is a generic function on both $Z(\mathcal{A})$ and $Z(\mathcal{A}^+)$. If γ^+ is a coherent f-monotone path of $(\mathcal{A}^+, f)$ then $\gamma = \gamma^+ \backslash (n+1)$ is a coherent f-monotone path of $(\mathcal{A}, f)$.*

PROOF. Without loss of generality, we assume $f_i = 1$ for all i. Further $\mathcal{A}^+$ is a single-element extension of $\mathcal{A}$ so duality tells us that $(\mathcal{A}^+)^* = \left\{\widehat{a_i^*}\right\}$ is a single-element lifting of $\mathcal{A}^* = \{a_i^*\}$ with a projection $\pi : \widehat{\mathcal{A}^*} \to \mathcal{A}^*$ mapping $\pi(\widehat{a_i^*}) \to a_i^*$ for $i \neq n+1$ and $\pi(\widehat{a_{n+1}^*}) = 0$.

We first show that γ is an f-monotone path of $(Z(\mathcal{A}), f)$. Each covector $\gamma^{+(i)}$ is an acyclic orientation of $\mathcal{A}^+$ of the form:

$$0 = \sum_{i=1}^{n+1} c_i \widehat{a_i^*},$$

with $c_i > 0$ for all i. We use the projection π to construct γ one acyclic orientation of $\mathcal{A}$ at a time:

$$\pi(0) = \pi\left(\sum_{i=1}^{n+1} c_i \widehat{a_i^*}\right) = \sum_{i=1}^{n+1} c_i \pi(\widehat{a_i^*}) = \sum_{i=1}^{n} c_i a_i^* = 0.$$

So γ is a gallery of $\mathcal{A}$. We can use projection again to show that γ is coherent for f. Since γ^+ is coherent in $\mathcal{A}^+$ for f we know there must exist

$$g_{\gamma(1)} < g_{\gamma(2)} < \cdots < g_{\gamma(n)} < g_{\gamma(n+1)}$$

satisfying

$$\sum_{i=1}^{n+1} g_i a_i^* = 0.$$

Applying π we see

$$\pi(0) = \pi\left(\sum_{i=1}^{n+1} g_i \widehat{a_i^*}\right) = \sum_{i=1}^{n+1} g_i \pi(\widehat{a_i^*}) = \sum_{i=1}^{n} g_i a_i^* = 0.$$

Note in particular that π does not change g_i so that inequalities

$$g_{\gamma(1)} < g_{\gamma(2)} < \cdots < g_{\gamma(n)}$$

still hold and so γ a coherent f-monotone $(Z(\mathcal{A}), f)$. □

COROLLARY 4.20. *Given γ^+ an f-monotone path of $(Z(\mathcal{A}^+), f)$ and $\gamma = \gamma^+ \backslash (n+1)$ an incoherent f-monotone path $(\mathcal{A}, f)$ then γ^+ is incoherent as well.*

The geometry here is obscured by duality. Since $\mathcal{A}$ and $\mathcal{A}^+$ are both hyperplane arrangements of $\mathbb{R}^d$ the extension γ^+ extending γ is exactly the same path in $\mathbb{R}^d$ with an $n+1$ inserted in the geometrically appropriate place. If γ is incoherent on $\mathcal{A}$, then any sequence of inequalities

$$\frac{g_{\gamma(1)}}{f_{\gamma(1)}} < \frac{g_{\gamma(2)}}{f_{\gamma(2)}} < \cdots < \frac{g_{\gamma(n)}}{f_{\gamma(n)}}$$

is inconsistent and remains inconsistent no matter the value of $g_{\gamma^+(n+1)}$.

EXAMPLE 4.21. *Consider the following two hyperplane arrangements*

$$\mathcal{A} = \begin{array}{c} \begin{matrix} a_1 & a_2 & a_3 & a_4 \end{matrix} \\ \begin{pmatrix} 1 & 0 & 0 & 1 \\ 0 & 1 & 0 & 1 \\ 0 & 0 & 1 & -1 \end{pmatrix} \end{array} \quad \textit{and} \quad \mathcal{A}^+ = \begin{array}{c} \begin{matrix} a_1 & a_2 & a_3 & a_4 & a_5 \end{matrix} \\ \begin{pmatrix} 1 & 0 & 0 & 1 & 1 \\ 0 & 1 & 0 & 1 & 2 \\ 0 & 0 & 1 & -1 & 3 \end{pmatrix} \end{array}.$$

We recognize $\mathcal{A}$ as the hyperplane arrangement from Example 3.3 so we know that the f-monotone paths $\{1324, 2314, 4132, 4231\}$ are incoherent for $f(x, y, z) = 3x + 2y + z$. We then know that

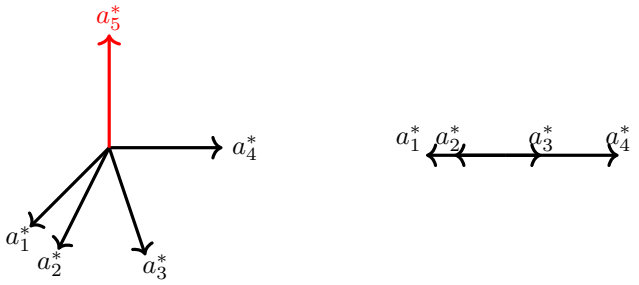

FIGURE 4.6. Single element extensions in the Dual

$\{13524, 23514, 25314, 41352, 42531\}$ *are incoherent in* $\mathcal{A}^+$ *for* f *since each* f*-monotone path of* $(\mathcal{A}^+, f)$ *is a lifting of an* f*-monotone path of* $(\mathcal{A}, f)$.

We close by illustrating how we use Lemma 4.19 in practice. Example 4.21 was a straightforward illustration of using Lemma 4.19. To use Corollary 4.20 in our classification of corank 2 monotone path graphs, we must understand it with duality.

EXAMPLE 4.22. *The hyperplane arrangements from example 4.21 have Gale duals*

$$\mathcal{A}^* = \begin{array}{c} \begin{matrix} a_1^* & a_2^* & a_3^* & a_4^* \end{matrix} \\ \begin{pmatrix} -1 & -1 & 1 & 1 \end{pmatrix} \end{array} \quad \textit{and} \quad \mathcal{A}^{+*} = \begin{array}{c} \begin{matrix} \widehat{a_1^*} & \widehat{a_2^*} & \widehat{a_3^*} & \widehat{a_4^*} & \widehat{a_5^*} \end{matrix} \\ \begin{pmatrix} -1 & -1 & 1 & 1 & 0 \\ -1 & -2 & -3 & 0 & 1 \end{pmatrix} \end{array}.$$

To show that $\mathcal{A}^+$ *is a single-element extension of* $\mathcal{A}$ *we must give a projection from* $\pi : \mathcal{A}^{+*}$ *onto* $\mathcal{A}^*$. *Figure 4.6 shows* $\mathcal{A}^*$ *and* $\mathcal{A}^{+*}$. *We see that* $\pi(v) = (1, 0) \cdot v$ *projects* $\mathcal{A}^{+*} \to \mathcal{A}^*$, *allowing us to say* $\mathcal{A}^+$ *has incoherent galleries for every* f.

The trick in using Corollary 4.20 is to see a projection $\mathcal{A}^{+*}$ to $\mathcal{A}^*$. In spite of the challenges Lemma 4.19 will be our main labor-saving tool for showing f-monotone paths are incoherent. In corank 1, Lemma 4.19 does not tell us anything useful because all corank 0 hyperplane arrangements are universally all-coherent [**BKS94**]. Corollary 4.20 will be most useful Section 6 in order to quickly show that $(\mathcal{A}, f)$ has incoherent galleries for small cases, leaving one case to deal with by hand, but the major extension tool we will need is a Lemma 4.24 for single-element liftings.

4.5. The Incoherent Lifting Lemma

Our fifth lemma is the analog of Lemma 4.19 for single-element liftings. This lemma will be the key to our classification of universally all-coherent hyperplane arrangements in both corank 1 and corank 2. We recall from Section 4.2 that when $\widehat{\mathcal{A}}$ is a single-element lifting of $\mathcal{A}$ we say a gallery $\widehat{\gamma}$ of $(\widehat{\mathcal{A}}, \widehat{c})$ is a lifting of a gallery γ of $(\mathcal{A}, c)$ when $\widehat{\gamma}/(n+1) = \gamma$

Our goal in this section is to prove that if γ is an incoherent f-monotone path for every $(Z(\mathcal{A}), f)$ realizing $(\mathcal{A}, c)$ then there is an incoherent $\widehat{f}$-monotone path $\widehat{\gamma}$ for every $(Z(\widehat{\mathcal{A}}), \widehat{f})$ realizing $(\widehat{\mathcal{A}}, \widehat{c})$.

EXAMPLE 4.23. *Following Example 3.3 we use the hyperplane arrangement introduced in Example 3.3. While we previously worked with $\mathcal{A}$ directly, we now revisit this example using $\mathcal{A}^*$.*

$$\mathcal{A}^* = \begin{pmatrix} -1 & -1 & 1 & 1 \end{pmatrix}.$$

For the function $f(x,y,z) = x+y+z$ we have $f_i = 1$ for all i. We were able to pick an incoherent f-monotone path γ by ordering γ negative, positive, negative, positive. This guaranteed that no matter what g_i we picked, we had $\sum_{i=1}^4 g_i a_i^* > 0$. We see that there are 8 such incoherent galleries for f.

We now look at a lifting $\widehat{\mathcal{A}}$ of $\mathcal{A}$ and in particular look at its dual $\widehat{\mathcal{A}}^*$

$$\widehat{\mathcal{A}}^* = \begin{pmatrix} -1 & -1 & 1 & 1 & 1 \end{pmatrix}.$$

Using the lifting $\widehat{f}$ guaranteed by Lemma 4.11; with $N = 10$ we have $\widehat{f}^* = (1,1,1,9/10,1/10)$. Our insight here is that $\sum_{i=1}^4 g_i a_i^* > 0$ so by making $g_5 a_5^* > 0$ we can make $\widehat{\gamma}$ incoherent, and we can make $g_5 a_5^* > 0$ by making $g_5 > g_3$ using $\widehat{\gamma} = 14235$. At the same time we think we can make $\gamma = 51423$ a coherent $\widehat{f}$-monotone path of $(Z(\mathcal{A}), \widehat{f})$ by making g_5 as negative as we want. Our intuition is good; $\widehat{\gamma} = 14235$ is incoherent for $(\widehat{\mathcal{A}}, \widehat{f})$ and $\gamma = 51423$ is coherent for $(\widehat{\mathcal{A}}, \widehat{f})$. That 51423 is coherent for $(\widehat{\mathcal{A}}, \widehat{f})$ is interesting and important; not every lifting of an incoherent f-monotone path is incoherent.

The lesson here is both the galleries $(n+1, \gamma)$ and $(\gamma, n+1)$ are important and we must check both when looking for incoherent galleries. As with Lemma 4.19 we will find coherence properties easier to deal with and use the contrapositive.

LEMMA 4.24. *Let $\mathcal{A}$ be a hyperplane arrangement and $\widehat{\mathcal{A}}$ a single-element lifting of $\mathcal{A}$. Suppose*

$$\widehat{\gamma}_g = (n+1, 1, 2, \ldots, n), \text{ and}$$
$$\widehat{\gamma}_h = (1, 2, \ldots, n, n+1)$$

are coherent $\widehat{f}$-monotone paths of $(Z(\widehat{\mathcal{A}}), \widehat{f})$ for some $\widehat{f}$. Then there is a generic functional f on $Z(\mathcal{A})$ for which γ is a coherent f-monotone path.

PROOF. We assume we have ordered $\widehat{\mathcal{A}}$ so that $\widehat{\mathcal{A}}^* = \widehat{\mathcal{A}} \cup \{\widehat{a}_{n+1}\}$. We know that $(\mathcal{M}(\mathcal{A}), (+)^n)$ is an acyclically oriented matroid and that γ is a gallery of $(\mathcal{M}(\mathcal{A}), (+)^n)$ we want to show that if

$$\widehat{\gamma}_g = (n+1, 1, 2, \ldots, n), \text{ and}$$
$$\widehat{\gamma}_h = (1, 2, \ldots, n, n+1)$$

are both coherent f-monotone paths for some generic $\widehat{f}$ on $Z(\mathcal{A})$ then there exists some generic f on $Z(\mathcal{A})$ for which γ is coherent. We may that $\widehat{\mathcal{A}}$ is chosen so $\widehat{f}_i = \widehat{f}(\widehat{a}_i) = 1$ for all i. Both $\widehat{\gamma}_g$ and $\widehat{\gamma}_h$ are coherent f-monotone paths so, there are linear dependencies $\{\widehat{g}_i\}$ and $\left\{\widehat{h}_i\right\}$ of $\mathcal{A}^*$ selecting $\widehat{\gamma}_g$ and $\widehat{\gamma}_h$ chosen according to Corollary 3.5 so that

$$0 = \widehat{g}_{n+1} < \widehat{g}_1 < \widehat{g}_2 < \cdots < \widehat{g}_n, \quad \text{and}$$
$$0 < \widehat{h}_1 < \widehat{h}_2 < \cdots < \widehat{h}_n < \widehat{h}_{n+1}.$$

We want to realize $(\mathcal{M}(\mathcal{A}), (+)^n)$ with a generic functional $f \in \left(\mathbb{R}^d\right)^*$ on $Z(\mathcal{A})$.

$$\text{Define} \quad f_i = 1 - \frac{\widehat{h}_i}{\widehat{h}_{n+1}} > 0.$$

We check that $\{f_i\}$ are induced by a functional $f_i = f(a_i)$ by computing

$$\begin{aligned}\sum_{i=1}^{n} f_i a_i^* =& \sum_{i=1}^{n} \left(1 - \frac{\widehat{h}_i}{\widehat{h}_{n+1}}\right) a_i^* \\ =& \sum_{i=1}^{n} a_i^* - \frac{1}{\widehat{h}_{n+1}} \sum \widehat{h}_i a_i^* \\ =& - a_{n+1}^* - \frac{-\widehat{h}_{n+1}}{\widehat{h}_{n+1}} a_{n+1}^* \\ =& 0.\end{aligned}$$

This gives f two important properties:

- Since $\widehat{h}_i < \widehat{h}_{n+1}$ for $1 \leq i \leq n$, we know $f_i > 0$.
- For $1 \leq i < k \leq n$ we know $f_i > f_k$ (since $\widehat{h}_i < \widehat{h}_k$).

We claim that γ is a coherent f-monotone path of $\mathcal{A}$ and we must find g which selects γ in the sense of Definition 2.39.

Pick $g_i = \widehat{g}_i$ for $1 \leq i \leq n$. Since $\widehat{g}_{n+1} = 0$, we know that

$$\sum_{i=1}^{n} g_i a_i^* = \sum_{i=1}^{n} \widehat{g}_i a_i^* + 0 a_{n+1}^* = \sum_{i=1}^{n+1} \widehat{g}_i a_i^* = 0,$$

and $g_i = g(a_i)$ are induced by a function $g \in \left(\mathbb{R}^d\right)^*$. Finally we must check that $\{g_i\}$ have a γ ordering. Given $1 \leq i < k \leq n$ we know

$$\frac{g_i}{f_i} < \frac{g_k}{f_i} < \frac{g_k}{f_k}$$

as desired. Thus γ is a coherent f-monotone path of $(Z(\mathcal{A}), f)$. □

The way we intend to use this lemma is not for coherence, but as an inductive tool to show that hyperplane arrangements must have incoherent galleries. The logical statement we want is the contrapositive of Lemma 4.24.

COROLLARY 4.25. *For a $\widehat{\mathcal{A}}$ a single-element lifting of $\mathcal{A}$, if $(Z(\mathcal{A}), f)$ has an incoherent f-monotone path for every f then $(Z(\mathcal{A}), f)$ has an incoherent $\widehat{f}$-monotone path for every $\widehat{f}$.*

This is the lemma we are searching for. Corollary 4.25 will be our most powerful tool in classifying monotone path graphs in coranks 1 and 2. It is worth keeping in mind, however that none of our lemmas are specific to coranks 1 or 2; our technical lemmas are powerful enough to use in arbitrary corank.

CHAPTER 5

Application: Corank 1

This chapter uses the results of Chapter 4 to give a complete classification of all monotone path graphs in corank 1. We begin by recalling the classification in Section 2.1, restricting our attention to pointed hyperplane arrangements $(\mathcal{A}, c)$ and count the galleries of $(\mathcal{A}, c)$ explicitly. From our classification we identify a unique family of universally all-coherent pointed irreducible hyperplane arrangements and find functionals to select any f-monotone path or cellular string of $(Z(\mathcal{A}), f)$. For all other corank 1 hyperplane arrangements, we describe the incoherent galleries explicitly for a minimal obstruction. We then lift these incoherent galleries to all hyperplane arrangements outside of our universally all-coherent family, using Lemma 4.24. After classifying pointed irreducible hyperplane arrangements in corank 1, we prove Corollary 5.8 to say precisely when reducible hyperplane arrangements have incoherent galleries. Galleries and flips of pointed hyperplane arrangements are simple enough to understand in corank 1 that we show a specific gallery of $G_2(\mathcal{A}, c)$ is L_2-accessible and prove the diameter of $G_2(\mathcal{A}, c) = |L_2|$ for every corank 1 pointed hyperplane arrangement. We assume that all hyperplane arrangements in this section are irreducible unless otherwise noted.

5.1. Combinatorial Model

Pointed hyperplane arrangements in corank 1 are classified in $\mathcal{A}^* \subset \mathbb{R}^1$ by counting the number k of negative vectors and irreducible when they do not contain the zero vector. When $k = 0$ $\mathcal{M}(\mathcal{A})$ has no acyclic orientation so we discard it and focus only on $k > 1$. Our first step is to describe the number $|\Gamma(\mathcal{A}, c)|$ of galleries. Table 5.1 presents the number of galleries for small n and $k \leq n/2$ which we use to check our analytic results. We count galleries for any k by looking at all permutations of n and removing those which do not correspond to galleries. When $k = 1$ we have a constructive description which we use to describe functionals g selecting arbitrary f-monotone paths.

LEMMA 5.1. *For a hyperplane arrangement $\mathcal{A}$ of $n = d + 1$ vectors in $\mathbb{R}^d$ with k negative vectors in $\mathcal{A}^*$, the number of galleries $|\Gamma(\mathcal{A}, c)|$ is*

$$|\Gamma(\mathcal{A}, c)| = n! - 2k!(n - k)!.$$

		k				
		1	2	3	4	5
	3	12	16			
	4	72	96			
	5	480	624	648		
d	6	3600	4560	4752		
	7	30240	37440	38880	39168	
	8	282240	342720	354240	357120	
	9	2903040	3467520	3568320	3594240	3600000
	10	32659200	38465280	39432960	39674880	39744000

TABLE 5.1. Gallery counts for hyperplane arrangements of $d+1$ vectors in $\mathbb{R}^d$ with $\mathcal{A}^*$ having k negative vectors

PROOF. We begin by presenting $\mathcal{A}^*$ explicitly

$$\mathcal{A}^* = \begin{array}{c} \begin{matrix} a_1^* & \dots & a_k^* & a_{k+1}^* & \cdots & a_n^* \end{matrix} \\ \begin{pmatrix} -1 & \dots & -1 & 1 & \cdots & 1 \end{pmatrix} \end{array},$$

and count the number of galleries in $\mathcal{A}$ by counting permutations of the n dual vectors and removing the permutations which are not paths on $Z(\mathcal{A})$. A permutation γ of $[n]$ is not a gallery when the $\gamma^{(i)}$ fails to capture the origin in $\mathcal{A}^*$. This happens when γ crosses all the negative dual vectors $\{a_1, \dots, a_k\}$ followed by all the positive dual vectors $\{a_{k+1}, \dots, a_n\}$, or all the positive dual vectors followed by all the negative dual vectors.

We count the permutations which are not galleries by ordering the k negative hyperplanes, ordering the $n-k$ positive hyperplanes and doubling the result for reversals. Subtracting from all $n!$ permutations gives the total:

$$|\Gamma(\mathcal{A}, c)| = n! - 2k!(n-k)!.$$

□

This enumeration of the galleries matches the computational results of Table 5.1.

EXAMPLE 5.2. *To illustrate permutations which are not galleries we use*

$$\mathcal{A}^* = \begin{array}{c} \begin{matrix} a_1^* & a_2^* & a_3^* & a_4^* \end{matrix} \\ \begin{pmatrix} -1 & -1 & 1 & 1 \end{pmatrix} \end{array}.$$

We previously worked with $\mathcal{A}^*$ in Example 3.3 where we enumerated all 16 *galleries of the monotone path graph by listing all paths on $(Z(\mathcal{A}), v)$. We can now revisit this result and count* 8 *non-galleries of $\mathcal{A}$, which have the form (positive,positive,negative,negative) or (negative,negative,positive,positive).*

$$\left\{ \begin{array}{cccc} 1234, & 1243, & 2134, & 2143 \\ 4321, & 3421, & 4312, & 4512 \end{array} \right\}$$

We then know that there are $16 = 24 - 8$ *galleries of* $\mathcal{A}$*, which we can check by referring back to Example 3.3.*

5.2. A Universally All-Coherent Family.

We now focus on the family of pointed hyperplane arrangements in which $\mathcal{A}^*$ has exactly 1 negative vector and claim this pointed hyperplane arrangement is universally all-coherent. Definition 3.2 describes universally all-coherent, pointed hyperplane arrangements, as those for which any cellular string of $(Z(\mathcal{A}), f)$ is coherent for any f. We prove this by enumerating the galleries constructively, then finding a functional g corresponding to each f-monotone path. We sketch a method to find g for an arbitrary cell but rely on Lemma 4.16 to prove all-coherence for a particular f and since our argument is for any f we conclude that $(\mathcal{A}, c)$ is universally all-coherent.

LEMMA 5.3. *For the corank 1 hyperplane arrangement with*

$$\mathcal{A}^* = \begin{array}{c} \begin{matrix} a_1^* & a_2^* & \cdots & a_n^* \end{matrix} \\ \begin{pmatrix} -1 & 1 & \cdots & 1 \end{pmatrix} \end{array}$$

and the chamber c *corresponding to the covector* $(+)^n$*, the number of galleries is:*

$$|\Gamma(\mathcal{A}, c)| = d!(d-1).$$

REMARK 5.4. *The number of galleries* $|\Gamma(\mathcal{A}, c)|$ *equals the number of ways to organize* n *books on two bookshelves so that each shelf receives at least one book* [**oIS10**]*. Such arrangements are well documented and the subject of the occasional research project* [**Riv14**].

PROOF. The bijection is straightforward. Since a_1^* is the only negative vector of $\mathcal{A}^*$, we know $\gamma(1) \neq 1$ and $\gamma(n) \neq 1$ and a_1^* divides the d remaining vectors into two pieces. There are $d-1$ possible positions for the negative vector and $d!$ orderings of the remaining vectors.

We check that this equals the expression for $|\Gamma(\mathcal{A}, c)|$ found in when $k = 1$ and $n = d + 1$ in Lemma 5.1:

$$n! - 2k!(n-k)!\Big|_{k=1} = (d+1)! - 2(d+1-1)! = d!(d+1-2) = d!(d-1).$$

□

Our goal is, for any generic $f \in \left(\mathbb{R}^d\right)^*$, to find a functional $g \in \left(\mathbb{R}^d\right)^*$ selecting an arbitrary f-monotone, and to extend that argument to an arbitrary cellular string using Lemma 4.16. When an f-monotone path is coherent we can use Lemma 5.3 to pick $\{g_i\}$ so that $g_1 = 0$. We know that there will be a positive vector to the left and right of in γ so our idea is simply to make these positive and negative vectors as large as we want to satisfy

$$\sum_{i=2}^{n} \frac{g_i}{f_i} = 0.$$

We make a similar argument for a cellular string. We locate the block σ_k containing a_1 and make $g_i = 0$ for all $a_i \in \sigma_i$. When every cellular string is coherent, the monotone path graph is equal to the fiber polytope.

LEMMA 5.5. *For the corank 1 hyperplane arrangement with*

$$\mathcal{A}^* = \begin{array}{c} \begin{matrix} a_1^* & a_2^* & \cdots & a_n^* \end{matrix} \\ \begin{pmatrix} -1 & 1 & \cdots & 1 \end{pmatrix} \end{array}$$

with $f^* = (f_1, \ldots, f_n)$ generic on $Z(\mathcal{A})$, any f-monotone path γ is coherent.

PROOF. Our proof has been sketched above. Using Lemma 5.3 we assume that $\mathcal{A}$ has been ordered to that $\gamma = (2, 3, \ldots, k, 1, \ldots, n)$. Pick arbitrary $\{g_i\}$ so that

- $g_1 = 0$,
- $\dfrac{g_3}{f_3} < \cdots < \dfrac{g_k}{f_k} < 0 = \dfrac{g_1}{f_1} < \dfrac{g_{k+1}}{f_{k+1}} < \cdots < \dfrac{g_n}{f_n}$,
- $\dfrac{|g_3|}{f_3} < \displaystyle\sum_{i=3}^{n} \frac{g_i}{f_i}$,
- and, $\dfrac{g_2}{f_2} = -\displaystyle\sum_{i=3}^{n} \frac{g_i}{f_i}$.

The third condition is the only non-arbitrary choice and is easily satisfied by making g_n adequately large. We then know that

$$\frac{g_2}{f_2} < \frac{g_3}{f_3},$$

so γ is a coherent f-monotone path of $Z(\mathcal{A})$. □

Thus, when $\mathcal{A}$ is of corank 1 with exactly $\mathcal{A}^*$ containing exactly 1 negative vector, every f-monotone path is coherent. Lemma 4.16 then tells us that $(\mathcal{A}, c)$ is universally all-coherent. As a corollary we know the diameter of $G_2(\mathcal{A}, c)$ is $|L_2|$.

5.3. Minimal Obstructions and Uniqueness

Now we find a minimal obstruction set in corank 1 and prove that our universally all-coherent family is unique by showing all other corank 1 pointed hyperplane arrangements are liftings of the minimal obstruction set and contain at least one incoherent f-monotone path by Lemma 4.24. The minimal obstruction set is simple, consisting of a single hyperplane arrangement $\mathcal{A}$, with 4 vectors in $\mathbb{R}^3$ and 2 negative vectors in $\mathcal{A}^*$. In Example 3.3 we found incoherent f-monotone paths for a specific f. Our task now is to find an incoherent f-monotone path in $\mathcal{A}$ for every f. We realize $\mathcal{A}$ as

$$\mathcal{A} = \begin{array}{c} \begin{matrix} a_1 & a_2 & a_3 & a_4 \end{matrix} \\ \begin{pmatrix} 1 & 0 & 0 & 1 \\ 0 & 1 & 0 & 1 \\ 0 & 0 & 1 & -1 \end{pmatrix} \end{array} \qquad \mathcal{A}^* = \begin{array}{c} \begin{matrix} a_1^* & a_2^* & a_3^* & a_4^* \end{matrix} \\ \begin{pmatrix} -1 & -1 & 1 & 1 \end{pmatrix} \end{array}$$

The graph, $G_2(\mathcal{A}, c)$, depends on $\mathcal{A}$ and c. As in Example 3.3 coherence of γ depends on the function f inducing an acyclic orientation on $\mathcal{A}$. We gain some intuition for which f-monotone paths are incoherent by looking at the fiber zonotope for any arbitrary f, whose vertices parametrize the coherent f-monotone paths [**BS92**].

EXAMPLE 5.6. *Using Lemma 3.6 we can write down the vectors which generate the fiber polytope. Using $f(x, y, z) = f_1x + f_2y + f_3z$ we can compute $f_4 = f_1 + f_2 - f_3$ and*

$$\mathcal{A}' = \left\{ \begin{array}{lll} v_{12} = \begin{pmatrix} -f_2 \\ f_1 \\ 0 \end{pmatrix} & v_{13} = \begin{pmatrix} -f_3 \\ 0 \\ f_1 \end{pmatrix} & v_{14} = \begin{pmatrix} f_3 - f_2 \\ f_1 \\ -f_1 \end{pmatrix} \\ v_{23} = \begin{pmatrix} 0 \\ -f_3 \\ f_2 \end{pmatrix} & v_{24} = \begin{pmatrix} f_2 \\ f_3 - f_1 \\ -f_2 \end{pmatrix} & v_{34} = \begin{pmatrix} f_3 \\ f_3 \\ -(f_1 + f_2) \end{pmatrix} \end{array} \right\}.$$

It is clear from these vectors that the fiber zonotope has at most 12 vertices and 12 edges. Lemma 5.1 gives 16 galleries of $G_2(\mathcal{A}, c)$ so we argue that the monotone path graph must contain at least 4 incoherent f-monotone paths. We would like to predict, given f, which f-monotone paths are incoherent. Looking at Figure 5.1 we guess that the incoherent f-monotone paths are from the set:

$$\left\{ \begin{array}{l} 1423, 2314, 1324, 2413 \\ 3241, 4123, 4231, 3142 \end{array} \right\}.$$

Each vector v_{ij} corresponds to a flip of $G_2(\mathcal{A}, c)$. We notice that the vectors v_{ij} will be parallel for specific f. Looking at the vectors v_{13} and v_{24} in $\mathcal{A}'$ we see that the vectors

$$v_{13} = \begin{pmatrix} -f_3 \\ 0 \\ f_1 \end{pmatrix} \quad v_{24} = \begin{pmatrix} f_2 \\ f_3 - f_1 \\ -f_2 \end{pmatrix}.$$

are parallel when $f_3 = f_1$ and speculate that a degeneracy of the $\mathcal{A}'$ causes the failure of coherence. In contrast, we see that 2314 is incoherent whenever $f_3 \leq f_4$ regardless of $\mathcal{A}'$. This motivates a geometric proof that the monotone path graph contains incoherent galleries.

LEMMA 5.7. *In the pointed hyperplane arrangement $(\mathcal{A}, c)$ of 4 vectors in $\mathbb{R}^3$ in which $\mathcal{A}^*$ has exactly 2 negative vectors, and $(\mathcal{A}, c)$ is realized by $f^* = (f_1, f_2, f_3, f_4)$ on $Z(\mathcal{A})$, the f-monotone path $\gamma = 2314$ is incoherent.*

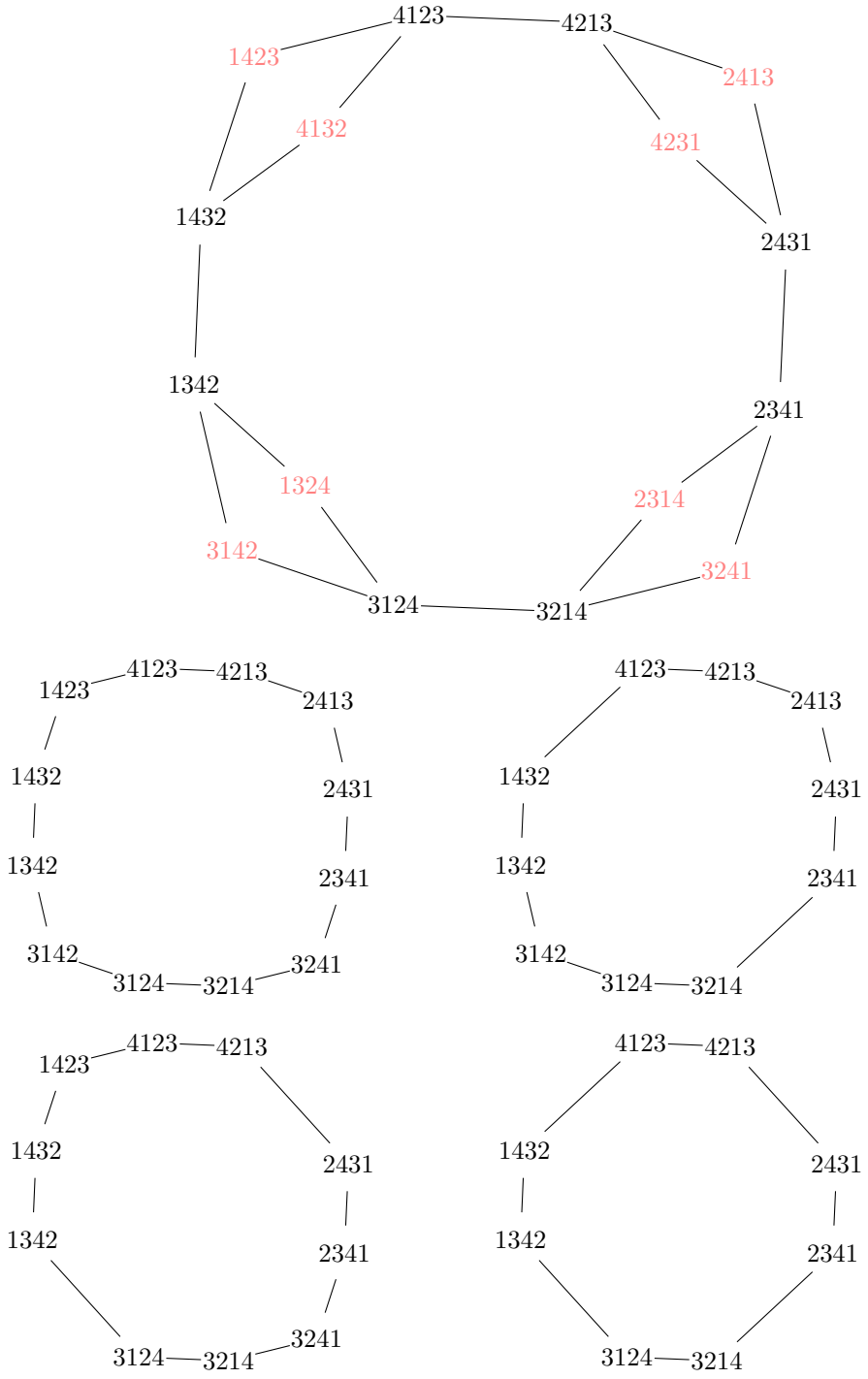

FIGURE 5.1. Monotone path graph of $\mathcal{A}$ and possible fiber polytopes.

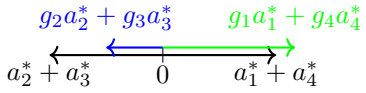

FIGURE 5.2. $\gamma = 2314$ is incoherent for every f

PROOF. The proof is elementary and we include it as a model for harder minimal obstructions in Lemma 6.6. We avoid fractions by choosing a_i so that $f_i = 1$ giving us:

$$\mathcal{A} = \begin{array}{c} \begin{matrix} a_1 & a_2 & a_3 & a_4 \end{matrix} \\ \begin{pmatrix} \frac{1}{f_1} & 0 & 0 & \frac{1}{f_1} \\ 0 & \frac{1}{f_2} & 0 & \frac{1}{f_2} \\ 0 & 0 & \frac{1}{f_3} & \frac{-1}{f_3} \end{pmatrix} \end{array}, \qquad \text{and} \quad \mathcal{A}^* = \begin{array}{c} \begin{matrix} a_1^* & a_2^* & a_3^* & a_4^* \end{matrix} \\ \begin{pmatrix} -f_1 & -f_2 & f_3 & f_4 \end{pmatrix} \end{array}.$$

With $f_1 + f_2 = f_3 + f_4$. Without loss of generality we assume that $f_1 \leq f_2$ and $f_3 \leq f_4$. Further we know that $f_1 \leq f_4$ and $f_3 \leq f_2$ so the vector $a_2^* + a_3^*$ points in the negative direction while $a_1^* + a_4^*$ points in the positive direction and $a_1^* + a_4^* + a_2^* + a_3^* = 0$.

We know 2314 is a gallery of $\mathcal{A}$ and if $\gamma = 2314$ is coherent we can find $\{g_1, g_2, g_3, g_4\}$ so that

$$g_1a_1^* + g_2a_2^* + g_3a_3^* + g_4a_4^* \text{ and } 0 < g_2 < g_3 < g_1 < g_4.$$

The vector $g_2a_2^* + g_3a_3^*$ is less negative than $a_2^* + a_3^*$ while the vector $g_1a_1^* + g_4a_4^*$ is more positive than $a_1^* + a_4^*$. Since $a_1^* + a_4^* + a_2^* + a_3^* = 0$ we then know that $g_1a_1^* + g_4a_4^* + g_2a_2^* + g_3a_3^* > 0$, contradicting our assumption that γ is coherent. □

COROLLARY 5.8. *Let $(\mathcal{A}, c)$ and $(\mathcal{A}', c')$ be pointed hyperplane arrangements, $\mathcal{A} \subset \mathbb{R}^d$ and $\mathcal{A}' \subset \mathbb{R}^{d'}$.*

(1) Suppose $\mathcal{A}' = \{a_{n+1}\}$ is an isthmus, $\widehat{f} \in \left(\mathbb{R}^{d+1}\right)^*$ is generic on $Z(\mathcal{A} \bigsqcup \mathcal{A}')$, and $\widehat{\gamma}$ is an $\widehat{f}$-monotone path on $Z(\mathcal{A} \bigsqcup \mathcal{A}')$. Then defining $f \in \left(\mathbb{R}^d\right)^*$ via

$$\mathbb{R}^d \xhookrightarrow{\iota} \mathbb{R}^{d+1} \xrightarrow{\widehat{f}} \mathbb{R}$$

and $\gamma = \widehat{\gamma} / \{a_{n+1}\}$, one has that:

- *f is generic on $Z(\mathcal{A})$,*
- *γ is f-monotone, and*
- *$\widehat{\gamma}$ is coherent if and only if γ is coherent.*

(2) If $\operatorname{corank} \mathcal{A} \geq 1$ and $\operatorname{corank} \mathcal{A}' \geq 1$ and $\widehat{f} \in \left(\mathbb{R}^{d+d'}\right)^*$ is a generic functional on $Z(\mathcal{A} \bigsqcup \mathcal{A}')$, then there is an incoherent $\widehat{f}$-monotone path of $Z(\mathcal{A} \bigsqcup \mathcal{A}')$

PROOF. To prove item (1), we assume that $\{a_i\}$ have been chosen so that $\widehat{f}_i = 1$ for all i and $\gamma = \widehat{\gamma} / \{a_{n+1}\} = (1, 2, \ldots, n)$. We define $f = \widehat{f} \circ \iota$ by the embedding $\iota : \mathbb{R}^d \xhookrightarrow{\iota} \mathbb{R}^{d+d'}$ as the first d coordinates. We check f is generic on by computing $f_i = f(a_i) = \widehat{f}(a_i) = 1 > 0$.

To show that $\widehat{\gamma}/\{a_{n+1}\} = (1, 2, \ldots, n)$ is an f-monotone path of $Z(\mathcal{A})$, we view $\widehat{\gamma}$ as a path on $Z(\mathcal{A} \bigsqcup \mathcal{A}')$. We understand $Z(\mathcal{A} \bigsqcup \mathcal{A}')$ as a prism over $Z(\mathcal{A})$ using Lemma 4.3. Removing a_{n+1} projects $Z(\mathcal{A} \bigsqcup \mathcal{A}')$ to $Z(\mathcal{A})$ along the isthmus a_{n+1} and the path $\widehat{\gamma}$ projects to γ, following edges of $Z(\mathcal{A})$. Therefore, γ is a f-monotone path

We suppose γ is a coherent f-monotone path of $(Z(\mathcal{A}), f)$, and recall that $f(a_i) = f_i = 1$ so there are $\{g_1, \ldots, g_n\}$ such that

$$0 < g_1 < \ldots g_n.$$

Let k be the position of a_{n+1} in $\widehat{\gamma}$ and define $\widehat{g}_i = g_i$ for $1 \leq i \leq n$ and

$$\widehat{g}_{n+1} = \begin{cases} 0 & \text{if } k = 1, \\ g_n + 1 & \text{if } k = n+1, \\ \frac{g_k + g_{k+1}}{2} & \text{otherwise.} \end{cases}$$

For $1 \leq i < k$ we know $\widehat{g}_i = g_i < \widehat{g}_{n+1}$ and for $k < i \leq n+1$ we also know $\widehat{g}_{n+1} < g_i = \widehat{g}_i$, so $\widehat{\gamma}$ is a coherent $\widehat{f}$-monotone path of $Z(\mathcal{A} \bigsqcup \mathcal{A}')$.

Now suppose that $\widehat{\gamma}$ is a coherent $\widehat{f}$-monotone path so there are $\{g_i\}$ selecting $\widehat{\gamma}$ and by ignoring g_{n+1} we have

$$\frac{g_1}{f_1} < \frac{g_2}{f_2} < \cdots < \frac{g_n}{f_n}.$$

We know that $\{g_1, \ldots, g_n, g_{n+1}\}$ are a linear dependence of $(\mathcal{A} \bigsqcup \mathcal{A}')^* = \mathcal{A}^* \cup \{0\}$, so

$$\sum_{i=1}^{n+1} g_i a_i^* = \sum_{i=1}^{n} g_i a_i^* + g_{n+1} \begin{pmatrix} 0 \\ \vdots \\ 0 \end{pmatrix} = \sum_{i=1}^{n} g_i a_i^* = 0.$$

Therefore, $\{g_1, \ldots, g_n\}$ is a linear dependence of $\mathcal{A}^*$ and γ is a coherent f-monotone path.

To prove item (2), we must show that $Z(\mathcal{A} \sqcup \mathcal{A}')$ has incoherent $\widehat{f}$-monotone paths for any $\widehat{f} \in \left(\mathbb{R}^{d+d'}\right)^*$. When $\mathcal{A}$ or $\mathcal{A}'$ are not universally all coherent, $Z(\mathcal{A} \sqcup \mathcal{A}')$ has incoherent $\widehat{f}$-monotone paths by Lemma 4.24. When $\mathcal{A}$ and $\mathcal{A}'$ are universally all-coherent, both $\mathcal{A}$ and $\mathcal{A}'$ are extensions of universally all-coherent corank 1 hyperplane arrangements. We show that $Z(\mathcal{A} \sqcup \mathcal{A}')$ has incoherent $\widehat{f}$-monotone paths when $\mathcal{A}$ and $\mathcal{A}'$ are both of universally all-coherent and of corank 1, and any higher corank will follow from Lemma 4.19. We assume that $|\mathcal{A}| = d + 1 \leq d' + 1 = |\mathcal{A}'|$, and assume that $\mathcal{A}$ and $\mathcal{A}'$ are ordered so that:

$$\mathcal{A} = \left\{ a_1, \ldots, a_d, a_{d+1} = \sum_{i=1}^{d} a_i \right\}, \text{ and}$$

$$\mathcal{A}' = \left\{ a'_{d-d'+1}, \ldots, a'_0, a'_1, \ldots, a'_d, a'_{d+1} = \sum_{i=1}^{d} a'_i \right\}.$$

We further assume $\mathcal{A}$ and $\mathcal{A}'$ are chosen so that $f(a_i) = 1$ for $1 \leq i \leq d$ and $f(a'_i) = 1$ for $d - d' + 1 \leq i \leq d'$. Then know $f(a_{d+1}) = d$ and $f(a'_{d+1}) = d'$. Using the combinatorial description

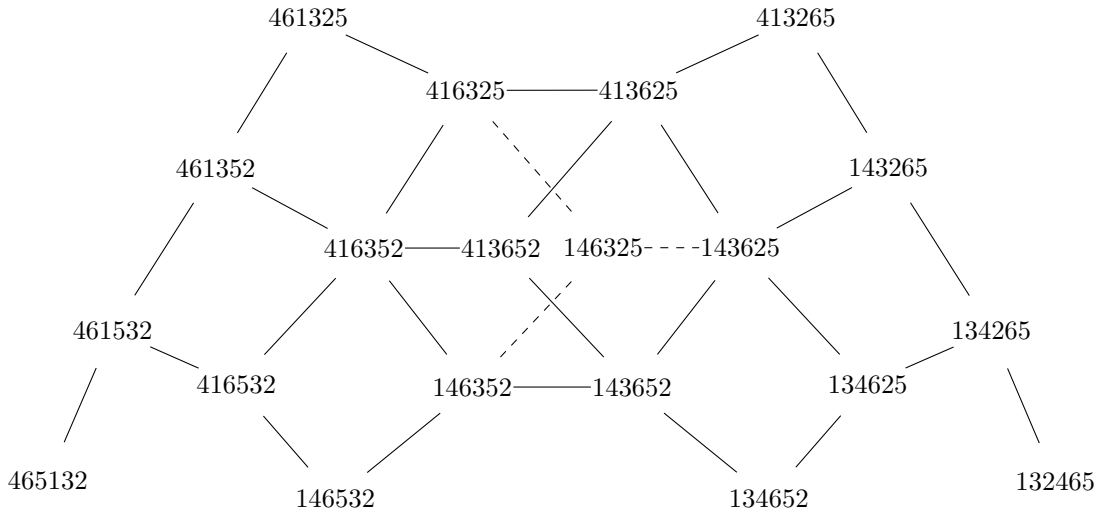

FIGURE 5.3. All shuffles of 132 and 465

in Lemma 5.3 we claim that

$$\begin{aligned}\gamma &= (a_1, \ldots, a_{d-1}, a_{d+1}, a_d) \text{ is a gallery of } (\mathcal{A}, c), \text{ and}\\ \gamma' &= (a'_{d-d'+1}, \ldots, a'_0, a'_1, \ldots, a'_{d-1}, a'_{d+1}, a'_d) \text{ is a gallery of } (\mathcal{A}', c').\\ \text{Define } \widehat{\gamma} &= (a'_{d-d'+1}, \ldots, a'_0, a'_1, a_1, \ldots, a'_{d-1}, a_{d-1}, a_{d+1}, a'_{d+1}, a'_d, a_d)\end{aligned}$$

as a shuffle of γ and γ' and an $\widehat{f}$-monotone path of $Z(\mathcal{A} \sqcup \mathcal{A}')$ by Lemma 4.8. We claim that $\widehat{\gamma}$ is an incoherent $\widehat{f}$-monotone path of $Z(\mathcal{A} \sqcup \mathcal{A}')$. Suppose $\widehat{\gamma}$ were coherent, then there would be $\{g_i, h_i\}$, chosen so that $h_0 < 0 < h_1$ and satisfying

$$\underbrace{h_{d-d'+1} < \ldots < h_0}_{h_i<0} < \underbrace{h_1 < g_1 < \cdots < h_{d-1} < g_{d-1}}_{h_i<g_i} < \frac{g_{d+1}}{d} < \frac{h_{d+1}}{d'} < h_d < g_d.$$

In particular we have $g_{d+1}/d < h_{d+1}/d'$. We compute:

$$\frac{h_{d+1}}{d'} = \sum_{i=d-d'+1}^{d} \frac{h_i}{d'} < \frac{1}{d'} \sum_{i=0}^{d} h_i < \frac{1}{d'} \sum_{i=0}^{d} g_i \leq \frac{1}{d} \sum_{i=0}^{d} g_i = \frac{g_{d+1}}{d},$$

a contradiction so $\widehat{\gamma}$ is an incoherent $\widehat{f}$-monotone path. Thus $Z(\mathcal{A})$ contains incoherent $\widehat{f}$-monotone paths for every $\widehat{f}$. □

Corollary 5.8 will be particularly useful for our classification, allowing us to focus on irreducible hyperplane arrangements. This completes our classification of universally all-coherent pointed hyperplane arrangements in corank 1. To put the result in a tidy package we state the classification as our first main theorem.

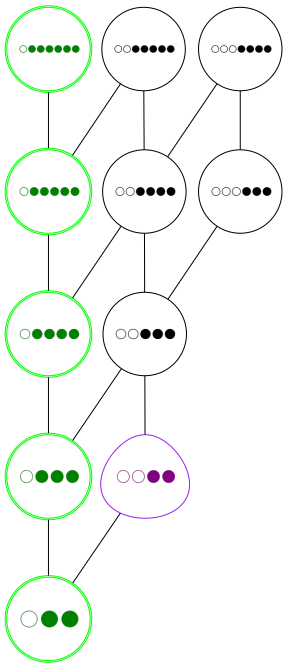

FIGURE 5.4. Classification of monotone path graphs in corank 1 ordered by single element lifting. Zonotopal arrangements distinguished by circular nodes

THEOREM 5.9. *For a pointed hyperplane arrangement $\mathcal{A}$ in corank* 1*,*

- *if $\mathcal{A}^*$ has exactly 1 negative vector, then $(\mathcal{A}, c)$ is universally all-coherent, and*
- *if $\mathcal{A}^*$ has* 2 *or more negative vectors then the monotone path graph has at least one incoherent f-monotone path for any f.*

The classification, with minimal obstruction class highlighted in red, the universally all-coherent family in green, is illustrated in Figure 5.4.

PROOF. Our previous lemmas contain all the arguments required for this proof. The classification of irreducible hyperplane arrangements in corank 1 can be see in Figure 5.4. Every hyperplane arrangement for which $\mathcal{A}^*$ has 2 or more negative vectors is a lifting of the minimal obstruction class in Lemma 5.7 and has incoherent galleries by Lemma 4.24. When $\mathcal{A}^*$ has exactly 1 negative vector, every gallery is coherent by Lemma 5.5. Moreover, every cellular string is coherent according to Lemma 4.16. Reducible hyperplane arrangements are addressed by Corollary 5.8 and universally all-coherent when $\mathcal{A}$ is a disjoint union of an all-coherent irreducible hyperplane arrangement and an isthmus, or series of isthmuses. □

5.4. Diameter bound

Having classified monotone path graphs into universally all-coherent and containing an incoherent path for every f we now return to the main question of [**RR12**] "For real hyperplane arrangements $\mathcal{A}$ and a choice of base chamber c, does the graph $G_2(\mathcal{A}, c)$ of minimal galleries from $-c$ to c have diameter exactly $|L_2|$?". Our strategy is to explicitly compute the diameter of $G_2(\mathcal{A}, c)$ when $\mathcal{A}^*$ has exactly 1 negative vector. By identifying $G_2(\mathcal{A}, c)$ with the one skeleton of $Z(\mathcal{A}')$, we know the diameter of $G_2(\mathcal{A}, c)$ is $|L_2|$. For all other pointed hyperplane arrangements, we find a gallery which is provably L_2-accessible using our understanding of the covectors of $\mathcal{M}(\mathcal{A}, (+)^n)$.

The first part of this strategy is simple. We have already shown that $G_2(\mathcal{A}, c)$ equals the one-skeleton of $Z(\mathcal{A}')$ when $\mathcal{A}^*$ has exactly 1 negative vector. To compute its diameter, we simply recall the well-known result of [**BS92**], and we know $\operatorname{Diam} G_2(\mathcal{A}) = \operatorname{Diam} G_1(\mathcal{A}') = |L_2|$

The second part of this strategy requires more work. It will be helpful to give $\mathcal{A}^*$ coordinates. To make L_2 separation easier to work with, we will use slightly nonstandard coordinates for $\mathcal{A}^*$:

$$\mathcal{A}^* = \begin{array}{c} \begin{matrix} a_1^* & \dots & a_{k-1}^* & a_k^* & \cdots & a_n^* \end{matrix} \\ \begin{pmatrix} -1 & \dots & -1 & 1 & \cdots & -1 \end{pmatrix} \end{array}.$$

In this ordering, $(1, 2, \dots, n)$ a gallery of $(\mathcal{A}, c)$. We find L_2 separation using modified bubble sort operations [**CLRS09**], [**Knu98**] and claim that $(1, 2, \dots, n)$ is L_2-accessible.

LEMMA 5.10. *For an irreducible hyperplane arrangement $\mathcal{A}$ of $n = d + 1$ hyperplane in $\mathbb{R}^d$ in which $\mathcal{A}^*$ has at least 2 negative vectors, $a_1^* = a_n^* = -1$, the gallery $(1, 2, \dots, n)$ is L_2-accessible in $G_2(\mathcal{A}, c)$.*

PROOF. For irreducible $\mathcal{A}$ of corank 1, $L_2(\mathcal{A}) = \left\{X_{i,j} \middle| 1 \le i < j \le n\right\}$. For an arbitrary γ separation set of γ and $(1, 2, \dots, n)$ is

$$L_2((1, 2, \dots, n), \gamma) = \left\{X_{i,j} \middle| i < j \quad \text{and} \quad \gamma(i) > \gamma(j)\right\}.$$

Any flip $X_{i,j}$ of γ with $i < j$ will reduce $L_2((1, 2, \dots, n), \gamma)$ by one. We must exhibit such a flip for every γ. We consider two cases:

- If $\gamma(1) \neq 1$ and $\gamma(n) \neq n$, and $\gamma(i) = 1$, $\gamma(j) = n$ then either $X_{1,\gamma(i-1)}$ or $X_{\gamma(j+1),n}$ is a flip of γ.

  Suppose $\gamma(1) \neq 1$, $\gamma(n) \neq n$, and $X_{1,\gamma(i-1)}$ is not a flip of γ. Our combinatorial description of Lemma 5.1 says γ has the form

  $$\gamma = \left(\underbrace{(i-1) \text{ negative vectors of } \mathcal{A}^*}\right) \gamma(i+1)1 \left(\underbrace{(n-i-1) \text{ positive vectors of } \mathcal{A}^*}\right)$$

  and $X_{\gamma(j+1),n}$ is a flip of γ that decreases the L_2 separation of γ and $(1, 2, \dots, n)$. A symmetric argument tells us that when $X_{\gamma(j+1),n}$ is not a flip of γ then $X_{1,\gamma(i-1)}$ is.

- If $\gamma(1) = 1$ and $\gamma(n) = n$ we take $k = \min\left\{l \middle| \gamma(l) < \gamma(l+1)\right\}$ and claim that $X_{k,\gamma'(k+1)}$ is a flip of γ. We know that $1 < k < n-1$ so any sign vector c with $c_{\gamma(k)} = c_{\gamma(k+1)} = 0$ corresponding to $X_{k,\gamma(k+1)}$ has $c_1 = -$ and $c_n = +$ so c will be a covector of $\mathcal{A}$.

□

EXAMPLE 5.11. *We will illustrate Theorem 5.10 using a hyperplane arrangement of* 10 *hyperplanes in* $\mathbb{R}^9$*, in which* $\mathcal{A}^*$ *has exactly* 2 *negative vectors. Our idea is to begin by first moving* 1 *to the left then 10 to the right. The result is the following path in* $G_2(\mathcal{A}, c)$*:*

step	*gallery*	*next flip*
0	$(10,3,2,4,9,8,7,6,5,1)$	$X_{1,5}$
1	$(10,3,2,4,9,8,7,6,1,5)$	$X_{3,10}$
2	$(3,10,2,4,9,8,7,6,1,5)$	$X_{2,10}$
$\vdots$	$\vdots$	$\vdots$
9	$(3,2,4,9,8,7,6,10,1,5)$	$X_{1,10}$
10	$(3,2,4,9,8,7,6,1,10,5)$	$X_{5,10}$
11	$(3,2,4,9,8,7,6,1,5,10)$	$X_{2,3}$
$\vdots$	$\vdots$	$\vdots$
	$(1,2,3,4,5,6,7,8,9,10)$	*complete*

At each step we avoid the permutations $(-,\ldots,-,1,10)$ *and* $(-,\ldots,-,10,1)$*. After moving* 10 *to the right, we know the origin is captured by* a^*_{10} *and* $a^*_{\gamma(9)}$*.*

We now prove our second main theorem which answers the main question of [**RR12**] in corank 1.

THEOREM 5.12. *For a hyperplane arrangement* $\mathcal{A}$ *of* $n = d+1$ *hyperplane in* $\mathbb{R}^d$ *with an acyclic orientation, the monotone path graph* $G_2(\mathcal{A}, c)$ *has diameter* $|L_2|$*.*

PROOF. We restrict our attention to irreducible hyperplane arrangements, relying on Lemma 4.9 to deal with disjoint unions. Let $\mathcal{A}^*$ be the dual of $\mathcal{A}$ and k be number of negative vectors in $\mathcal{A}$. When $k = 1$, Theorem 5.5 tell us that $G_2(\mathcal{A}, c)$ is universally all-coherent, written as $Z(\mathcal{A}')$, and thus has diameter $|\mathcal{A}'| = |L_2(\mathcal{A})|$. When $k > 1$ Theorem 5.10 tells us that there is an L_2-accessible node and [**RR12**] guarantees that the diameter of $G_2(\mathcal{A}, c) = |L_2|$. Thus $G_2(\mathcal{A}, c)$ has diameter $|L_2|$ for all k. □

CHAPTER 6

Application: Corank 2

This chapter uses the results of Chapter 4 to provide a complete classification of monotone path graphs in corank 2. Following the logical progression of Chapter 5, we begin with a classification of pointed irreducible hyperplane arrangements using affine Gale diagrams, identifying two infinite families of universally all-coherent pointed irreducible hyperplane arrangements and giving minimal obstructions for all other arrangements. For both universally all-coherent families we will give combinatorial descriptions of the galleries of $(\mathcal{A}, c)$ and find functionals making every f-monotone path coherent, for every f. Outside the two infinite families, we use Lemma 4.24 to reduce all monotone path graphs to a finite set of minimal obstructions. Eight minimal obstructions are single-element extensions of corank 1 hyperplane arrangements containing incoherent f-monotone paths. Applying Lemma 4.19, these eight corank 2 hyperplane arrangements have incoherent f-monotone paths. The remaining minimal obstruction is the subject of Section 6.3; we carefully find an incoherent f-monotone path for every f. We conclude this chapter with our third main theorem, which is the classification of monotone path graphs in corank 2 into universally all-coherent, and containing an incoherent f-monotone path for every f. We assume that all hyperplane arrangements in this section are irreducible unless otherwise noted.

For an arrangement $\mathcal{A}$ of $n = d + 2$ hyperplanes in $\mathbb{R}^d$, the dual $\mathcal{A}^*$ consists of $d + 2$ vectors in $\mathbb{R}^2$. To highlight our classification and guide our results we present Figure 6.1 showing the universally all-coherent families and the minimal obstructions in corank 2. We focus on green affine Gale diagrams which correspond universally all-coherent families. The purple affine Gale diagram is the special case in Section 6.3. All remaining minimal obstructions are red and illustrated in illustrate in Table 6.2.

6.1. First Universally All-Coherent Family

In corank 2, there are two analogs to the universally all-coherent family of Section 5.2. The first, which we call *type I*, consists of $n = d + 2$ vectors in $\mathbb{R}^d$ with 4 parallelism classes in $\mathcal{A}^*$. We remark that we have to include the cross-ratio to prove coherence, but will not need the cross-ratio to enumerate the galleries of $(\mathcal{A}, c)$. We illustrate the dual configuration and affine Gale diagram in Figure 6.2.

We describe $\mathcal{A}^*$, including its cross-ratio $\mu > 0$, in coordinates as

$$\mathcal{A}^* = \begin{array}{c} \begin{matrix} a_1^* & a_2^* & a_3^* & a_4^* & \cdots & a_n^* \end{matrix} \\ \begin{pmatrix} 0 & -1 & 1 & 1 & 1 & \cdots & 1 \\ 1 & -1 & 0 & -\mu & -\mu & \cdots & -\mu \end{pmatrix} \end{array}.$$

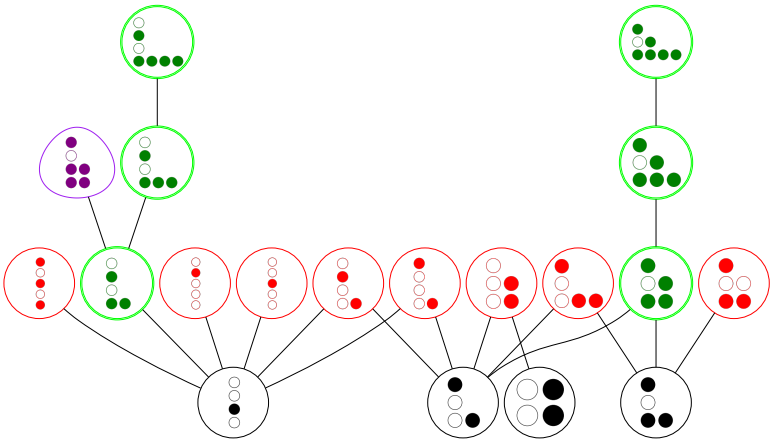

FIGURE 6.1. Classification of monotone paths in corank 2. Universally all-coherent pointed hyperplane arrangements are green, minimal obstructions are red, and the exceptional case from Section 6.3 is purple.

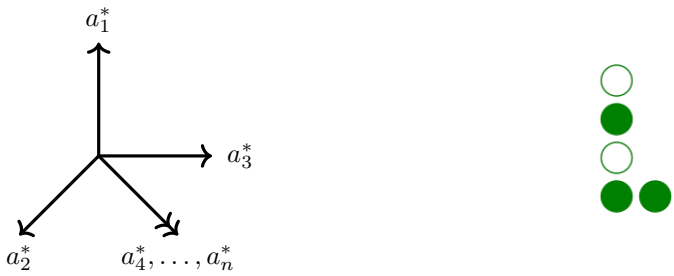

FIGURE 6.2. Type I universally all-coherent hyperplane arrangement in corank 2; dual vectors and sample affine gale dual.

LEMMA 6.1. *When $(\mathcal{A}, c)$ is type I, the number of galleries of $(\mathcal{A}, c)$ is:*

$$|\Gamma(\mathcal{A})| = 2(d-1)!\binom{d+1}{3}.$$

PROOF. When $(\mathcal{A}, c)$ is of type I, its galleries have a combinatorial description based on three observations:

- The only possible orderings of $\{a_1^*, a_2^*, a_3^*\}$ are (a_3^*, a_2^*, a_1^*) and (a_1^*, a_2^*, a_3^*).
- There are no galleries γ with $\gamma(1) \in \{1, 2, 3\}$ and $\gamma(n) \in \{1, 2, 3\}$.
- The vectors $\{a_4^*, \ldots, a_{d+2}^*\}$ are interchangeable.

The idea of is to build galleries based on these observations using the following enumeration.

- Pick an ordering of $\{a_1^*, a_2^*, a_3^*\}$ in one of 2 possible ways.
- Choose locations for a_1^*, a_2^*, a_3^* in γ by picking i, j, and k to which for $\gamma(i) = a_1, \gamma(j) = a_2$, and $\gamma(k) = a_3$. A fixed ordering of a_1^*, a_2^*, a_3^* eliminates the first or last position of γ, so i, j, and k are elements of a $d+1$ set and we must choose 3 elements.
- The vectors $\left\{a_4^*, \ldots, a_{d+2}^*\right\}$ are interchangeable and ordered in $(d-1)!$ ways.

Taken together this gives

$$|\Gamma(\mathcal{A}, c)| = 2(d-1)!\binom{d+1}{3}$$

galleries of $(\mathcal{A}, c)$. □

To show that $(\mathcal{A}, c)$ of type I is universally all-coherent, we must show that $(Z(\mathcal{A}), f)$ is all-coherent for any f realizing $(\mathcal{A}, c)$. We start from a generic f and show that $(Z(\mathcal{A}), f)$ is all-coherent by finding g_i which select an arbitrary f-monotone path and using Lemma 4.16 to extend coherence to any cellular string of $(Z(\mathcal{A}), f)$.

LEMMA 6.2. *When $(\mathcal{A}, c)$ is of type I, for any generic functional f on $Z(\mathcal{A})$ realizing $(\mathcal{A}, c)$, and an f-monotone path γ we have that*

- *there are $a, b > 0$ and a positive real partition $b = \sum_{i=4}^{n} b_i$ so that the f-valuation of $\mathcal{A}$ is:*

$$f^* = (a + b(1+\mu), a + b, a, b_4, \ldots, b_n)\,, \text{ and}$$

- *the f-monotone path γ is coherent.*

PROOF. We take $f^* = (f_1, \ldots, f_n)$ to be a positive linear dependence on $\mathcal{A}^*$. Since $\{a_4^*, \ldots, a_n^*\}$ are parallel in $\mathcal{A}^*$ we can simplify this to a linear dependence of

$$\begin{array}{cccc} a_1^* & a_2^* & a_3^* & a_4^* \\ \begin{pmatrix} 0 & -1 & 1 & 1 \\ 1 & -1 & 0 & -\mu \end{pmatrix} \end{array}.$$

This matrix has a kernel spanned by

$$\left\{ \begin{pmatrix} 1 \\ 1 \\ 1 \\ 0 \end{pmatrix}, \begin{pmatrix} 1+\mu \\ 1 \\ 0 \\ 1 \end{pmatrix} \right\}.$$

Define $a = f_3 > 0$ and $b = \sum_{i=4}^{n} f_i > 0$. The vector $(a + b(1+\mu), a + b, a, b)$ is a linear combination of kernel elements and therefore a linear dependence. Further, $f^* = (a + b(1+\mu), a + b, a, b, f_4, \ldots, f_n)$ is the same linear dependence with ba_4^* partitioned into the parallel vectors $\{a_4^*, \ldots a_n^*\}$ and satisfies our first condition.

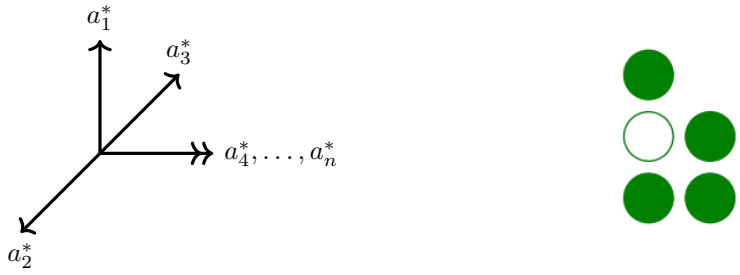

FIGURE 6.3. Type II universally all-coherent hyperplane arrangement in corank 2; dual vectors and sample affine gale dual.

We now find g by describing g_i explicitly and checking that g_i are a linear dependence $\sum g_i a_i^* = 0$ of $\mathcal{A}^*$. Mirroring our enumeration of the galleries we begin by picking the ordering (a_1^*, a_2^*, a_3^*) of $\{a_1^*, a_2^*, a_3^*\}$. We recall that $\gamma(1) \neq 1$ so we assume that $\gamma(1) = 4$ by re-indexing. We set

$$g_1 = 1 \quad g_2 = 1 \quad g_3 = 1$$

so that

$$\frac{g_1}{f_1} = \frac{1}{a+b+b\mu} < \frac{g_2}{f_2} = \frac{1}{a+b} < \frac{g_3}{f_3} = \frac{1}{a}.$$

We order $\{g_5, \ldots, g_n\}$ according to γ and pick them so that

$$\frac{g_{\gamma(i)}}{f_{\gamma(i)}} < \frac{g_{\gamma(i+1)}}{f_{\gamma(i+1)}} \quad \text{for } 5 < i < n, \text{and}$$
$$\frac{|g_5|}{f_5} < \frac{g_5}{f_5} + \cdots + \frac{g_n}{f_n}$$

We set $\frac{g_4}{f_4} = -\left(\frac{g_5}{f_5} + \cdots + \frac{g_n}{f_n}\right)$ so that $g_4 < 0 < \frac{g_1}{f_1}$ and $\sum_{i=1}^n g_i a_i^* = 0$. If we instead pick the ordering (a_3^*, a_2^*, a_1^*) of $\{a_3^*, a_2^*, a_1^*\}$ we make a symmetric argument by multiplying g_i by -1. We conclude every f-monotone path of $(\mathcal{A}, c)$ is coherent and therefore $(\mathcal{A}, c)$ is all-coherent by Lemma 4.16 for every f, and $(\mathcal{A}, c)$ is universally all-coherent. □

6.2. Second Universally All-Coherent Family

The second class of universally all-coherent hyperplane arrangements in corank 2, which we call *type II*, consists of $d+2$ hyperplanes in $\mathbb{R}^d$. We characterize this arrangement by its dual, which has 3 parallelism classes in standard position; we do not need to include a cross-ratio in our computations. We illustrate $\mathcal{A}^*$ with Figure 6.3 and give it coordinates

$$\mathcal{A}^* = \begin{array}{c} \begin{array}{cccccc} a_1^* & a_2^* & a_3^* & a_4^* & \cdots & a_n^* \end{array} \\ \begin{pmatrix} 0 & -1 & 1 & 1 & \cdots & 1 \\ 1 & -1 & 1 & 0 & \cdots & 0 \end{pmatrix} \end{array}.$$

We use the same logical progression as Section 6.1, first enumerating the galleries combinatorially, then explicitly finding a g which selects every gallery and using Lemma 4.16 to then claim that $\mathcal{A}$ is universally all-coherent.

LEMMA 6.3. *For $(\mathcal{A}, c)$ of type II, the number of galleries of $(\mathcal{A}, c)$ is*

$$|\Gamma(\mathcal{A}, c)| = (d-1)! \left(\sum_{k=1}^{d-2} (k+2)(k+1) \right)$$

PROOF. We begin with four observations.

(1) The non parallel vectors $\{a_1^*, a_2^*, a_3^*\}$ can only be ordered in two ways, (a_1^*, a_2^*, a_3^*) or (a_3^*, a_2^*, a_1^*),
(2) there is no gallery with $\gamma(1) = 1$ and symmetrically, no gallery with $\gamma(n) = 1$,
(3) there is no gallery which begins with either (a_1^*, a_2^*, a_3^*), or (a_3^*, a_2^*, a_1^*), and symmetrically no gallery which ends with (a_1^*, a_2^*, a_3^*), or (a_3^*, a_2^*, a_1^*),
(4) the parallel vectors $\left\{a_4^*, \ldots, a_{d+2}^*\right\}$ can be ordered arbitrarily.

We begin by choosing one of the two orderings of $\{a_1^*, a_2^*, a_3^*\}$ and assume that a_1^* is in position k. For the ordering (a_1^*, a_2^*, a_3^*) we know $1 < k < d$ for a total of $d-2$ choices for k. Symmetrically, for the ordering (a_3^*, a_2^*, a_1^*) we know $3 < k < d+1$ for a total of $d-2$ choices for k. Given any choice k for the position a_1^*, the remaining two non-parallel vectors are inserted prior in any of the $\binom{k+2}{2}$ ways. We then pick any ordering of the parallel vectors, $\left\{a_4^*, \ldots, a_{d+2}^*\right\}$, in $(d-1)!$ possible ways. Each choice of k gives a distinct gallery, so we count the total number of galleries as

$$|\Gamma(\mathcal{A}, c)| = (d-1)!2 \sum_{k=1}^{d-2} \binom{k+2}{2} = (d-1)! \sum_{k=1}^{d-2} \frac{(k+2)!}{k!} = (d-1)! \sum_{k=1}^{d-2} (k+2)(k+1).$$

□

Next, we show $(\mathcal{A}, c)$ is universally all-coherent by showing that $(Z(\mathcal{A}), f)$ is all-coherent for any f realizing $(\mathcal{A}, c)$. We start from a generic f and show that $(Z(\mathcal{A}), f)$ is all-coherent by finding g_i which select an arbitrary f-monotone path and using Lemma 4.16 to extend coherence to any cellular string of $(Z(\mathcal{A}), f)$.

LEMMA 6.4. *When $(\mathcal{A}, c)$ is of type II and for any generic functional f on $Z(\mathcal{A})$ realizing $(\mathcal{A}, c)$ and an f-monotone path γ we have that*

- *there are $a, b > 0$ and a positive real partition $a = \sum_{i=4}^{n} a_i$ so that the f-valuation of $\mathcal{A}$ is:*

$$f^* = (a, a+b, a, a_4, \ldots, a_n), and$$

- *the f-monotone path γ is coherent.*

PROOF. We take $f^* = (f_1, \ldots, f_n)$ to be a positive linear dependence on $\mathcal{A}^*$. Since $\{a_4^*, \ldots, a_n^*\}$ are parallel in $\mathcal{A}^*$ we can simplify this to a linear dependence of

$$\begin{array}{cccc} a_1^* & a_2^* & a_3^* & a_4^* \\ \begin{pmatrix} 0 & -1 & 1 & 1 \\ 1 & -1 & 1 & 0 \end{pmatrix} \end{array}.$$

This matrix has a kernel spanned by

$$\left\{ \begin{pmatrix} 1 \\ 1 \\ 0 \\ 1 \end{pmatrix}, \begin{pmatrix} 0 \\ 1 \\ 1 \\ 0 \end{pmatrix} \right\}.$$

Define $a = f_3 > 0$ and $b = \sum_{i=4}^n f_i > 0$. The vector $(a, a+b, a, a)$, is a linear combination of kernel elements and therefore a linear dependence. Further, $f^* = (a, a+b, a, a_4, \ldots, a_n)$ is the same linear dependence with aa_4^* partitioned into the parallel vectors $\{a_4^*, \ldots a_n^*\}$ and satisfies our first condition.

We now find a functional g selecting an arbitrary f-monotone γ by finding $\{g_i\}$ and checking it is a linear dependence. We mirror the enumeration of $\Gamma(\mathcal{A}, c)$ and begin by assuming $\{a_1^*, a_2^*, a_3^*\}$ are ordered as (a_1^*, a_2^*, a_3^*) of in γ and set

$$g_1 = 0, \quad g_2 = 1, \quad g_3 = 1.$$

So that

$$\frac{g_1}{f_1} = \frac{0}{a} < \frac{g_2}{f_2} = \frac{1}{a+b} < \frac{g_3}{f_3} = \frac{1}{b}, \qquad \text{and}$$
$$g_1 a_1^* + g_2 a_2^* + g_3 a_3^* = 0.$$

We must have

$$\sum_{i=4}^n g_i a_i^* = 0.$$

Lemma 6.3 guarantees $\gamma(1) \neq 1$, so we assume $\gamma(1) = 4$. We find values for g_i with $i \geq 5$ just as in Lemma 6.2 with a γ ordering then pick g_4 so that

$$g_4 + \cdots + g_{d+2} = 0.$$

Since a_1^* is never first, g_4 is negative so $\{g_i\}$ exist. For the symmetric ordering of $\{a_1^*, a_2^*, a_3^*\}$ we make a symmetric argument by multiplying g_i by -1. We conclude every f-monotone path of $(\mathcal{A}, c)$ is coherent and therefore $(Z(\mathcal{A}), f)$ is all-coherent by Lemma 4.16 and $(\mathcal{A}, c)$ is universally all-coherent. □

6.3. Exceptional Case

The final arrangement we deal with is the minimal obstruction not dealt with by Corollary 4.20. This hyperplane arrangement $\mathcal{A}$ consists of 6 vectors in $\mathbb{R}^4$ and is a single-element lifting of the type I universally all-coherent arrangement with 5 vectors. $\mathcal{A}^*$ is a minor deformation Example 4.10 and retains

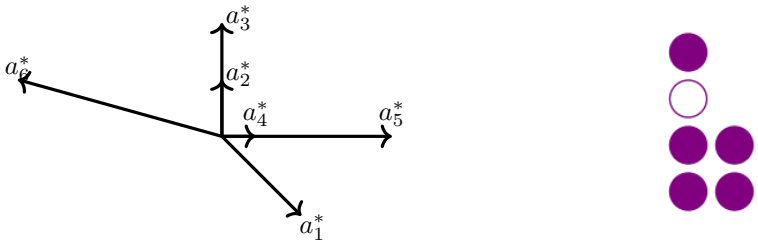

FIGURE 6.4. Dual vector configuration of the exceptional case.

just enough of the shuffle structure to contain incoherent f-monotone paths for every f. The exceptional arrangement $\mathcal{A}$ has 4 parallelism classes so we must include the cross-ratio in our calculations. We start by describing the galleries of $\mathcal{A}$ and computing the incoherent f-monotone paths for various f. Once we understand how f dictates which paths are coherent, we prove that there is always an incoherent path.

We first describe $\mathcal{A}$ using its dual $\mathcal{A}^*$. We incorporate a generic f on $Z(\mathcal{A})$ into our description of $\mathcal{A}^*$ so that for any f we have $f(a_i) = 1$ by making $\sum_{i=1}^{n} a_i^* = 1$.

$$\mathcal{A}^* = \begin{array}{c} \begin{matrix} a_1^* & a_2^* & a_3^* & a_4^* & a_5^* & a_6^* \end{matrix} \\ \begin{pmatrix} f_1 & 0 & 0 & f_4 & f_5 & -f_6 \\ -f_1 & f_2 & f_3 & 0 & 0 & \mu f_6 \end{pmatrix} \end{array}$$

We can describe any $\{f_1, \ldots, f_6\}$ using only four parameters and we pick $\{f_2, f_3, f_4, f_5\}$. From these parameters we compute f_1 and f_6 as

$$f_1 = \frac{-1}{\mu - 1}\left(f_2 + f_3 + \mu f_4 + \mu f_5\right), \quad \text{and} f_6 = \frac{-1}{\mu - 1}\left(f_2 + f_3 + f_4 + f_5\right).$$

and we must check that $f_1, f_6 > 0$ and $(1, 1, 1, 1, 1, 1)$ is a positive linear dependence on $\mathcal{A}^*$. We know that if $f_2, f_3, f_4, f_5 > 0$ then $f_1 > 0$ and $f_6 > 0$ and check $\sum_{i=1}^{6} a_i^*$:

$$\begin{aligned} a_1^* + a_6^* &= \begin{pmatrix} f_1 - f_6 \\ -f_1 + \mu f_6 \end{pmatrix} \\ &= \begin{pmatrix} \frac{-1}{\mu-1}\left(f_2 + f_3 + \mu f_4 + \mu f_5 - f_2 - f_3 - f_4 - f_5\right) \\ \frac{-1}{\mu-1}\left(-f_2 - f_3 - \mu f_4 - \mu f_5 + \mu f_2 + \mu f_3 + \mu f_4 + \mu f_5\right) \end{pmatrix} \\ &= \frac{-1}{\mu - 1}\begin{pmatrix} \mu f_4 + \mu f_5 - f_4 - f_5 \\ -f_2 - f_3 + \mu f_2 + \mu f_3 \end{pmatrix} \\ &= \frac{-1}{\mu - 1}\begin{pmatrix} (\mu - 1)\left(f_4 + f_5\right) \\ (\mu - 1)\left(f_2 + f_3\right) \end{pmatrix} \\ &= -\begin{pmatrix} f_4 + f_5 \\ f_2 + f_3 \end{pmatrix} = -\left(a_2^* + a_3^* + a_4^* + a_5^*\right). \end{aligned}$$

$\langle f_2, f_3, f_4, f_5\rangle$	421653	431652	521643	531642
$\langle 1,1,1,1\rangle$	inc.	inc.	inc.	inc.
$\langle 1,1,2,3\rangle$	coh.	coh.	inc.	inc.
$\langle 1,2,1,1\rangle$	inc.	coh.	inc.	coh.
$\langle 1,2,1,2\rangle$	inc.	coh.	inc.	inc.
$\langle 4,1,2,3\rangle$	coh.	inc.	coh.	inc.
$\langle 2,3,4,1\rangle$	inc.	inc.	coh.	coh.

TABLE 6.1. Summary of examples from Section 6.3

EXAMPLE 6.5. *We compute the monotone path for a fixed μ. The monotone path graph contains 152 galleries and has diameter 15. We can also compute the fiber polytope and check that it has at most 148 galleries so we expect at least 4 incoherent galleries for every f. Remarkably, the cross-ratio does not change coherence/incoherence for this configuration.*

We use our computer to generate a list of incoherent nodes for fixed μ and a variety of f, which is summarized in Table 6.1.

We must show that there is an incoherent path for every choice of $\{f_2, f_3, f_4, f_5\}$. Based on Table 6.1 we guess that incoherent galleries of $\mathcal{A}$ will always start with one of $\{a_4^*, a_5^*\}$, followed by one of $\{a_2^*, a_3^*\}$, then followed by a_1^* and a_6^* in order, the unused element of $\{a_4^*, a_5^*\}$, and the final unaccounted for vector from $\{a_2^*, a_3^*\}$. We write this using a regular expression.

$$\gamma = (\{a_4^*, a_5^*\}, \{a_2^*, a_3^*\}, a_1^*, a_6^*, \{a_5^*, a_4^*\}, \{a_3^*, a_2^*\}).$$

In Table 6.1, we see that there is no path which is incoherent for every f but, when we restrict our attention to the functionals in which $f_2 \leq f_3$ and $f_4 \leq f_5$, we suspect that $\gamma = 521643$ is incoherent.

LEMMA 6.6. *Suppose $(Z(\mathcal{A}), f)$ is the exceptional pointed hyperplane arrangement above with dual $\mathcal{A}^*$. The gallery $\gamma = 421653$ is coherent if and only if*

$$\frac{f_3}{f_5} < \frac{f_3 + f_5}{f_4 + f_5} < \frac{f_2}{f_4}. \tag{1}$$

PROOF. Our proof is geometric in nature and clear with adequate illustrations. All our diagrams rely on $\sum a_i^* = 0$. When γ is coherent, we also know that $\sum g_i a_i^* = 0$. Our diagrams will focus on 6 vectors:

$$\begin{aligned} v_{24} &= a_2^* + a_4^* & w_{24} &= g_2 a_2^* + g_4 a_4^* \\ v_{16} &= -a_1^* - a_6^* & w_{16} &= -g_1 a_1^* - g_6 a_6^* \\ v_{35} &= a_4^* + a_5^* & w_{35} &= g_4 a_4^* + g_5 a_5^*. \end{aligned}$$

Our convention will be to draw v_{ij} in black, w_{ij} in green, and both v_{16} and w_{16} as with dotted lines. We a priori know that v_{24} and v_{35} will lay in the first quadrant and v_{16} will lay in the third quadrant. By using Lemma 3.4 we can pick $g_i > 0$ and know that w_{24} and w_{35} will also lay in the first quadrant while

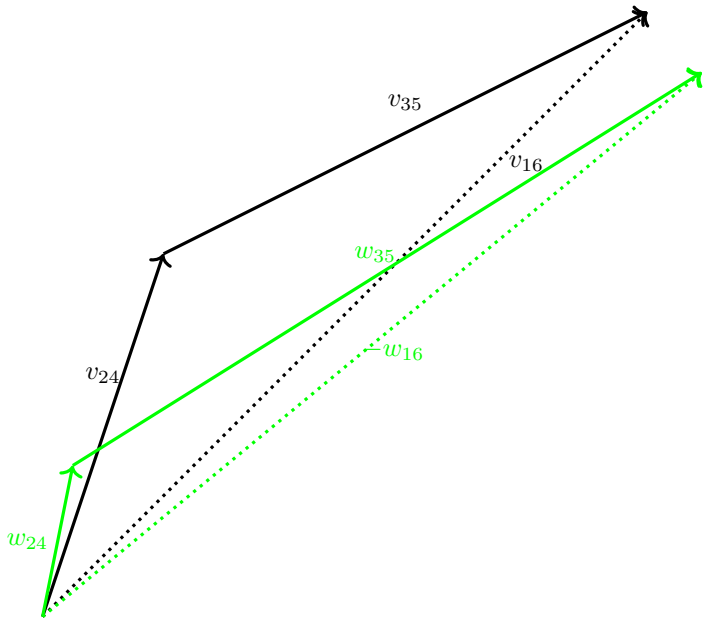

FIGURE 6.5. $\gamma = 421653$ is coherent when $\frac{f_3}{f_5} < \frac{f_3+f_5}{f_4+f_5} < \frac{f_2}{f_4}$.

w_{16} will lay in the third quadrant. Our presentation of $\mathcal{A}^*$ allows us to visualize information about g_i in the following way:

- When $g_4 < g_2$, w_{24} has a larger slope than v_{24}.
- When $g_5 < g_3$, w_{35} has a larger slope than v_{35}.
- When $g_1 < g_6$, w_{16} has a smaller slope than v_{35}.

First we will check is that if Equation 1 holds then $\gamma = 421653$ is coherent. Figure 6.5 show v_{24}, v_{16}, v_{35} satisfying Equation 1 . We pick g_1 and g_6 so that $|v_{16}| = |w_{16}|$ and g_2, g_3, g_4, g_5 so that $\sum g_i a_i^* = 0$. Since the solid green arrows are steeper than the solid black arrows, $g_4 < g_2$ and $g_5 < g_6$, and the dotted green arrow is less steep than the dotted black arrow, so we know $g_1 < g_6$. We also see that $g_2 + g_4 < 1 < g_3 + g_5$. We conclude that $\gamma = 421653$ is coherent.

In reverse, we must show that if Equation 1 is not satisfied, then $\gamma = 421653$ is incoherent. We first consider the case that

$$\frac{f_3}{f_5} = \frac{f_3 + f_5}{f_4 + f_5} = \frac{f_2}{f_4}.$$

We now assume

$$\frac{f_3}{f_5} \geq \frac{f_3 + f_5}{f_4 + f_5} \geq \frac{f_2}{f_4}.$$

Figure 6.6 guides our proof. Suppose there exist $g_4 < g_2 < g_1 < g_6 < g_5 < g_3$ with $\sum g_i a_i^* = 0$, and chosen so that $|v_{16}| = |w_{16}|$. Since w_{35} cannot point down, we must have

$$\frac{g_2 f_2}{g_4 f_4} > \frac{g_2 f_2 + g_3 f_3}{g_4 f_4 + g_5 f_5}.$$

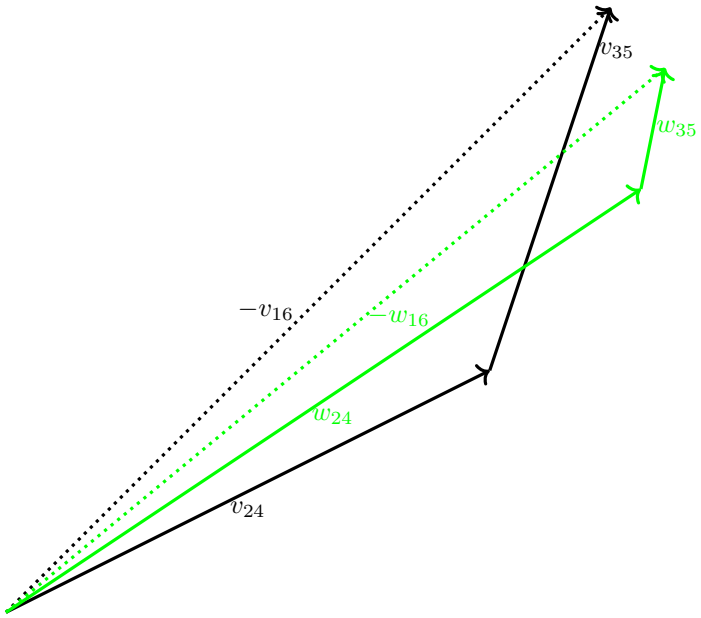

FIGURE 6.6. $\gamma = 421653$ is incoherent when $\frac{f_3}{f_5} \geq \frac{f_3+f_5}{f_4+f_5} \geq \frac{f_2}{f_4}$.

which contradicts Figure 6.6. To make $\sum g_i a_i^* = 0$ we have had to shrink w_{35} while stretching w_{24}. This in turn means that $g_2 + g_4 > g_3 + g_5$, contradicting our hypothesis on $\{g_i\}$.

□

Lemma 6.6 gives a method of seeing which galleries in $\mathcal{A}$ are incoherent. In $\mathcal{A}$, the ordering of $\{a_2^*, a_3^*\}$ and the ordering of $\{a_4^*, a_5^*\}$ were arbitrary so we can relabel vectors and see which labeling make 421653 incoherent. To make this easier, we state this for an arbitrary gallery γ in the following corollary.

COROLLARY 6.7. *Suppose $\mathcal{A}^*$ is the dual configuration in Lemma 6.6 and γ is a gallery of the form $\{4,5\}\,\{2,3\}\,16\,\{5,4\}\,\{3,2\}$, then*

$$\frac{f_{\gamma(6)}}{f_{\gamma(5)}} < \frac{f_3+f_5}{f_4+f_5} < \frac{f_{\gamma(2)}}{f_{\gamma(1)}}.$$

PROOF. Since both the pairs a_2^*, a_3^* and a_4^*, a_5^* are parallel we can label them arbitrarily and after reordering, have $\gamma = 421653$ is coherent. □

This corollary explains the results of Table 6.1 and why $\gamma = 521643$ is incoherent for every f. When $f_2 \leq f_3$ and $f_4 \leq f_5$ we have:

$$\frac{f_2}{f_5} \leq \frac{f_2+f_3}{f_4+f_5} \leq \frac{f_3}{f_4},$$

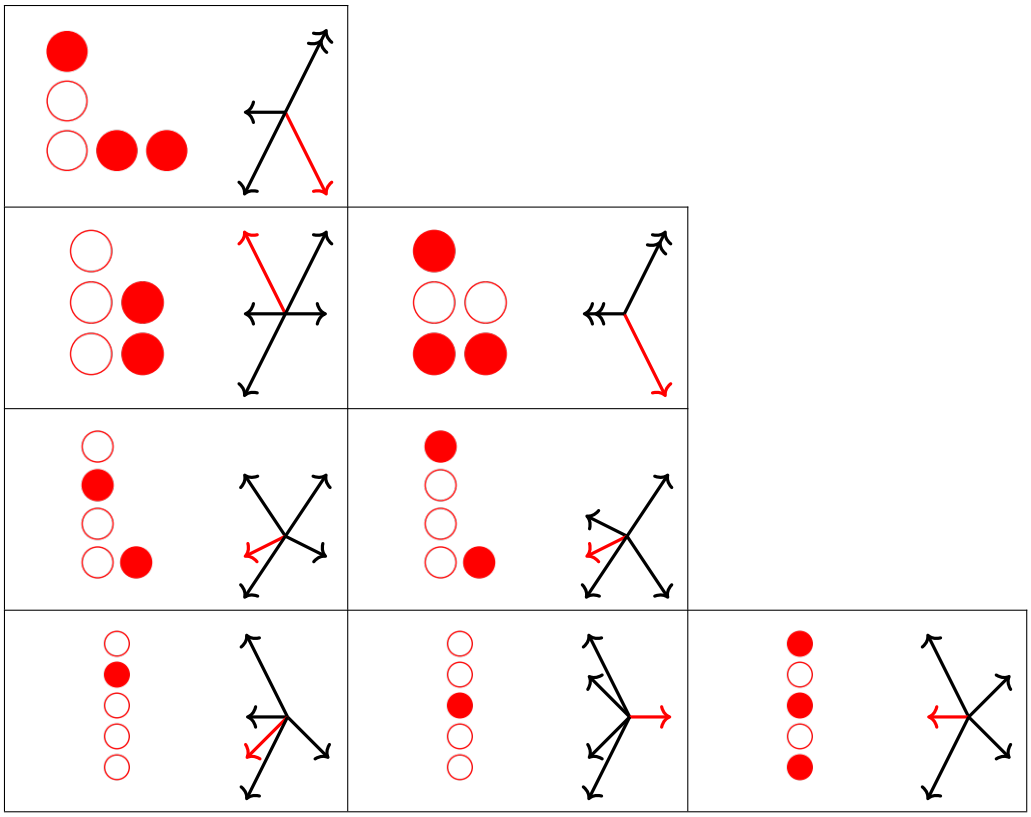

TABLE 6.2. Minimal obstructions in corank 2. Projection along the red vector results in the hyperplane arrangement of Section 5.3.

so $\gamma = 521643$ is incoherent according to Corollary 6.7. We have shown that $\mathcal{A}$ has an incoherent f-monotone path for every f and are ready to give a complete classification of universally all-coherent hyperplane arrangements in corank 2.

6.4. Corank 2 classification

We claim that every pointed hyperplane arrangement in corank 2 is either one of our two universally all-coherent families or has an incoherent f-monotone path for every f. Section 6.3 gave a single minimal obstruction however Figure 6.1 has pointed hyperplane arrangements which we claim have incoherent galleries. We recall that deleting a vector from $\mathcal{A}$ is equal to projecting parallel to a vector in $\mathcal{A}^*$ [**Zie95**, Prop. 6.1] so we rely on Lemma 4.19 to prove that $\mathcal{A}$ has incoherent f-monotone paths. Table 6.2 shows each of the affine Gale duals, along with a representative dual vector configuration with a single vector highlighted in red. Projecting parallel to each of the red vectors results in a vector configuration which contains an incoherent f-monotone path γ according to Lemma 5.7 so each configuration in Table 6.2 has an incoherent gallery by Lemma 4.19. We now can state the main theorem of this Chapter.

THEOREM 6.8. *In corank 2 there are exactly two infinite families of universally all-coherent pointed hyperplane arrangements. All other corank 2 families have at least one incoherent f-monotone path for every f and Figure 6.1 illustrates the minimal obstructions to universal all-coherence.*

PROOF. When $\mathcal{A}$ is reducible, Corollary 5.8 describes precisely when $\mathcal{A} = \mathcal{A}_1 \bigsqcup \mathcal{A}_2$ has incoherent galleries; $\mathcal{A}$ has incoherent galleries when $\mathcal{A}_1$ and $\mathcal{A}_2$ are both of corank 1. When $\mathcal{A}_1$ is of corank 2 and $\mathcal{A}_2$ is of corank 0, the disjoint union $\mathcal{A} = \mathcal{A}_1 \bigsqcup \mathcal{A}_2$ has incoherent galleries when $\mathcal{A}_1$ has incoherent galleries, i.e., when $\mathcal{A}_1$ is not of type I or type II.

When $\mathcal{A}$ is an irreducible hyperplane arrangement, the two universally all-coherent infinite families are the subject of Lemma 6.2 and Lemma 6.4. The minimal obstruction consisting of 6 vectors in $\mathbb{R}^4$ contains an incoherent f-monotone path for every f by Lemma 6.6. The remaining hyperplane arrangements are single element extensions of the corank 1 hyperplane arrangement of Section 5.7; These arrangements always contain an incoherent f-monotone path by Lemma 4.19 and are illustrated in Table 6.2. □

CHAPTER 7

Further Research

We now turn our attention to topics of ongoing investigation. Some of these questions, such as the main question of [**RR12**] we asked at the outset of our research and have remained elusive. Others are question that came up during our work and deserve further investigation.

7.1. When does the diameter equal $|L_2|$?

With Theorem 5.12 we have an answer to the diameter question of [**RR12**] in corank 1, obtained by find an L_2-accessible node for any graph $G_2(\mathcal{A}, c)$. Such methods cannot give a complete answer in corank 2, as Example 7.1 has no L_2-accessible galleries.

EXAMPLE 7.1. *A hyperplane arrangement we have looked at but have not featured prominently is the arrangement:*

$$\mathcal{A} = \begin{array}{c} \begin{matrix} a_1 & a_2 & a_3 & a_4 & a_5 \end{matrix} \\ \begin{pmatrix} 1 & 0 & 0 & 1 & 1 \\ 0 & 1 & 0 & -1 & -2 \\ 0 & 0 & 1 & 1 & 3 \end{pmatrix} \end{array}$$

,with Gale dual:

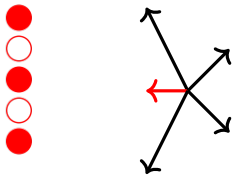

This example has diameter equal to $|L_2|$ automatically since $\mathcal{A} \subset \mathbb{R}^3$ [**CM93**, Theorem 2.5]*,* [**RR12**, Remark 2.6] *and is a minimal obstruction to universal all-coherence in corank 2. A careful inspection of the graph $G_2(\mathcal{A}, c)$, illustrated in Figure 7.1, where we have labeled each flip with the pair of hyperplanes that intersect at its non-trivial cell, reveals $G_2(\mathcal{A}, c)$ has no L_2-accessible galleries.*

7.2. What are the universally all-coherent families in higher corank?

We have classified all universally all-coherent pointed hyperplane arrangements in coranks 1 and 2. Corank 3 is what Sturmfels calls "the threshold for counterexamples" [**Stu88**] and poses additional challenges over coranks 1 and 2. In particular, a finite enumeration of classes in corank 3 is impossible. Our main tools of classification Lemma 4.16 and Lemma 4.24 are valid for arbitrary corank and our computational tools are powerful enough to look at examples.

Computational results indicate that there are pointed hyperplane arrangements which are all-coherent for certain f in corank 3 and above and therefore universally all-coherent by Theorem 4.17. These families extend the type I family of Section 6.1 in corank k and take the form $\mathcal{A}^* = \{e_1, \ldots, e_k, v, v, \ldots, v\}$

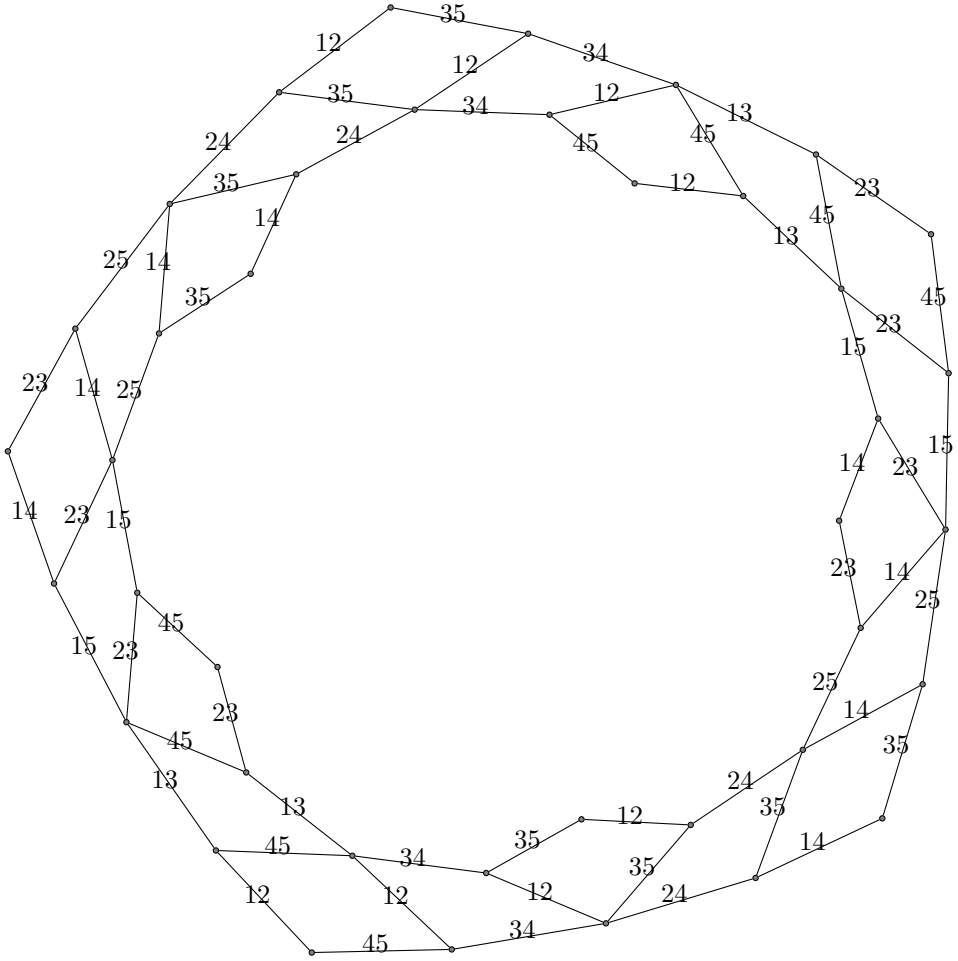

FIGURE 7.1. The monotone path graph with no L_2-accessible nodes discussed in Example 7.1.

for generic v. We have listed gallery counts for these arrangements when n is small in Table 7.1. We strongly suspect that this family is universally all-coherent and that a proof of coherence for these families is directly analogous to the proof given in Section 6.1. Table 7.1 suggests that the number of galleries in galleries will be counted by

$$\Gamma(\mathcal{A}, c) = k!(d-1)!\binom{d+1}{k+1},$$

and we expect an enumeration of the galleries to be similar to the enumeration in Lemma 6.1. We have not, however, attempted to give functionals selecting galleries for an arbitrary f, preferring to keep our focus on corank 2.

		k							
		3	4	5	6	7	8	9	10
	1	12	16						
	2	72	120	180					
n	3	480	960	1680	2688				
	4	3600	8400	16800	30240	50400			
	5	30240	80640	181440	362880	665280	1140480		
	6	282240	846720	2116800	4656960	9313920	17297280	30270240	
	7	2903040	9676800	26611200	63866880	138378240	276756480	518918400	922521600

TABLE 7.1. Number of galleries in of suspected universally all-coherent pointed hyperplane arrangements in dimension d with corank k

In addition, we expect to find corank k analogs of the type II universally all-coherent family. Proving universal all-coherence is important but is not the most exciting task. The main reason to further study these examples is to try to find all possible, all-coherent pointed hyperplane arrangements. After finding *all* all-coherent pointed hyperplane arrangements and removing them from the list of all hyperplane arrangements, you know where to look for minimal obstructions.

7.3. What are the minimal obstructions in corank $k > 2$?

In addition to our suspected family of universally all-coherent pointed hyperplane arrangements in corank k, we can ask about minimal obstructions in corank k. Corank 1 has a single minimal obstruction. Corank 2 has 9 minimal obstructions but 8 of them were extensions of the corank 1 minimal obstruction. Given the difficulty of classifying monotone path graphs in corank 3 and above we have no good intuition into the question of "what are the minimal obstructions?". We are specifically interested in hyperplane arrangements analogous to the purple arrangements of Figure 7.2 which are minimal obstructions to all-coherence, but extensions only of universally all-coherent hyperplane arrangements in corank 2. To help us, the results of Chapter 4 are independent of corank and our computational tools are available to generate examples.

7.4. Cyclic hyperplane arrangements?

Since a classification is challenging in corank 3 and above we can direct our efforts at particularly nice families of pointed hyperplane arrangements. Methods of single-element liftings and single-element extensions have proven useful in the analysis of *cyclic polytopes* [**ERR00**], [**ADLRS00**] and we have a very similar story for cyclic hyperplane arrangements. We define the family of *cyclic* hyperplane

arrangements:

$$\mathcal{A}(n,d) = \begin{array}{c} \begin{array}{cccc} a_1 & a_2 & \cdots & a_n \end{array} \\ \begin{pmatrix} 1 & 1 & \cdots & 1 \\ t_1 & t_2 & \cdots & t_n \\ \vdots & \vdots & & \vdots \\ t_1^{d-1} & t_2^{d-1} & \cdots & t_n^{d-1} \end{pmatrix} \end{array},$$

with $t_1 < t_2 < \ldots < t_n$. Based on our results, we claim $(\mathcal{A}(n,d), c)$ has is universally all-coherent when $n = d+1$ and c is a reorientation of the $k = 1$ corank 1 hyperplane arrangement and all has incoherent f-monotone paths for all other c. Further, we claim that when $n-d \geq 2$ the cyclic hyperplane arrangement $(\mathcal{A}(n,d), c)$ has incoherent f-monotone paths for any f realizing $(\mathcal{A}(d+1,d), c)$ and for every c.

PROPOSITION 7.2. *Given a pointed, cyclic hyperplane arrangement $(\mathcal{A}(n,d), c)$ with $d > 2$ and f realizing c, the monotone path graph*

- *When $n - d = 1$, the pointed hyperplane arrangement $(\mathcal{A}(n,d), c)$ is universally all-coherent when c is a reorientation of the universally all-coherent corank 1 pointed hyperplane arrangement (e.g., $c = --+-+\cdots-+$), and has incoherent f-monotone paths for all other c.*
- *When $n - d \geq 2$, the pointed hyperplane arrangement $(\mathcal{A}(n,d), c)$ has incoherent galleries for every f.*

PROOF. $\mathcal{A}(n,d)$ is irreducible and when $n = d+1$ we compute the dual as $\mathcal{A}^* = \left(a_1^*, \ldots, a_{d+1}^*\right)$ using the Vandermonde determinant, so

$$a_i^* = (-1)^{(i+1)} \prod_{\substack{1 \leq j < k \leq d+1 \\ j,k \neq i}} (t_k - t_j) / t_i.$$

We know that $t_k - t_j > 0$ for $1 \leq j < k \leq d+1$ so the sign of a_i^* depends only on i. When $c = --+-+\cdots-+$, we have a_1^* as negative dual vector, and all other $\{a_i^*\}$ are positive dual vectors. The pointed hyperplane configuration $(\mathcal{A}, c)$ then realizes the unique universally all-coherent cyclic hyperplane arrangement is that of Section 5.2.

For all other corank 1 cyclic hyperplane Section 5.3 proves that there is an incoherent f-monotone path for every f by giving a minimal obstruction when $d = 3$ and realizing $\mathcal{A}(d+1,d)$ a single-element lifting of $\mathcal{A}(d,d-1)$ which has incoherent f-monotone paths for every f, by Lemma 4.24.

When $d > 3$ and $n-d = 2$, the pointed cyclic hyperplane arrangements $\mathcal{A}(n,d)$ have no parallelism in the dual and are single-element liftings of the parallelism free classes in Table 6.2. These minimal obstructions arrangements all contain incoherent f-monotone paths according to Theorem 6.8 so they form a minimal obstruction set and any $\mathcal{A}(d+2,d)$ with $d > 2$ contains incoherent f-monotone paths by Lemma 4.24. For $n - d \geq 2$ we know that $\mathcal{A}(n,d)$ is a single element extension of a corank 2 cyclic hyperplane arrangement and will have incoherent f-monotone paths for every f according to Lemma 4.19. □

Existence of incoherent f-monotone paths nodes do not determine the diameter $G_2(C(n,d),c)$ so the main question of Reiner and Roichman remains unsolved for cyclic hyperplane arrangements. Cyclic hyperplane arrangements do give insight into the diameter of $G_2(\mathcal{A}(n,d),c)$. The cyclic arrangement $\mathcal{A}(8,4)$ is the first realized example we know of, in which the diameter of $G_2(\mathcal{A},c)$ is strictly greater than $|L_2|$. Non-realized examples previously demonstrated that the diameter is strictly greater than $|L_2|$ for acyclically oriented matroids in rank 4 [**RG93**, §3], [**RR12**, p.2785-2786]. In Example 7.3 we improve this result by demonstrating that the cyclic hyperplane arrangements, $\mathcal{A}(8,4)$ realize an example in which the diameter bound strictly greater than $|L_2|$. We feel our methods are only scratching the surface of this rich family and it is worth studying in further detail.

EXAMPLE 7.3. *The cyclic hyperplane arrangement $\mathcal{A}(8,4)$ has 8 vectors in $\mathbb{R}^4$ and the chamber $c=(-)^4(+)^4$ specifies an acyclic orientation. Making use of our computer we can check that*

$$|\Gamma(\mathcal{A},c)| = 4896,$$
$$\operatorname{Diam} G_2(\mathcal{A},c) = 30, \quad \textit{and}$$
$$|L_2| = 28.$$

Yet the shortest path between $\gamma = 34127856$ and $-\gamma = 65872143$ has length 30 and crosses the L_2 intersection $X_{1,2}$ multiple times.

In fact of the 128 chambers of $\mathcal{A}$ the diameter equals $|L_2|$ for 96 chambers and is strictly greater for remaining 32 chambers. At this time we know of nothing special about the 32 chambers of $\mathcal{A}$ which make the diameter greater than $|L_2| = 28$.

We know that the diameter of $G_2(\mathcal{A}(n,3))$ equals $|L_2|$ and also that the diameter of $G_2(\mathcal{A}(d+1,d))$ equals $|L_2|$, yet by $d=4$, and $n=8$, we have a cyclic arrangement $\mathcal{A}(8,4)$, whose diameter is greater than $|L_2|$. We believe that Example 7.3 is the smallest realized case in which diameter exceeds $|L_2|$ but we do not yet understand why, nor are our methods powerful enough to guess when the diameter will exceed $|L_2|$.

7.5. Computational Results and Applications to other Fields?

Our computational tools have provided new results for the number of reduced words in reflection arrangements. A simple modification of Dijkstra's algorithm provides a powerful tool to count paths on a pointed zonotope [**Dij59**]. We used this method to compute the number of galleries in pointed hyperplane arrangements without producing the monotone path graph. This allowed us to compute the number of reduced words for some reflection arrangements which were previously unknown, as well as provide confirmation of results obtained in other ways. We highlight these computations in Table 7.2.

The simplex method [**Mur83**] of optimization is deeply concerned with understanding f-monotone paths on *polytopes* [**AK08**] and its worst case run time proportional to the diameter 1-skeleton of polytopes.

Arrangement	$\operatorname{Diam} G_2(\mathcal{A}, c) = \lvert L_2 \rvert$?	$\lvert \Gamma(\mathcal{A}) \rvert$	$\exists L_2$-accessible
H_3	Y	152	Yes, 4
D_4	Y	2316	Y
D_5	Y	12985968	Unknown
D_6	Y	3705762080	Unknown
F_4	Y	2144892	Unknown

TABLE 7.2. Summary of computational results.

CONJECTURE 7.4 (Hirsch). *For $n > d > 2$ the diameter of a polytope in $\mathbb{R}^d$ with m facets is no larger than $m - d$.*

Our results of Theorem 5.12 and Example 7.3 fit into this context as geometrically motivated graphs with unexpected diameters. Diameter is known for zonotopes is known and well understood, however the diameter of monotone path graphs remains an interesting question.

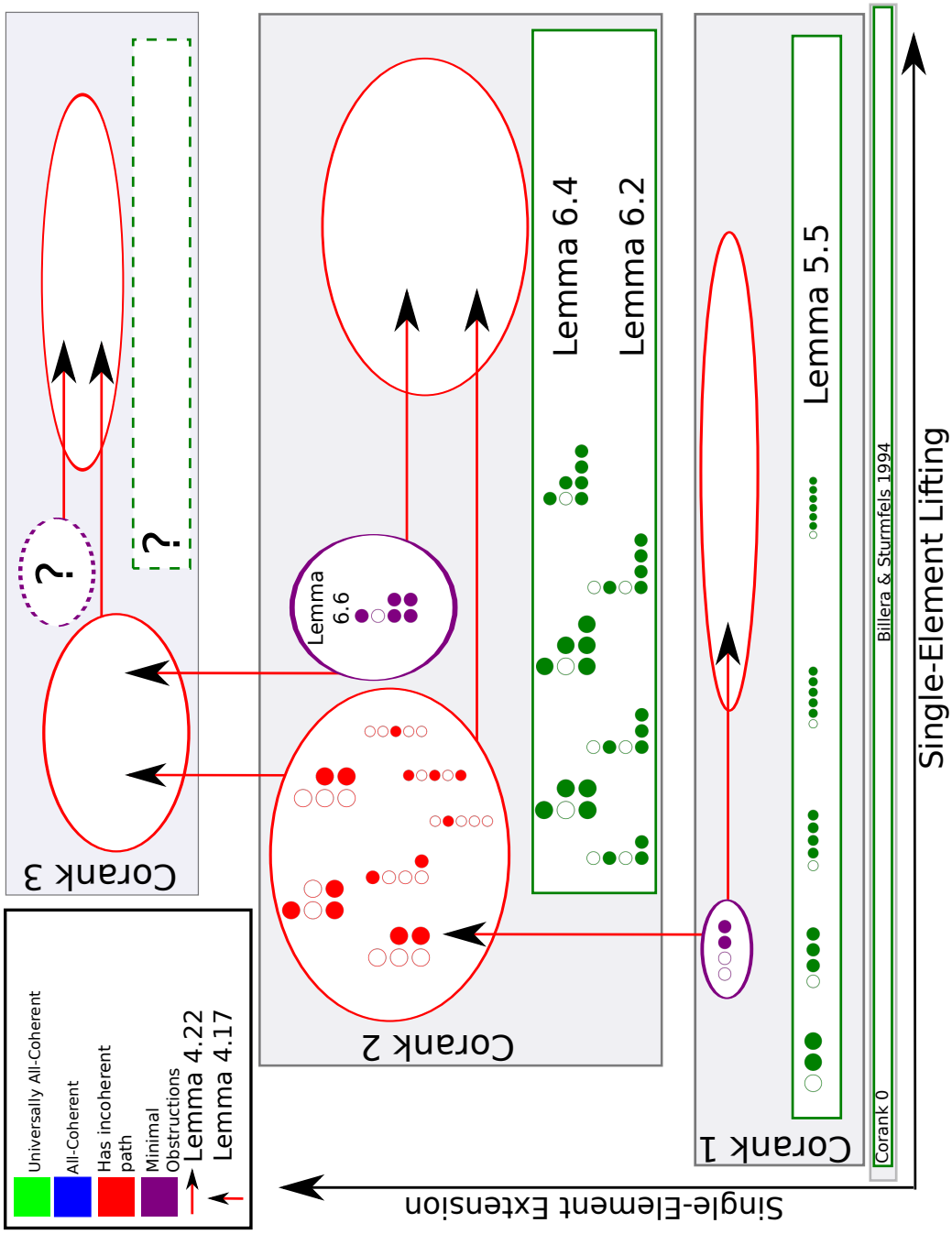

FIGURE 7.2. Summary of results and unsolved questions.

References

[ADLRS00] Christos A. Athanasiadis, Jesús A. De Loera, Victor Reiner, and Francisco Santos, *Fiber polytopes for the projections between cyclic polytopes*, European J. Combin. **21** (2000), no. 1, 19–47, Combinatorics of polytopes.

[AK08] David Avis and Bohdan Kaluzny, *Computing monotone disjoint paths on polytopes*, Journal of Combinatorial Optimization **16** (2008), no. 4, 328.

[AS01] Christos A. Athanasiadis and Francisco Santos, *Monotone paths on zonotopes and oriented matroids*, Canadian Journal of Mathematics **53** (2001), no. 6, 1121.

[BKS94] Louis J. Billera, M. M. Kapranov, and B. Sturmfels, *Cellular strings on polytopes*, Proceedings of the American Mathematical Society **122** (1994), no. 2, 549.

[BLVS+93] Anders Björner, Michel Las Vergnas, Bernd Sturmfels, Neil White, and Günter M. Ziegler, *Oriented matroids*, Encyclopedia of Mathematics and its Applications, vol. 46, Cambridge University Press, Cambridge, 1993.

[BS92] Louis J. Billera and Bernd Sturmfels, *Fiber polytopes*, The Annals of Mathematics **135** (1992), no. 3, 527.

[CFGdO00] Raul Cordovil, Komei Fukuda, and A. Guedes de Oliveira, *On the cocircuit graph of an oriented matroid*, Discrete & Computational Geometry **24** (2000), no. 2, 257.

[CLRS09] Thomas H. Cormen, Charles E. Leiserson, Ronald L. Rivest, and Clifford Stein, *Introduction to algorithms*, third ed., MIT Press, Cambridge, MA, 2009.

[CM93] R. Cordovil and M. L. Moreira, *A homotopy theorem on oriented matroids*, Discrete Math. **111** (1993), no. 1-3, 131–136, Graph theory and combinatorics (Marseille-Luminy, 1990).

[Dij59] Edsger W. Dijkstra, *A note on two problems in connexion with graphs*, Numerische Mathematik **1** (1959), no. 1, 269.

[DLRS10] Jesús A. De Loera, Jörg Rambau, and Francisco Santos, *Triangulations*, Algorithms and Computation in Mathematics, vol. 25, Springer-Verlag, Berlin, 2010, Structures for algorithms and applications.

[ERR00] Paul H. Edelman, Jörg Rambau, and Victor Reiner, *On subdivision posets of cyclic polytopes*, European Journal of Combinatorics **21** (2000), no. 1, 85.

[FL78] Jon Folkman and Jim Lawrence, *Oriented matroids*, J. Combin. Theory Ser. B **25** (1978), no. 2, 199–236.

[FPS01] Komei Fukuda, Alain Prodon, and Tadashi Sakuma, *Notes on acyclic orientations and the shelling lemma*, Theoretical Computer Science **263** (2001), no. 1-2, 9.

[Gal56] David Gale, *Neighboring vertices on a convex polyhedron*, Linear inequalities and related system, Princeton University Press, Princeton, N.J., 1956, pp. 255–263.

[GKZ94] I. M. Gel′fand, Mikhail M. Kapranov, and Andrei V. Zelevinsky, *Discriminants, resultants, and multidimensional determinants*, Mathematics: Theory & Applications, Birkhäuser Boston, Inc., Boston, MA, 1994.

[Grü67] Branko Grünbaum, *Convex polytopes*, With the cooperation of Victor Klee, M. A. Perles and G. C. Shephard. Pure and Applied Mathematics, Vol. 16, Interscience Publishers John Wiley & Sons, Inc., New York, 1967.

[HIK11] Richard Hammack, Wilfried Imrich, and Sandi Klavžar, *Handbook of product graphs*, second ed., Discrete Mathematics and its Applications (Boca Raton), CRC Press, Boca Raton, FL, 2011, With a foreword by Peter Winkler.

[Knu98] Donald E. Knuth, *The art of computer programming. vol. 3*, Addison-Wesley, Reading, MA, 1998, Sorting and searching, Second edition.

[LV77] Michel Las Vergnas, *Acyclic and totally cyclic orientations of combinatorial geometries*, Discrete Math. **20** (1977), no. 1, 51–61.

[McM71] P. McMullen, *On zonotopes*, Trans. Amer. Math. Soc. **159** (1971), 91–109.

[Mur83] Katta G. Murty, *Linear programming*, John Wiley & Sons, Inc., New York, 1983, With a foreword by George B. Dantzig.

[oIS10] The Online Encylopedia of Integer Sequences, *A062119 from oeis*, published electronically at http://oeis.org, 2010.

[RG93] Jürgen Richter-Gebert, *Oriented matroids with few mutations*, Discrete Comput. Geom. **10** (1993), no. 3, 251–269.

[Riv14] L. M. Rivera, *Integer sequences and k-commuting permutations*, ArXiv e-prints (2014).

[RR12] Victor Reiner and Yuval Roichman, *Diameter of graphs of reduced words and galleries*, Transactions of the American Mathematical Society **365** (2012), no. 5, 2779.

[San12] Francisco Santos, *A counterexample to the hirsch conjecture*, Ann. of Math. (2) **176** (2012), no. 1, 383–412.

[Sta97] Richard P. Stanley, *Enumerative combinatorics. vol. 1*, Cambridge Studies in Advanced Mathematics, vol. 49, Cambridge University Press, Cambridge, 1997, With a foreword by Gian-Carlo Rota, Corrected reprint of the 1986 original.

[Sta99] ———, *Enumerative combinatorics. vol. 2*, Cambridge Studies in Advanced Mathematics, vol. 62, Cambridge University Press, Cambridge, 1999, With a foreword by Gian-Carlo Rota and appendix 1 by Sergey Fomin.

[Sta07] ———, *An introduction to hyperplane arrangements*, Geometric combinatorics, vol. 13, Amer. Math. Soc., Providence, RI, 2007, pp. 389–496.

[Stu88] Bernd Sturmfels, *Some applications of affine gale diagrams to polytopes with few vertices*, SIAM J. Discrete Math. **1** (1988), no. 1, 121–133.

[Zie95] Günter M. Ziegler, *Lectures on polytopes*, Graduate Texts in Mathematics, vol. 152, Springer-Verlag, New York, 1995.

APPENDIX A

Incoherent tigers in acyclic cages

Die Mathematiker sind eine Art Franzosen; redet man zu ihnen, so bersetzen sie es in ihre Sprache, und dann ist es alsobald ganz etwas anders.[a]

[a]Mathematicians are [like] a sort of Frenchmen; if you talk to them, they translate it into their own language, and then it is immediately something quite different.

Johann Wolfgang von Goethe

Welcome to the part of my thesis written for non-mathematicians. This section is an attempt to answer the question "what exactly is it you study?". A typical answer to this question drops some buzz words, includes a variety of tangentially related applications, but never says much of anything. To me this misses the point in the same way that "I work in that building" misses the point of the question "what do you do". A better answer allows non-mathematicians to interact with the same problems I think about day-to-day, in a less technical way, which is what this appendix attempts to do.

At the highest level I study mathematics (Duh!). The particular flavor of math is combinatorics, which is the mathematical study of objects which you can count. Within combinatorics I enjoy counting objects of geometric or algebraic interest (e.g., counting solutions to an equation). The topic of this thesis is coherent monotone paths, specifically trying to answer the question "which monotone paths are coherent".

Already, we are dealing with technical objects without a formal definition. Chapters 2 and 3 of this dissertation give meaning to monotone paths and coherent galleries. Instead of asking you to read those 30 pages, I am going pose some problems involving a tiger. The problems about tigers are actual examples from this thesis; they will not look technical at first, but that is because I have replaced the frightening technical words like "acyclic", "monotone", and "bijection" with more friendly words like "tiger" and "fence". These problems aren't designed to trick anyone and if you make an honest attempt to solve the problem, you'll have a good idea of the methods I used in this thesis.

Acyclic tiger cages: Suppose you are a zoo keeper and your job is to keep a tiger from escaping its cage. The Tigers live on a line and the cage is four fences, two on either side of the tiger as illustrated in Figure A.1.

FIGURE A.1. The tiger problem

Occasionally, you must rotate the fences, which means you to take every fence and move it to the opposite side of the tiger. The catch is that you cannot let the tiger escape while you are rotating fences. You can move any fence at any time, you can move each fence only once, and you must move all of them.

This is not possible with only one fence on each side of the tiger, but with our tiger cage has fences. Using the fence labeling in figure A.1 you can move the fences in the order 1423 or 2431, but you cannot move the fences in the order 1234; after moving the first two fences, your tiger will escape out the left side of the cage, as illustrated in A.1. We can now ask our first problem:

Counting Problem 1: In how many ways can you move all the fences exactly once without ever letting the tiger escape.

You should pause here, get out a pencil, and try this problem for yourself. It is a fun problem, just try some rotations and see if you notice any patterns. You can't count all the rotations with just your fingers, but if you use both fingers and toes you can get there.

A standard answer to this question is to create the decision tree illustrated in Figure A.2. You can see 4 choices for the first fence you move, 2 choices for the second, 2 choices for the 3rd fence, and only 1 choice for the last fence. This gives a total of $4 * 2 * 2 = 16$ possible ways to rotate the fences. The tree is reasonably large so I have drawn it using a shorthand. In our shorthand we write $+$ or $-$ for each fence: We write $-$ if we still must move the fence and $+$ if we have already moved the fence. This shorthand calls the starting fence arrangement $----$ and the final fence arrangement $++++$ and a fence rotation is a path between these, such as 1423, which we write in shorthand:

$$---- \to +--- \to +--+ \to ++-+ \to ++++ .$$

The tiger will escape if our shorthand is ever $--++$ or $++--$.

Counting fence rotations is a problem that I solved in this thesis. I called a fence rotations a *gallery* in Definition 2.10. The counting problem you just solved was important enough that it was Lemma 5.1.

Lemma 5.1 says that if a tiger is surrounded by n fences with $k < n$ fences to his right, then the number of fence rotations is

$$n! - 2(n-k)!k!.$$

I encourage you to use $n = 4$ and $k = 2$ to check your answer to Counting Problem 1. My solution is different from the decision tree; to count the number of fence rotations, I count ways to let the tiger free

and remove that from the all possible ways to rotate the fences. Once you have done that you can use Lemma 5.1 for 20 fences or 100 fences with ease. Which way do you think is easier?

When we look at the decision tree more closely we see some repetition. Some fence arrangements come up multiple times, for instance the cage $+-+-$ is seen when we move fence 1 followed by fence 3 and seen again when we move fence 3 followed by fence 1. The decision tree was great for counting fence rotations but is does not distinguish between fence arrangements when we get to the same arrangement multiple ways. This is confusing! we want to understand all fence arrangements which keep the tiger from escaping. By redrawing the decision tree with each fence draw configuration drawn once, we have a more clear picture of ways to keep the tiger from escaping. See Figure A.3.

This picture looks like a 3d shape and remarkably it *is* a 3d shape that you can think of as being a weird 12-sided die or a stretched cube. Suddenly we are doing geometry while talking about tigers in a zoo. This is so cool that we need to give it a name, so we call it the *Tiger tope*. In this setting, fence rotations are paths from $----$ to $++++$ on the tiger tope.

We can now say how similar two fence rotations are because they can partly overlap as paths on the tiger tope. We can say that 1342 "is close to" 1324 because they are the same for the first two fence moves and differ only by moving the last two fences in opposite orders. We call this flipping two fences because we can move both fences at once without letting the tiger escape.

If you look at all the possible fence rotations you found, you can arrange them together and connect the fence arrangement which are flips (like 1324 and 1342). This gives you a picture which looks like Figure A.4 and which we call the fence diagram. A fancier word for it is the monotone path graph (Definition 2.37) which are the geometric objects that this dissertation is about.

Congratulations, you now understand the geometric half of this thesis. The remaining half of the thesis is the question of which monotone paths are "coherent". To explain coherence, we will go back to our tiger and ask a second counting problem. After understanding the solution you will be ready to understand the main results of this thesis.

Coherent tigers: Lets start with the same tiger in the same cage and we still want to rotate the fences without letting the tiger escape. Further suppose that you cannot move the fences yourself (perhaps there was an unfortunate tiger accident), but you can still ask people to move the fences for you. You have interns who are all hanging out by the fences to the left of the tiger and you have tiger lovers who are all hanging out to the right of the tiger. To get the interns and the tiger lovers to move fences, you must follow these rules:

(1) You must pay interns to move the fences from left to right.
(2) Tiger lovers pay you for the opportunity to move fences from right to left.
(3) As the fences move, the tiger gets more hungry and active, which excites the tiger lovers and scares the interns. The result is that for each fence moved, more money is exchanged (you must either pay more to the interns or the tiger lovers will pay you more to move fences for you).

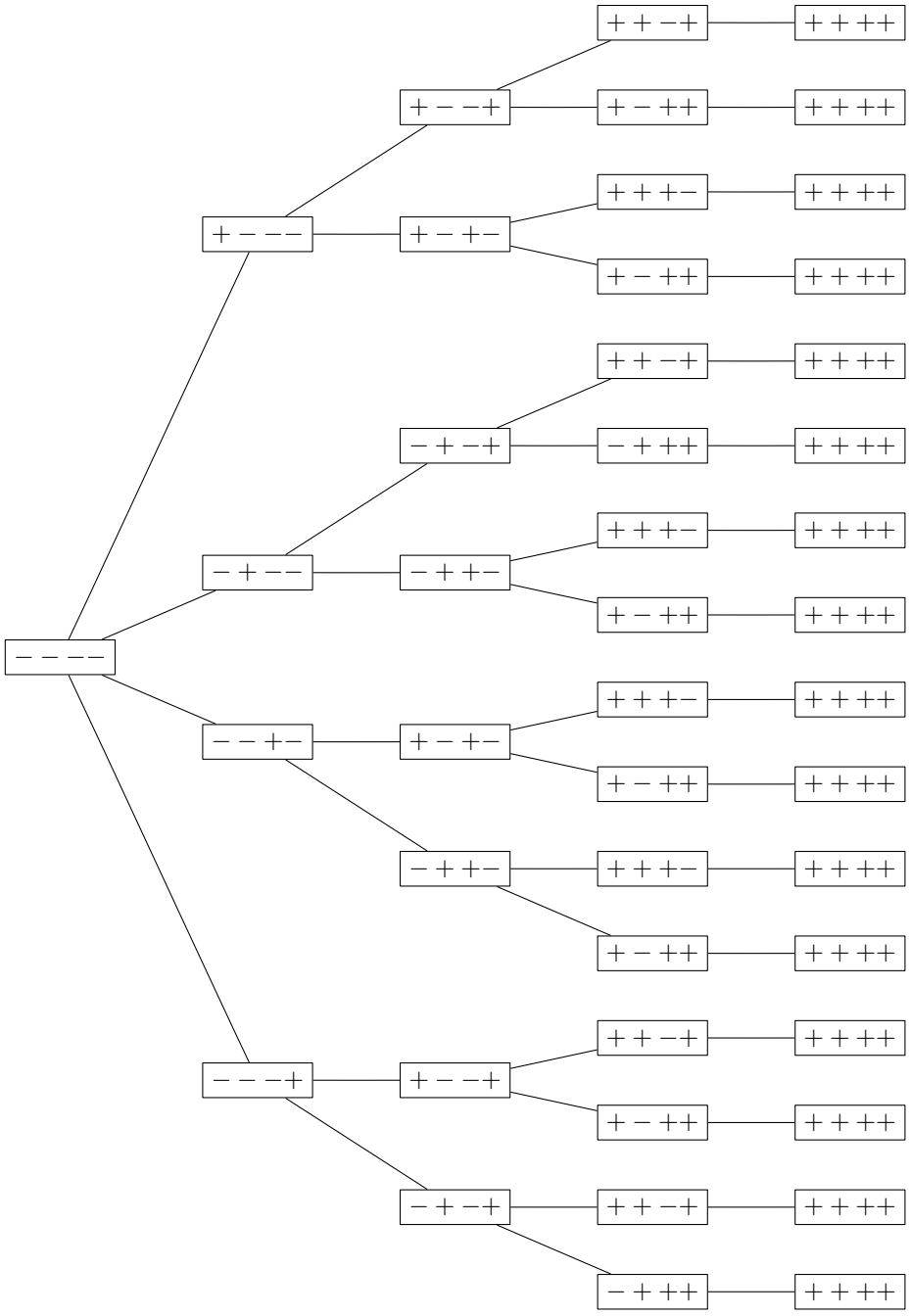

FIGURE A.2. The tiger decision tree

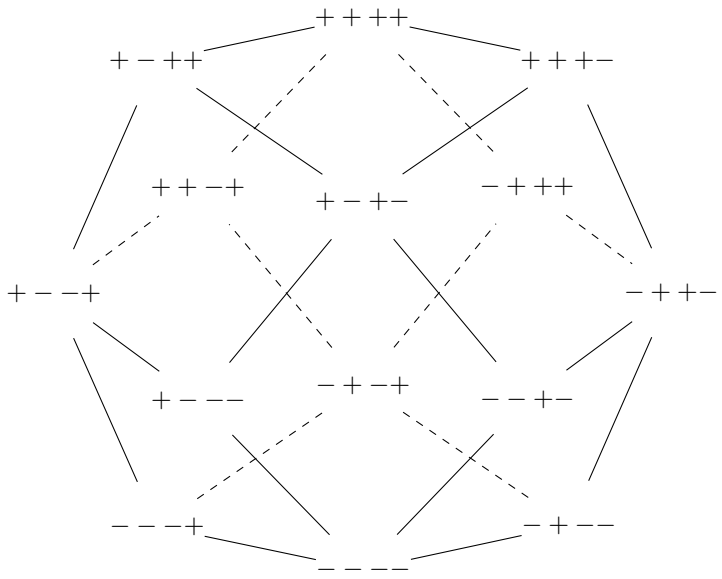

FIGURE A.3. The tiger-tope

Counting Problem 2 As a non-profit zoo, you can't make money moving the fences, but you shouldn't lose money either. Which of the 16 fence rotations can convince the tiger lovers and interns to move without losing or making money?

An example is in order here. We can convince tiger lovers and interns to rotate the fences in the order 1342 by paying an intern \$1 to move fence 1, then charge a tiger lover \$2 to move fence 3, then get another tiger lover to pay \$3 to move fence 4, and finally pay \$4 to have an intern move fence 2. We paid \$5 to interns and we got \$5 from tiger lovers. In contrast there is no way to pay people to move the fences in the order 1324 since you will make money from moving 1 followed by 4 and you will also make money from 2 followed by 4, so you are doomed to make money for the zoo.

You should again pause here, get out your pencil and try this problem yourself. Checking all 16 fence rotations might get dull, but try a few and see if you notice any patterns.

The fence rotations that balance tiger lovers and interns are called *coherent*. That is the same notion of coherence as in the title of this dissertation and was Definition 2.39. The fence rotations which cannot be done for free are *incoherent*. Understanding which galleries are coherent and which galleries are incoherent is the major question of this thesis, and you now understand it! This dissertation is a careful analysis of two generalizations of the tiger problem.

The first is to ask about more fences or different arrangements of the fences. Both of these possibilities are addressed in Chapter 5 which presents 2 major results, which we will paraphrase in the language of tigers and fences:

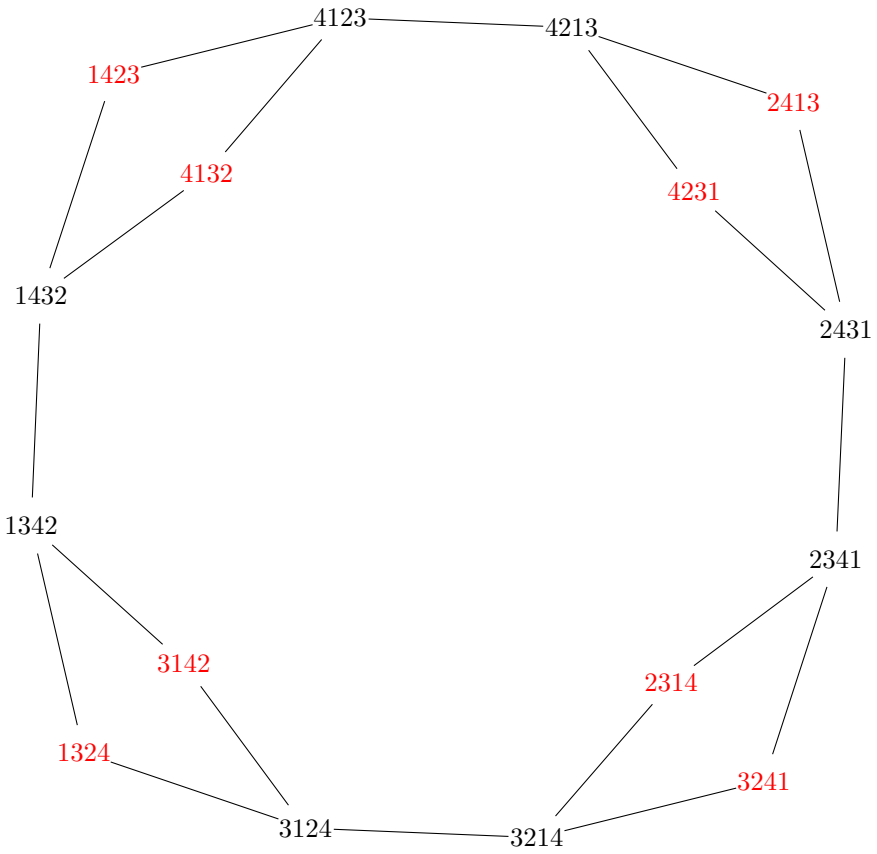

FIGURE A.4. The tiger fence diagram

(1) Theorem 5.5: If you have a tiger enclosed by n fences but only 1 of them is to the left of the tiger, you can always pay your tiger lovers and interns to rotate the fences for you. That is, there are no incoherent fence rotations when $k = 1$.
(2) Theorem 5.7 When $k > 1$ there will always be a fence rotation which you cannot pay tiger lovers and interns to do for you, without making or losing money. The proof of this is particularly interesting, because it uses a technical Lemma 4.24 to say "If there is an incoherent fence rotation for n fences I cannot make every ordering coherent by adding more fences". This Lemma is hugely important because it lets us carefully solve bite sized problems (like you just did!) then draw conclusions about all other tiger cages. 5.4

A second way to generalize the tiger problems is to consider a tiger who lives on a plane. The definitions of fence rotations, coherent and incoherent become more involved here but we have analogous results

(1) Lemma 6.2 and Theorem 6.4 give conditions making every fence rotation coherent.

(2) Lemma 6.6 shows that all other configurations have at least 1 incoherent fence rotation. Lemma 4.24 is again the primary tool we use, so this again reduces down to checking 9 bite sized problems carefully.

If you are still reading, thank you for your patience. The question which I should still answer is "who cares"? I doubt that I will receive any calls from zoo keepers asking how to rotate fences around their one-dimensional tigers. Mathematicians are interested in this problem because when a tiger cage has only coherent fence rotations the fence rotation graph will look like a sphere (in d dimensions). This may seem abstract and impractical but I agree with De Loera, Santos, and Rambau who wrote: "We firmly believe that understanding the fundamentals of geometry and combinatorics pays up for algorithms and applications." [**DLRS10**]. The algorithms and applications they are referring to include:

- The simplex algorithm for optimization. Galleries are monotone paths so we are describing the same objects used in linear programming. Unfortunately our description does not help solve linear programming problems but this illustrates that these are practical objects. Interestingly, the Hirsch conjecture for linear programming was solved by Santos [**San12**] whom we consulted for Lemma 4.16.
- Triangulations, which are a natural ways to decompose convex regions into smaller, bite-sized convex regions. Triangulations like galleries, can be coherent or incoherent and are used in everything from meshing for numerical methods and algebra problems to computer graphics, or volume computations.
- Gröbner Bases, which are methods of working with multivariate polynomials on computers. They are cutting edge math which uses triangulations to replace polynomials with monomials and solve nonlinear systems of equations.

Finally, I think this is a beautiful topic full of cool math and that makes it worth studying for its own sake. I have avoided talking about applications because I wanted to give readers the chance to actually do some math and appreciate its beauty for themselves.

APPENDIX B

Classification of affine Gale diagrams and monotone path graphs

This thesis is not complete without a classification of pointed zonotopes. Our starting point is a vector configuration $V = \{v_1, \ldots, v_n\}$. We recall that the covectors of $\mathcal{M}(V)$ are sign vectors of valuations of functionals f on V and the maximal covectors are sign vectors of generic functionals for which $f(v_i) \neq 0$. The zonotope $Z(V) \sum_{i=1}^{n} [-v_i, v_i]$ has vertices corresponding to maximal covectors of V and the Gale dual V^* of V is a vector configuration whose linear dependencies correspond to the maximal covectors of V. Our strategy for classification of pointed zonotopes will be to classify all affine Gale diagrams. The choice of an affine gale diagrams includes the choice of an acyclic orientation of $\mathcal{M}(V)$ so affine Gale diagrams will correspond to pointed zonotopes and pointed hyperplane configurations.

We give a partial ordering on affine Gale diagrams using single-element extensions which we recall from Chapter 2.2.

DEFINITION B.1. *We say that a vector configuration V^+ is a single-element extension of V if $V^+ = V \cup \{v_{n+1}\}$*

DEFINITION B.2. *We say that a vector configuration $\widehat{V} = \left\{\widehat{v}_i \in \mathbb{R}^{d+1} \,\middle|\, 1 \leq i \leq n+1\right\}$ is a single-element lifting of $V = \left\{v_i \in \mathbb{R}^d \,\middle|\, 1 \leq i \leq n\right\}$ if there is a linear surjection $\mathbb{R}^{d+1} \overset{\pi}{\longmapsto} \mathbb{R}^d$ so that*

$$\pi(\hat{v}_{n+1}) = 0$$
$$\pi(\hat{v}_i) = c_i \cdot v_i \, 1 \leq i \leq n$$

Without loss of generality, we typically assume that $c_i = 1$.

The important things to recall about single-element liftings and extensions are:

- Single element extensions of V^* correspond to single-element liftings of V.
- Single element extensions increase corank.
- Any function $h \in \left(\mathbb{R}^d\right)^*$ of V can be extended to V^+, however acyclic orientations of V do not necessarily extend to acyclic orientations of V^+ as $h(v^*_{n+1})$ may not be positive.
- Single element liftings preserve corank.
- Acyclic orientations of $\mathcal{A}$ can always be lifted to acyclic orientations of $\widehat{\mathcal{A}}$, using Lemma 4.11.
- If $\widehat{V}$ is a single-element lifting of V then $\widehat{V}^*$ is a single-element extension of V^*

$$\left(\widehat{V}\right)^* = (V^*)^+$$

- If V^+ is a single-element extension of V then $(V^+)^*$ is a single-element lifting of V^*

$$\left(V^+\right)^* = \widehat{V^*}$$

B.1. Corank 1

For V a vector configuration of $d+1$ vectors in $\mathbb{R}^d$ the dual configuration $V^* = \left\{v_1^*, \ldots, v_{d+1}^*\right\}$ is a configuration of $d+1$ vectors in $\mathbb{R}^1$. These vectors can either point in the *positive* direction or the *negative* direction. We know from Definition 2.26 that the magnitudes $|v_i^*|$ do not change $\mathcal{M}(V)$, so the positive vectors are interchangeable and the negative vectors are interchangeable. The vector configuration V is uniquely determined by the number k of *negative* vectors in V^*. Without loss of generality, we can assume that $0 \leq k \leq \frac{d+1}{2}$.

The $k = 0$ vector configuration will have no acyclic orientation; all v_i^* will be positive and thus there no $\{h_i > 0\}$ such that $\sum h_i v_i^* = 0$. All other vector configurations will have an acyclic orientation. Figure B.1 illustrates corank 1 vector configurations for small n, ordered by single-element extension, which will be lifting in the dual.

We represent each pointed zonotope with a series of black and white dots. We draw positive vectors as black dots and negative vectors as white dots. We denote vector configurations with an acyclic orientation using a circle diagram, while those with no acyclic orientation are contained in an square.

B.2. Corank 2

To give an equivalent classification in corank 2 we extend these tricks by writing vectors as elements of V^* in standard position and calling them positive or negative. This was accomplished by [**Gal56**] and more fully developed in [**Grü67**] and [**McM71**] but is presented in many survey works of which we are particularly fond of [**Zie95**] and [**BLVS$^+$93**]. We first write V^* in a canonical form.

DEFINITION B.3. *When $d \geq 3$ and $n - d = 2$, we say that the vectors of V^* are in standard position when $v_1^* = \pm \begin{pmatrix} 0 \\ 1 \end{pmatrix}$, $v_2^* = \pm \begin{pmatrix} 1/2 \\ 1/2 \end{pmatrix}$, and $v_3^* = \pm \begin{pmatrix} 1 \\ 0 \end{pmatrix}$. Any remaining v_i are given coordinates $\pm \begin{pmatrix} 1 \\ -\mu \end{pmatrix}$ and we call μ the cross-ratio of v_i^*.*

To classify the elements of V^* as positive or negative vectors in 2 dimension, we introduce an affine hyperplane and look at which half-space contains each element of V^*. This gives a picture known as an affine Gale diagrams.

DEFINITION B.4. *Given a vector configuration V consisting of n vectors in $\mathbb{R}^d$, the* Affine Gale Diagram *is a set of vectors in $\mathbb{R}^{n-d-1}$ each labeled as "positive" or "negative". The affine Gale diagram encodes the geometric information of V which we construct as follows:*

(1) Find V^* so that $\mathcal{M}(V)^* = \mathcal{M}(V^*)$.

(2) Pick $\mathcal{L}$, a generic affine hyperplane of $\mathbb{R}^{n-d}$ with normal vector ℓ.

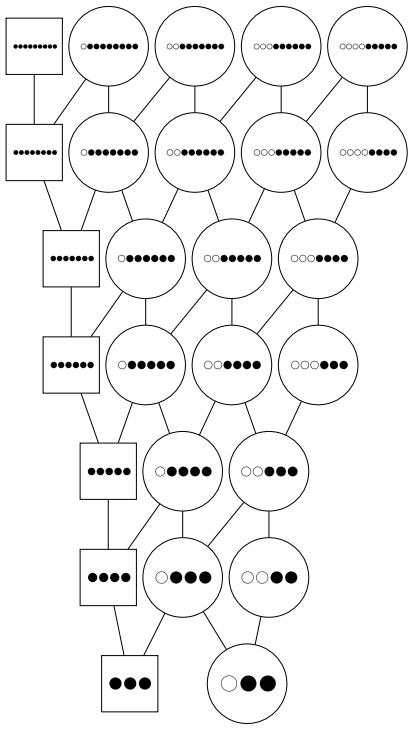

FIGURE B.1. Affine Gale diagrams in corank 1.

(3) Project $v_i^* \in V^*$ onto $\mathcal{L}$.
(4) Label $v_i^* \in V^*$ as positive or negative based on the sign of $v_i^* \cdot \ell$.

Our convention when drawing pictures of affine Gale diagrams is to draw positive vectors as black dots and negative vectors as white dots. We will draw our affine gale diagrams so that classes of parallel vectors in V^* will "line up" on the x axis, while non parallel vectors have distinct y values form a "pile". We recognize that the absolute position of the remaining vectors may depend on the cross-ratio, even when the oriented matroid does not.

Affine Gale diagrams make it possible to classify corank 2 vector configurations, however we can not tell when two affine Gale diagrams represent the same vector configuration. We address this with a brief lemma.

LEMMA B.5. *Two affine Gale diagrams are equivalent if they differ by any sequence of moves of the form :*

- *Reversing the order of the vectors.*
- *Pulling a vector from the top, switching its sign, and putting it back on the bottom.*

PROOF. This proof follows from the definition of affine Gale diagrams. Reversing the signed vectors corresponds to flipping the normal vector of $\mathcal{L}$. Cycling signed vectors corresponds to rotating the hyperplane $\mathcal{L}$. When $\mathcal{L}$ rotates through a vector v_i^* the sign of v_i^* and it switches from being first to last, thus the signed vector changes color and moves from first to last. □

We now classify realized oriented matroids in corank 2 using affine Gale diagrams. This classification is well-known [**Gal56**], however a complete classification is tedious and typically left to the reader [**Zie95**] or treated as a counting problem [**LV77**]. We include our classification because we found it useful as a written reference, and having the complete classification ordered by single extensions liftings makes patterns clear.

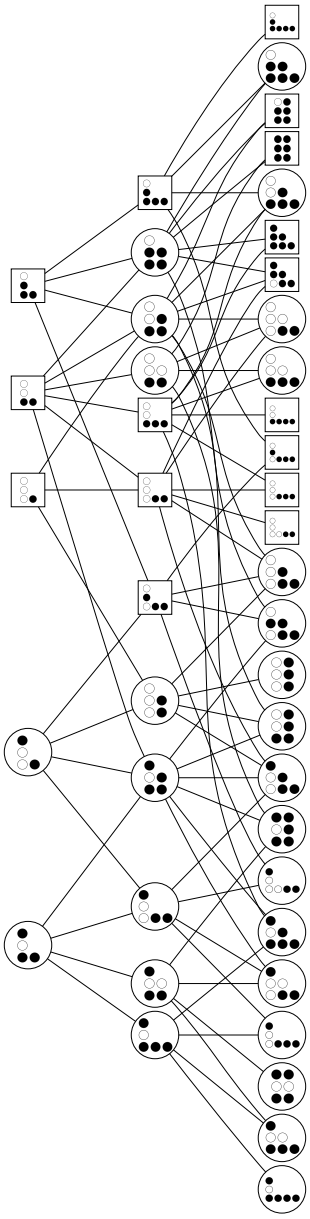

FIGURE B.2. Affine Gale diagrams in corank 2 with exactly 3 parallelism classes

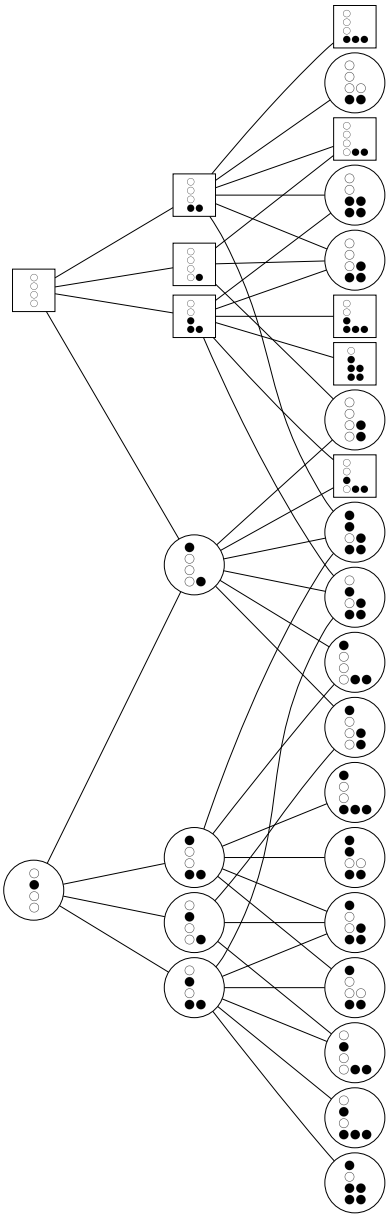

FIGURE B.3. Affine Gale diagrams in corank 2 with exactly 4 parallelism classes

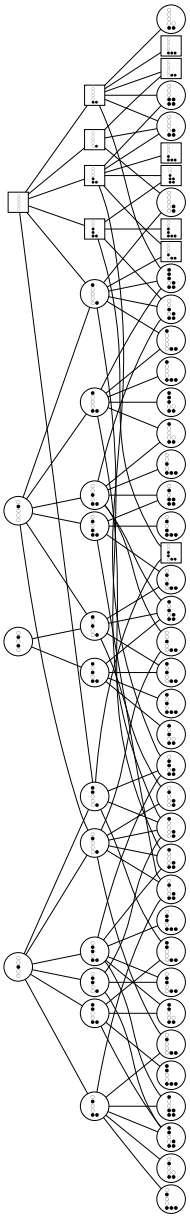

FIGURE B.4. Affine Gale diagrams in corank 2 with exactly 5 parallelism classes